The Dissertation Committee for Wen Li Certifies that this is the approved version of the following dissertation:

Development and Understanding of New Membranes Based on Aromatic Polymers and Heterocycles for Fuel Cells

Committee:

Arumugam Manthiram, Supervisor

Benny D. Freeman

Christopher W. Bielawski

Paulo J. Ferreira

Harovel G. Wheat

Development and Understanding of New Membranes Based on Aromatic Polymers and Heterocycles for Fuel Cells

by

Wen Li, B. S.; M. S.

Dissertation

Presented to the Faculty of the Graduate School of

The University of Texas at Austin

in Partial Fulfillment

of the Requirements

for the Degree of

Doctor of Philosophy

The University of Texas at Austin

August, 2009

Dedication

To my wife, son, and parents

Acknowledgements

I would like to express my deepest appreciation to my dissertation advisor, Dr. Arumugam Manthiram, for his supervision throughout the duration of this work. His guidance and encouragement have fostered independent thinking and individual initiative, yet he has always been available for consultation. I would also like to thank Drs. Christopher Bielawski, Benny Freeman, Paulo Ferreira, and Harovel Wheat for serving on my dissertation committee and providing helpful advice and support during this study.

I also wish to take this opportunity to thank past and present members of Dr. Manthiram's group for the exchange of ideas and friendship. It has been a great pleasure working with and learning from them during this work. In particular, I would like to thank Dr. Yongzhu Fu (former graduate student) and Dr. Jeong K. Lee (former postdoctoral follow) in Dr. Manthiram's group, for all their help. I would also like to thank Dr. Karalee Jarvis for her help with the TEM characterization.

Lastly, and most importantly, I wish to thank my wife, son, and parents, for all their support with endless love. It takes many efforts to finish this long course, and it would not have been possible without them.

This work was supported by Office of Naval Research MURI grant No. N00014-07-1-0758 and the Welch Foundation Grant No. F-1254.

Development and Understanding of New Membranes Based on Aromatic Polymers and Heterocycles for Fuel Cells

Publication No._____

Wen Li, Ph.D.

The University of Texas at Austin, 2009

Supervisor: Arumugam Manthiram

Direct methanol fuel cells (DMFC) are appealing as a power source for portable devices as they do not require recharging with an electrical outlet. However, the DMFC technology is confronted with the high crossover of methanol fuel from the anode to the cathode through the currently used Nafion membrane, which not only wastes the fuel but also poisons the cathode platinum catalyst. With an aim to overcome the problems encountered with the Nafion membrane, this dissertation focuses on the design and development of new polymeric membrane materials for DMFC and a fundamental understanding of their structure-property-performance relationships.

Several polymeric blend membranes based on acid-base interactions between an aromatic acidic polymer such as sulfonated ploy(ether ether ketone) (SPEEK) and an aromatic basic polymer such as heterocycle tethered poly(sulfone) (PSf) have been explored. Various heterochylces like nitro-benzimidazole (NBIm), 1*H*-Perimidine (PImd), and 5-amino-benzotriazole (BTraz) have been tethered to PSf to understand the

influence of pKa values and the size of the hetrocycles. The blend membranes show lower methanol crossover and better performance in DMFC than plain SPEEK due to an enhancement in proton conductivity through acid-base interactions and an insertion of the heterocycle side groups into the ionic clusters of SPEEK as indicated by small angle X-ray scattering and TEM data. The SPEEK/PSf-PImd blend membrane shows the lowest methanol crossover due to the larger size of the side groups, while the SPEEK/PSf-BTraz blend membrane shows the highest proton conductivity and maximum power density.

To further investigate the methanol-blocking effect of the heterocycles, *N*,*N*'-Bis-(1H-benzimidazol-2-yl)-isophthalamide (BBImIP) having two amino-benzimidazole groups bonded to a phenyl ring has been incorporated into sulfonated polysulfone (SPSf) and SPEEK membranes. With two 2-amino-benzimidazole groups, which could greatly increase the proton transfer sites, and three phenyl rings, which are compatible with the aromatic polymers, the BBImIP/SPSf and BBImIP/SPEEK blend membranes show suppressed methanol crossover and increased fuel cell performance in DMFC.

Novel sulfonated copolymers based on poly(aryl ether sulfone) (SPS-DP) that exhibit low methanol crossover have been synthesized and explored as a methanol-barrier center layer in a multilayer membrane configuration having SPEEK as the outer layers. These multilayer membranes exhibit better performance in DMFC than plain SPEEK and Nafion 115 membranes due to suppressed methanol crossover.

To address the issue of incompatibility between the new hydrocarbon-based membranes synthesized and the Nafion ionomer used in the catalyst layer in fabricating membrane-electrode assemblies (MEAs), the MEAs have been fabricated with the SPEEK membranes and 10 to 30 % SPEEK ionomer in the catalyst layer. These MEAs exhibit better performance in DMFC compared to the MEAs fabricated with the SPEEK membranes and Nafion ionomer in the catalyst layer due to lower interfacial resistance.

TABLE OF CONTENTS

LIST OF TABLES

LIST OF FIGURES

CHAPTER 1

Introduction

1.1 FUEL CELLS

The increasing worldwide energy consumption and the rapid depletion of fossil fuels (Fig.1.1) have created enormous interest in alternative energy sources such as solar, wind, nuclear, biofuels, and hydrogen. The ideal alternative energy source should be easily accessible, environmental friendly, and cost competitive compared to the existing energy supplies. In this regard, the fuel cell technology that employs hydrogen as a fuel has attracted much attention in recent years.

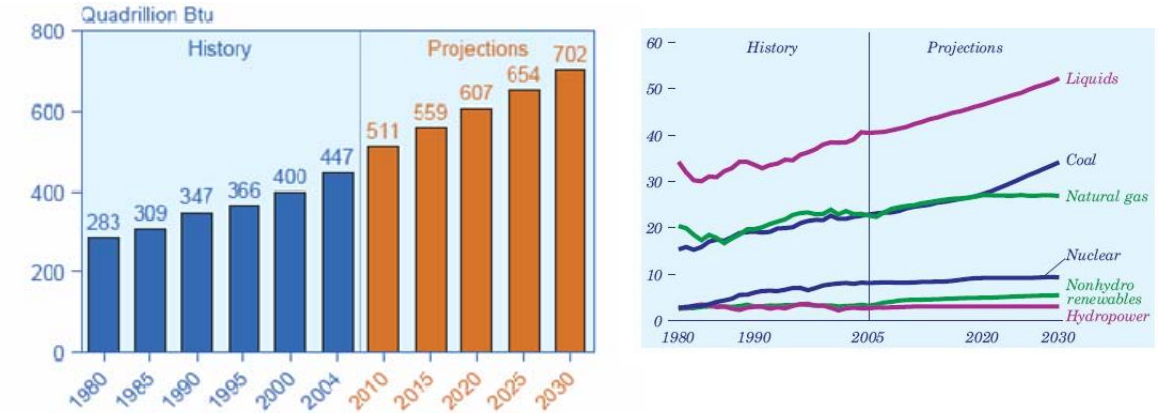

Figure 1.1: Worldeide energy consumption and energy consumption from various sources (1980-2030) [1].

Fuel cells are energy conversion devices, which convert the chemical energy stored in a fuel directly into electrical energy. They have higher conversion efficiency and less emission compared to the traditional combustion engines. When pure hydrogen

and oxygen are used as fuel and oxidant respectively, zero emission could be achieved as water is the only product in the reaction.

Like other electrochemical devices, a fuel cell consists of a positive electrode (cathode), a negative electrode (anode), and an ion-conducting electrolyte. The production of electricity by the fuel cells involves the oxidation of a fuel and the reduction of an oxidant, which are fed, respectively, into the anode and cathode compartments. This process generates ion flow through the electrolyte and electron flow through the external circuit. Unlike a battery, a fuel cell can continue to provide power as long as the fuel and oxidant are available. In contrast, a battery is an energy storage device, which chemically stores electrical energy during charging and provides electricity during the discharging process.

1.1.1 Major Types of Fuel Cells

Based on the type of electrolyte used, five major types of fuel cells have been widely investigated: (i) proton exchange membrane fuel cell (PEMFC), (ii) alkaline fuel cell (AFC), (iii) phosphoric acid fuel cell (PAFC), (iv) molten carbonate fuel cell (MCFC), and (v) solid-oxide fuel cell (SOFC). While all the five fuel cell types are based on the same electrochemical principles, they operate at different temperatures, incorporate different materials, and often differ in their fuel tolerance and performance characteristics. Table 1.1 provides an overview of the key characteristics of these major types of fuel cells, while Fig. 1.2 provides a convenient graphical summary [2-5].

Table 1.1: Comparison of the characteristics of the five major types of fuel cells.

	PEMFC&DMFC	AFC	PAFC	MCFC	SOFC
Electrolyte	Proton exchange membrane	Potassium hydroxide in asbestos matrix	Phosphoric acid in SiC	Molten carbonate in $LiAlO_2$	Ceramic oxide ion conductor
Electrode	Carbon	Transition metals	Carbon	Nickel and Nickel oxide	Oxide, oxide/metal cermet
Operating Temperature	50 – 130 ^oC	50 – 250 ^oC	180 – 200 ^oC	650 ^oC	600 – 1000 ^oC
Charge Carrier	H^+	OH^-	H^+	CO_3^{2-}	O^{2-}
Catalyst	Pt/PtRu	Pt	Pt	Electrode material	Electrode material
Fuel	Pure or reformed H_2 / CH_3OH	H_2 and CH_3OH	Reformed H_2	Reformed H_2 and CH_4	Reformed H_2 and hydrocarbons
CO Tolerance	Poison (<50 ppm)	Poison (<50 ppm)	Poison (<1 %)	Fuel	Fuel
Electrical Efficiency (%)	40-50	50	40	45-55	50-60
Power Density (mW/cm^2)	300-1000	150-400	150-300	100-300	250-350
Internal Reforming	No	No	No	Yes	Yes
Power Range (kW)	0.001-1000	1-100	50-1000	100-100,000	10-100,000
Major Applications	Portable, Transportation, Stationary	Space, Stationary, Transportation	Stationary	Stationary, Transportation	Stationary, Transportation
Balance of Plant	Low-moderate	Moderate	Moderate	Complex	Moderate

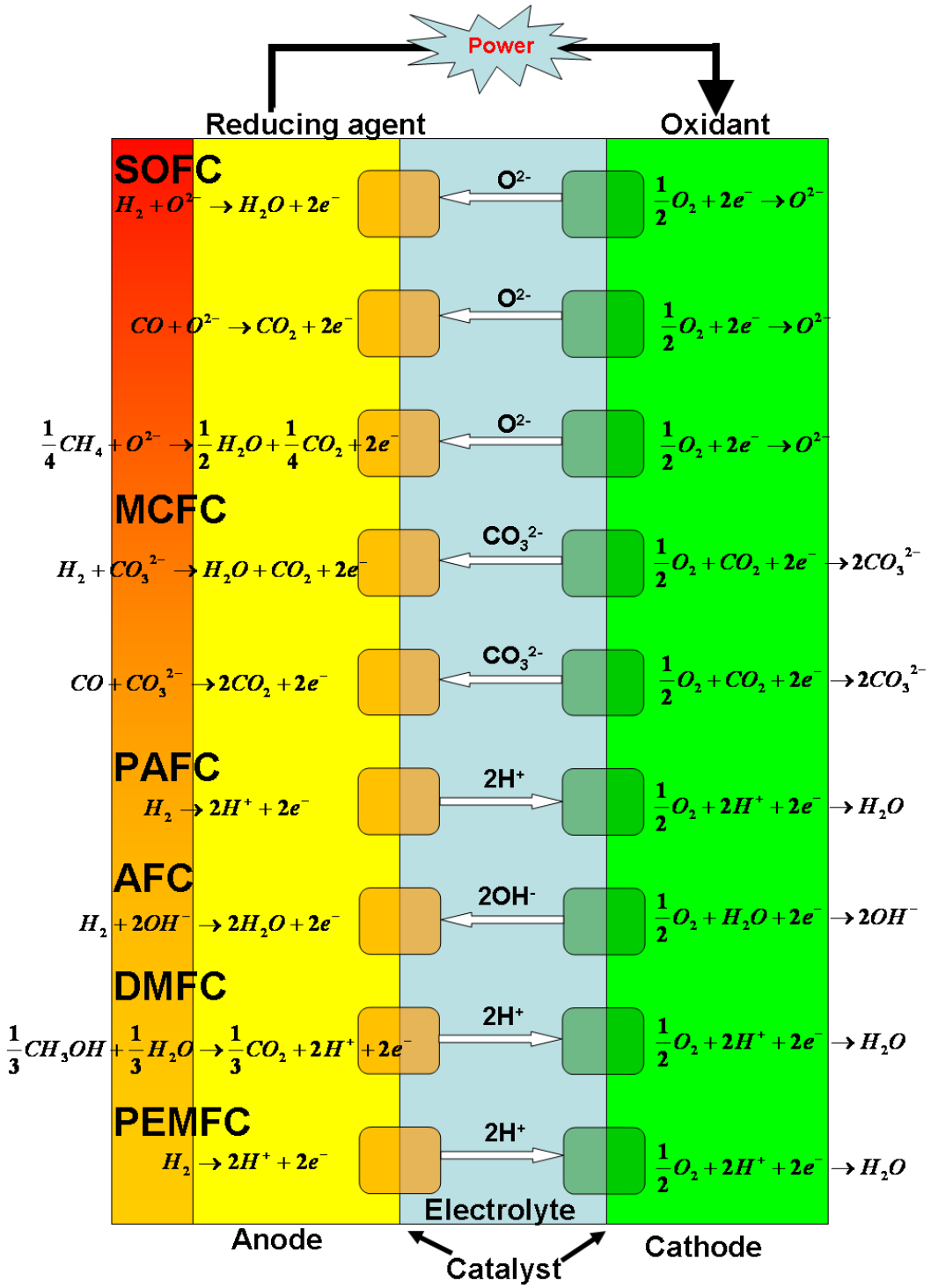

Figure 1.2: Graphical summary of major types of fuel cells.

While both PAFCs and AFCs benefited from early historical development, the other fuel cell types have caught up in recent years and have become more appealing in the long run. Among the five primary fuel cell types, PEMFCs and SOFCs offer great potential for widespread practical applications. For instance, they can be applied for residential power and other small-scale stationary power applications. The high-temperature fuel cells (SOFC and MCFC) offer some advantages like high efficiency and good fuel flexibility. They also generate higher-quality waste heat, which can be used in combined heat and power applications. While all the fuel cells operate best on hydrogen, these higher-temperature fuel cells offer improved impurity tolerance and the possibility for internal reforming of hydrocarbon fuels to yield hydrogen. However, the high-temperature fuel cells suffer from disadvantages like slow startup time and thermal degradation [6]. On the other hand, low-temperature fuel cells such as PEMFC and DMFC are widely considered as the most promising types of fuel cells for portable, transportation, and stationary applications due to their high energy/power density, low operating temperature, absence of liquid electrolyte, and easy maintenance [2].

1.1.2 Proton Exchange Membrane Fuel Cell (PEMFC) and Direct Methanol Fuel Cell (DMFC)

1.1.2.1 Proton Exchange Membrane Fuel Cell (PEMFC)

Proton Exchange Membrane Fuel Cell (PEMFC), which uses pure hydrogen as the fuel and oxygen/air as the oxidant, is a promising power source for transportation and stationary applications due to its high power density, rapid startup, quick response to power demand, and low emission. The electrochemical reactions with their standard-state potential involved in the PEMFC are given below:

Anode reaction: $H_2 \rightarrow 2H^+ + 2e^-$ $E^o = 0.00V$ (1.1)

Cathode reaction: $\frac{1}{2}O_2 + 2H^+ + 2e^- \rightarrow H_2O$ $E^o = 1.23V$ (1.2)

Overall reaction: $\frac{1}{2}O_2 + H_2 \rightarrow H_2O$ $E_{cell}^{\ o} = 1.23V$ (1.3)

In PEMFC, hydrogen is supplied as a fuel into the anode side and oxidized to protons and electrons on the surface of the catalyst. While the electrons flow through the external circuit, the protons are transported through the electrolyte to the cathode side. The oxygen or air is supplied as the oxidant into the cathode side and reduced with protons on the surface of the catalyst to produce water. The overall reversible cell potential for a PEMFC is 1.23 V at the standard state.

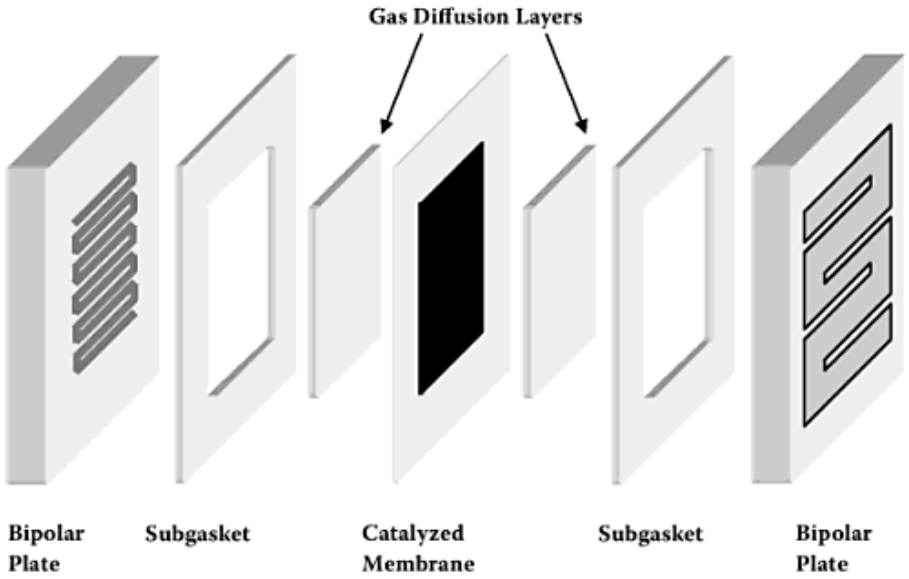

Figure 1.3: Schematic view of a proton exchange membrane fuel cell and a seven-layer membrane-electrode assembly (MEA) [7].

Fig.1.3 is a schematic view of a typical PEMFC. The main component of a PEMFC is the membrane-electrode assembly (MEA) which usually refers to a five-layer structure. It includes a cathode gas diffusion layer (GDL), a cathode catalyst layer, a

proton conducting membrane, an anode catalyst layer, and an anode GDL. Recently, a set of subgaskets are also included in the MEA, which is usually referred as seven-layer MEA.

The GDL is usually prepared by depositing a mixture of carbon powder and polytetrafluoroethylene (PTFE) onto a carbon paper or carbon cloth. The carbon materials provide electronic conductivity for the GDL, while the PTFE helps to adjust the hydrophobicity of the GDL, ensuring fast liquid and gas transfer during cell operation. The catalyst layers on both the anode and cathode sides in a typical PEMFC are the same, which consist of carbon-supported Pt catalyst and Nafion dispersion. By combining the carbon/Pt/Nafion together in this layer, good electrochemical activity, electronic conductivity, and proton conductivity could be achieved in the electrode.

The proton exchange membrane is one of the main components in the MEA. Naifon (product of Dupont) membrane is currently used in PEMFC due to its high proton conductivity and good resistance to chemical attack. In addition, as a solid electrolyte, the cell using the solid polymer membrane is much easier to seal compared to the cells with liquid electrolyte such as that in an MCFC. Also, the better corrosion resistance of the Nafion membrane leads to better durability for PEMFC compared to the other types of fuel cells.

1.1.2.2 Direct Methanol Fuel Cell (DMFC)

Direct methanol fuel cell (DMFC) is a promising power source for portable electronic devices. Because the liquid methanol is fed directly into the fuel cell, steam reforming of the fuel is not required and methanol is much easier to store compared to hydrogen, which needs high pressure or low temperature. Also, the energy density of methanol is much higher than that of compressed hydrogen. The electrochemical reactions with the standard-state potentials involved in DMFC are given below:

Anode reaction: $CH_3OH + H_2O \rightarrow CO_2 + 6H^+ + 6e^-$ $E^o = 0.03V$ (1.4)

Cathode reaction: $\frac{3}{2}O_2 + 6H^+ + 6e^- \rightarrow 3H_2O$ $E^o = 1.23V$ (1.5)

Overall reaction: $CH_3OH + \frac{3}{2}O_2 \rightarrow CO_2 + 2H_2O$ $E_{cell}^{\ o} = 1.20V$ (1.6)

In DMFC, MEA is also a key component, which is very similar to that in a PEMFC as shown in Fig. 1.4. Methanol is supplied as a fuel into the anode side and oxidized to protons, electrons, and carbon dioxide in the presence of water. While the electrons flow through the external circuit, the generated protons move from the anode to the cathode through the proton conducting electrolyte. At the cathode side, the supplied oxygen or air is reduced with protons to produce water. The overall reversible potential of a DMFC is 1.20 V under standard conditions, which is very similar to that in PEMFC.

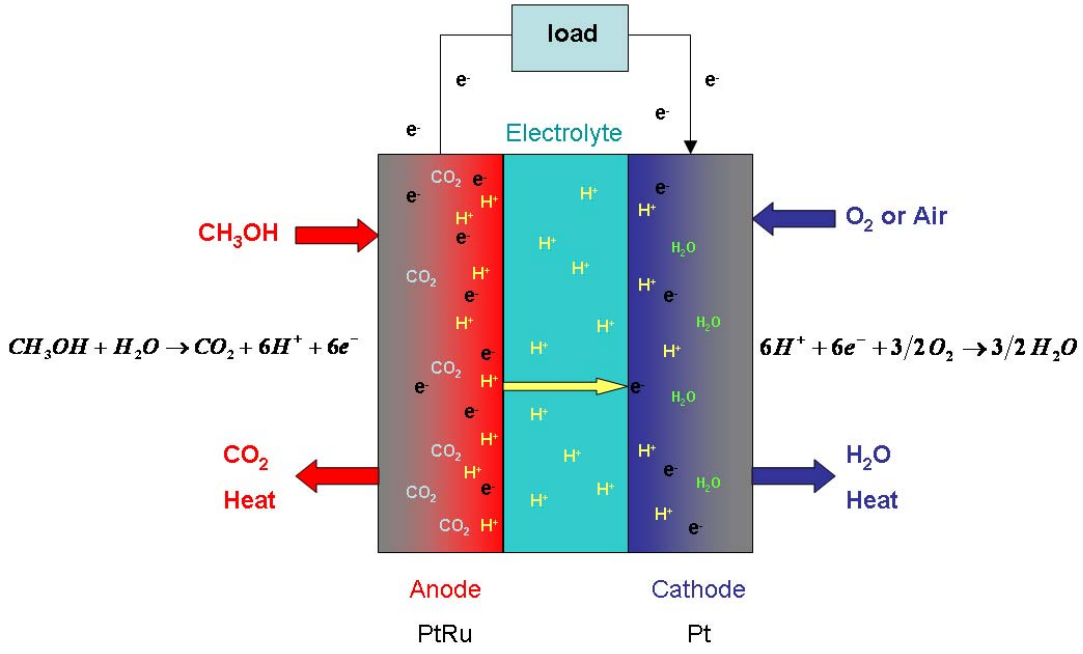

Figure 1.4: Schematic representation of a direct membrane fuel cell.

Unlike in PEMFC, the anode catalyst in DMFC is carbon-supported PtRu or PtRu black, while carbon-supported Pt or Pt black serve as the cathode as in PEMFC. Also, the catalyst loading in DMFC is much higher (1-10 mg/cm^2) to overcome the poor kinetics of the methanol oxidation reaction and oxygen reduction reaction. The high catalyst loading on the cathode side is also due to the high methanol permeation from the anode side to the cathode side during fuel cell operation. The methanol crossover poisons the Pt catalyst, wastes fuel, and generates undesired mix-potential at the cathode resulting in performance loss [8,9]. All these problems mentioned above are hampering the commercialization of the DMFC technology.

1.1.3 Challenges in PEMFC and DMFC Technologies

Since the discovery of proton exchange membrane fuel cells in the early 1960s [10], a lot of efforts have been made on the research and development of the PEMFC and DMFC technologies. However, several challenges still need be overcome before fuel cells can become a successful and competitive alternative energy technology. The research related to PEMFC and DMFC are focused on overcoming the following challenges: cost, safety, extreme condition operation, competitiveness with other technologies, and hydrogen storage and transportation. Interestingly, most of these challenges are related to the materials employed, especially the catalysts and proton exchange membranes.

1.1.3.1 Challenges of Electrocatalysts

Platinum is by far the most effective catalyst used jn PEMFC and DMFC. Nearly all the current PEMFC and DMFC use pure platinum to catalyze the oxygen reduction reaction (ORR) and hydrogen oxidation reaction (HOR). However, due to its high cost and low catalyst activity for ORR at low temperatures, current platinum-based catalysts

are not feasible for commercial applications. In order to lower the cost of fuel cells, researchers have reduced the platinum loading in PEMFC from 4 mg/cm^2 to 0.35 mg/cm^2 by optimizing the catalyst structure and particle size of the platinum catalyst during the past decades. The development of carbon-supported platinum (Pt/C) catalyst is a typical example. By depositing the platinum particles (2 ~ 4 nm size) onto porous conducting carbon, the platinum utilization efficiency is greatly improved. In late 1980s', researchers from Las Alamos Nation Laboratory also developed a novel MEA fabrication strategy: by depositing Pt/C catalyst directly onto the proton exchange membrane, the catalyst utilization efficiency is further improved, the catalyst loading is further decreased to 0.1 mg/cm^2 while maintaining a good fuel cell performance [11-14]. The efficiency of platinum by this method is about ten times higher than that of the electrodes produced by conventional methods.

Another strategy to reduce the catalyst loading is to increase the catalyst activity by alloying platinum with other elements [15-19]. The evolution of Pt alloys in PEMFC was carried out by Mukerjee et al. [15] in the early 1990s. Various binary PtM (M = Ni, Cr, Co) alloys with Pt_3M ordered structure have been found to show enhanced catalytic activity for ORR in PEMFC. Later, Shim et al.[16] prepared Pt-Fe-M (M = Cr, Mn, Co, Ni, Cu) ternary alloys and tested in PEMFC. Also, different binary PtM (M = Co, Cr, Ni) and ternary Pt-Co-M (M = Cr, Ni) alloys have been prepared and the ordered Pt-Co exhibits the best performance among all the samples evaluated [17]. Shukla et al. [19] prepared Pt-Fe alloys and tested in DMFC. The ordered Pt-Fe alloy shows higher catalytic activity for ORR than Pt in DMFC. Meanwhile, lots of effects have also been made on the research and development of non-platinum based catalysts for ORR such as transition metal oxides and sulfides [21-24], metal carbides [25], and non-platinum based metal alloys [26-29].

The catalytic activity for methanol oxidation reaction (MOR) has also been extensively studied for many years. Various PtM (M = Ru, Sn, Os, Ir, Mo, W, Cu, Zn, Cd, In, Ti, Cr, Mn, Fe, Co, and Ni) alloys have been investigated in the literature and Pt-Ru alloy shows the best catalytic activity for methanol oxidation [30, 31]. Meanwhile, there are also a lot of interests on the various other MOR catalysts such as Pt/transition metal oxide composite materials and Pt/perovskite type oxides materials [32-35].

In summary, despite five decades of research, up to now the most active electrocatalysts for ORR and MOR are the expensive Pt, Pt-based alloys, or their composites. Non-platinum based electrocatalyts are less expensive, but the activity of these catalysts is lower than that of Pt-based electrocatalyts.

1.1.3.2 Challenges of Membranes

In the early 1960's, sulfonated polystyrene membranes were first used as electrolytes in PEMFC, but they were replaced in 1966 by the Nafion membrane, which has been proved to be superior in performance and durability to sulfonated polystyrene for more than 40 years.

Nafion membrane shows the advantages of high proton conductivity and stability under harsh chemical and physical environments. However, since proton conduction in Nafion depends on the water content in it, the operating temperature of the fuel cell is limited by the boiling point of water. Also, a complex humidification system is required to maintain good fuel cell performance. In addition, the high methanol permeability is also a huge barrier for the commercialization of DMFC.

Regarding the challenges discussed above, there is great interest in developing novel proton exchange membranes for PEMFC and DMFC. The following section will discuss in detail the status of membrane studies.

1.2 PROTON EXCHANGE MEMBRANES IN FUEL CELLS

Proton exchange membrane (PEM) plays a critical role in the performance as well as long-term stability of PEMFC and DMFC. Although varying depending on the applications, common requirements of a proton exchange membrane in PEMFC and DMFC include: (i) high proton conductivity, (ii) poor electronic conductivity, (iii) low cost, (iv) low permeability of fuels and oxidants through the membrane, and (v) high chemical and mechanical durability. In addition, a low ruthenium crossover is also required for DMFC where PtRu alloy is used as the anode catalyst [36].

1.2.1 Poly(perfluorosulfonic acid) (PFSA) Membranes

Many efforts have been made on the research and development of poly(perfluorosulfonic acid) (PFSA) membranes such as Nafion (Dupont), Aciplex (Asahi Chemical company), Flemion (Asahi Glass Company), and XUS (Dow Chemical) due to their high proton conductivity and good resistance to chemical attack resulting in good performance durability (> 6000 h in PEMFC for Nafion) [36, 37]. The chemical structures of some PFSA membranes are shown in Fig. 1.5.

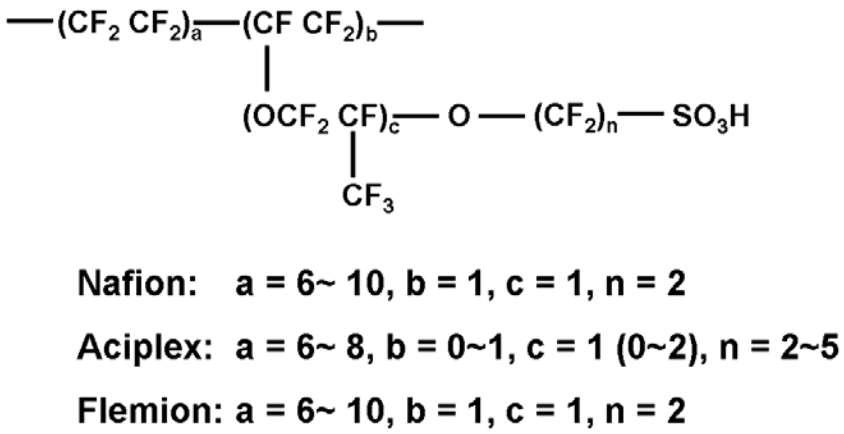

Figure 1.5: Chemical structures of poly(perfluorosulfonic acid) membranes.

Nafion is the most investigated PFSA membrane and widely used in PEMFC and DMFC currently. The proton and water transport properties of Nafion could be well explained by the cluster-network model (Fig. 1.6) based on the small-angle X-ray scattering (SAXS) and wide-angle X-ray diffraction (WAXD) studies on its structure [38]. The hydrophobic polytetrafluoroethylene (PTFE) backbone of PFSA polymers provides thermal and chemical stability and forms a hydrophobic crystal region, while the perfluorinated side chains terminating with hydrophilic sulfonic acid groups ($-SO_3H$) form a hydrophilic region (clusters and channels). The clusters formed by the absorbed water and side chains are around 4 nm wide, which are periodically arranged among the hydrophobic region. The distance between the clusters is around 5.0 nm, and the clusters are connected by channels with a diameter of 1 nm.

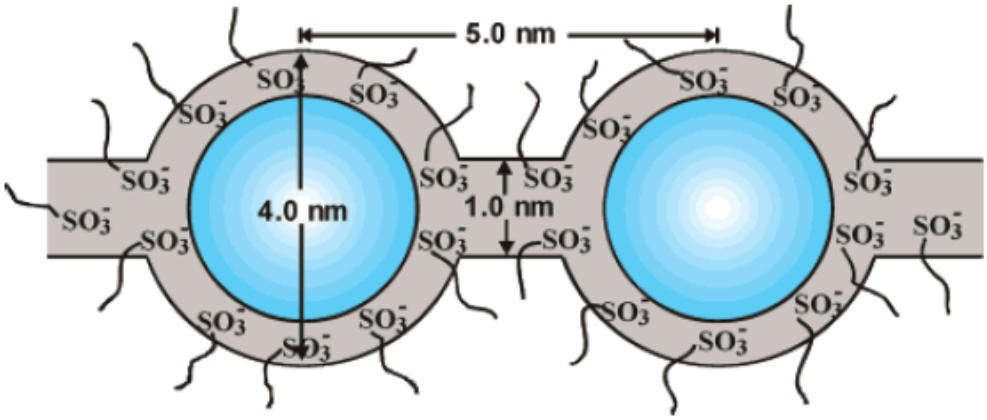

Figure 1.6: Cluster network model for the morphology of hydrated Nafion membranes [38].

As mentioned above, Nafion shows several advantages, but there are a few disadvantages when applying Nafion membrane in PEMFC and DMFC.

(1) Low operating temperature: The proton conductivity of Nafion membrane decreases dramatically when the water content decreases in the membrane [39, 40]. In order to maintain high proton conductivity, Nafion membrane is required to be saturated

in water during cell operation. So the operating temperature of PEMFC is limited to <100 ^{o}C at ambient pressure, and a complex humidification system is required to control the moisture of both the membrane and electrodes.

However, as shown Fig. 1.7, an operating temperature >120 ^{o}C is desired to maximize the catalyst activity and minimize the poisoning effect of CO on the Pt catalyst surface. Therefore, a low operating temperature will decrease the catalytic activity and increase the cost of purifying hydrogen to reach a low CO level (< 10 ppm) [41].

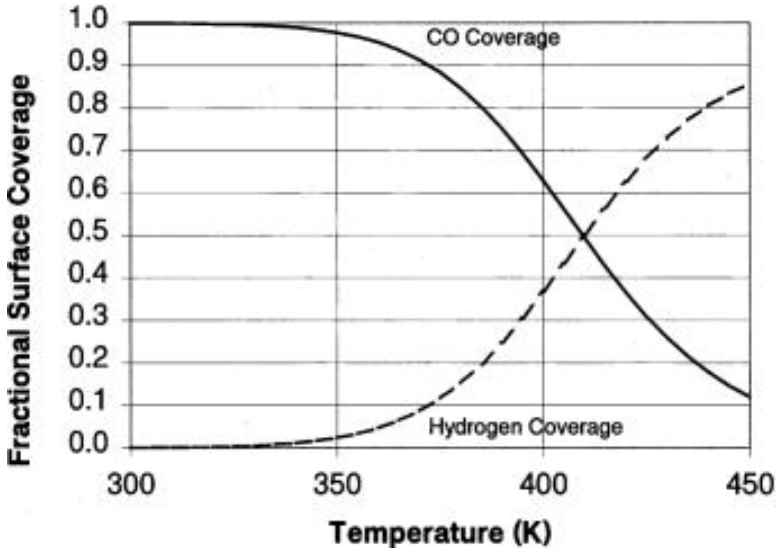

Figure 1.7: Langumuir-type adsorption of H_2 and CO on a smooth platinum surface as a function of temperature. These adsorption isobars are computed for 100 ppm CO in 1 bar H_2, based on the adsorption equilibrium constants for CO and H on Pt (111) surfaces [41].

(2) High methanol crossover in DMFC: Another problem in applying Nafion in DMFC is the high methanol permeability. During the cell operation, the methanol fuel migrates from the anode to the cathode side through the membrane by means of (i) active transport along with the protons and their solvated water (electro-osmotic drag) and (ii) diffusion through the Nafion membrane itself due to concentration gradient [42, 43]. The

methanol permeability not only wastes the fuel but also leads to an undesired reaction taking place at the cathode platinum catalyst, resulting in a severely reduced overall cell performance. Meanwhile, higher Pt catalyst loading on the cathode side is also required to overcome the oxidation of methanol crossover through the membrane, resulting in a higher cost of DMFC [44, 45].

(3) High cost: The average cost of Nafion membrane is \$600 - 1000/m^2 [46, 47], which contributes significantly to the overall cost of PEMFC and DMFC. The high cost of Nafion membrane is associated with the complicated processing procedure of perfluorinated monomers. In DMFC, a thicker Nafion membrane is required to minimize the methanol crossover, which will further increase the membrane cost.

These difficulties associated with the Nafion membranes have attracted enormous interests to develop alternative membranes that offer a higher operating temperature (T > 120 ^{o}C) and/or lower methanol permeability with low cost. In the rest of this chapter, the approaches to develop lower methanol permeable membranes will be discussed mainly. Before discussing the details of these approaches, it would be helpful to understand the mechanisms involved in proton conduction.

1.2.2 Proton Conduction Mechanism

Two types of proton conduction mechanisms are involved in the proton exchange membranes, vehicle-type and Grotthuss-type (hopping) mechanisms which are illustrated in Fig.1.8 [48, 49].

In the vehicle mechanism, the proton movement occurs with the aid of moving carriers (vehicle) such as water (H_3O^+ and $H_5O_2^+$) or other proton solvent (imidazole). The overall proton conductivity is mainly determined by the diffusion coefficient of the vehicles.

In the Grotthuss-type mechanism, the protons are passed through hydrogen bonds (proton hopping). The movement of the proton solvent is not needed, but the reorganization of the proton environment consisting of reorientation of individual species or even more extended ensembles is necessary for the formation of an uninterrupted path for proton migration. The proton transfer and reorganization rate of its environment affect directly this mechanism.

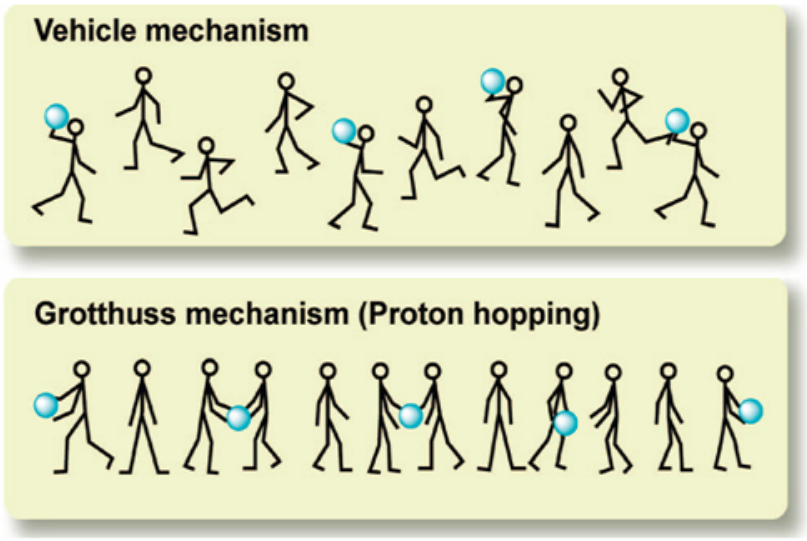

Figure 1.8: Illustration of proton transport mechanisms. Top: Vehicle mechanism; Bottom: Grotthuss mechanism [50].

These two proton conduction mechanisms are correlated. In all the sulfonated or phosphonated proton exchange membranes, the vehicle-type mechanism is predominant while the Grotthuss-type mechanism is also present. In the polybenzimidazole-doped system, the Grotthuss-type mechanism is dominant and vehicle-type mechanism is present as well. Generally, both mechanisms can be present and make differing contributions to proton conduction [51].

1.2.3 Proton Exchange Membranes with suppressed Methanol Crossover

High methanol crossover of the PFSA membranes like Nafion is a critical issue for DMFC. A proton exchange membrane with reduced methanol permeability is desirable to improve the cell performance and lower the cost of DMFC. The strategies employed to suppress methanol crossover are discussed below.

1.2.3.1 Modification of Nafion Membrane

Modification of the currently used Nafion membranes is an effective strategy to lower methanol crossover in DMFC. The modification is mainly focused on changing the distribution of the clusters in Nafion by incorporating or blending it with other inorganic/organic additives.

Silica modified Nafion: Incorporation of organic Si or inorganic silica additives into Nafion membrane is a widely used approach to modify Nafion membrane for DMFC applications. Nafion-slica membranes were prepared by solution casting of the mixtures of Si source and Nafion solutions. The nano-sized silica particles in the casting membranes could effectively block the migration of methanol through the membrane [52-54].

Cs^+ doped Nafion: The proton and methanol transport phenomena in Cs-doped Nafion membranes were studied by Tricoli [55]. The cesium-doped Nafion membranes were found to be highly impermeable to methanol. Also, the methanol permeability in the membrane was reduced by one order of magnitude due to the presence of cesium ion. The partially doped membranes retained good proton conductivity as well.

Metal-impregnated Nafion: Jiang et al. [56] reported that impregnating Pd nano-particles into Nafion membrane could lower methanol crossover resulting in the increased fuel efficiency and deceased cathode catalyst poisoning. Jung et al. [57] also studied the PtRu doped Nafion in DMFC, and it was found that small amount of PtRu in Nafion acts

as a methanol barrier through the chemical oxidation of methanol on PtRu particles in the membrane, which helps to lower the methanol crossover. However, proton conductivity of the metal-impregnated Nafion membranes decreased with increasing amount of impregnated metal particles.

Polymers composite Nafion membranes: Polymers such as polyfurfuryl alcohol (PFA)[58], poly(vinylacohol) (PVA)[59], polypyrrole [61-64], and poly(3,4-ethylenedioxythiophene) (PEDO) [60] have been chemically and electrochemically added with Nafion to form blend membranes. The resulting polymer composite membranes have been studied by methanol permeability and proton conductivity measurements. The presence of the polymers in the cluster destroys the distribution of sulfonic acid groups and blocks methanol crossover through the membrane. But it also blocks the proton conduction channels in the membrane, resulting in a decrease in the proton conductivity of the membranes.

Surface modification of Nafion: By applying a plasma [65] or an electron beam [66], the surface structure of Nafion membrane could be changed. A thin methanol barrier layer on the surface was created after the modification, resulting in a much suppressed methanol crossover and up to 50 % increase in the power output in DMFC compared to the use of plain Nafion membrane.

Although these approaches could reduce methanol crossover, they generally tend to decrease proton conductivity and some times lead to a loss in mechanical strength. In view of this, there has been considerable interest to develop new membrane materials that can suppress methanol crossover while offering acceptable proton conductivity.

1.2.3.2 Sulfonated Aromatic Polymer Membranes

Among the various polymer materials being investigated, aromatic polymers are a family of materials with high glass transition temperature, high thermal stability, good

mechanical properties, and excellent resistance to hydrolysis and oxidation. Accordingly, aromatic polymers attached with sulfonic acid groups have been widely investigated as candidates to substitute PFSA membranes in DMFC.

1.2.3.2.1 Sulfonation of Commercially Available Polymers

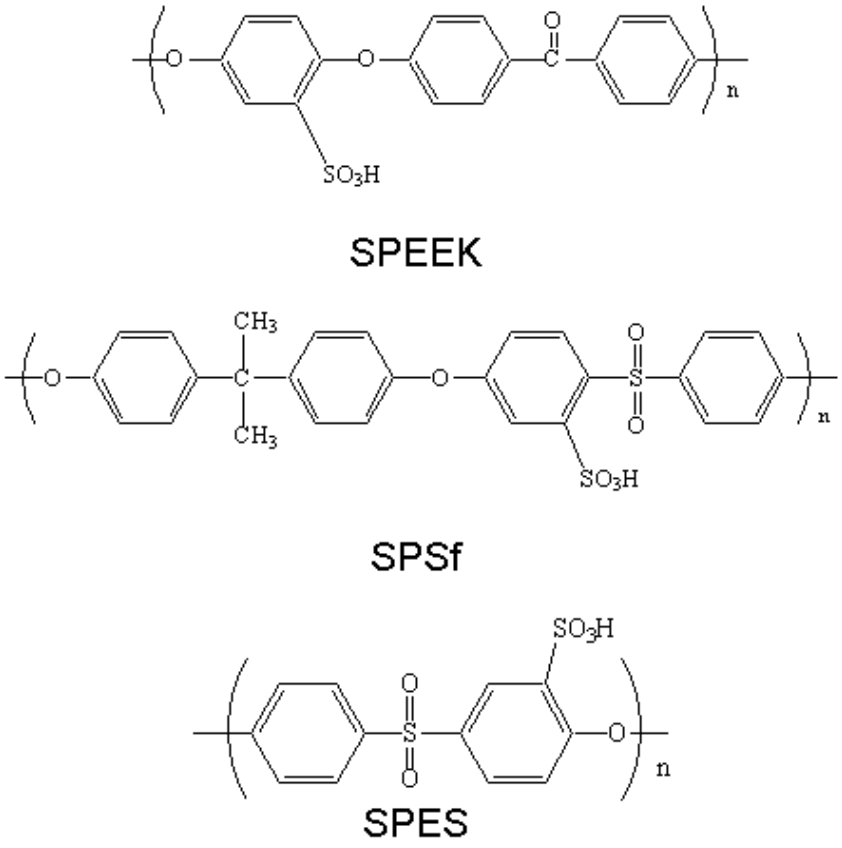

Figure 1.9: Chemical structures of some sulfoanted polymers. SPEEK: sulfonated poly (ether ether ketone), SPSf: sulfonated polysulfone, SPES: sulfonated poly(ethersulfone).

Sulfonated derivatives of commercially available aromatic polymers are among those being actively investigated due to the easy access of the low cost precursors. Sulfonated poly(ether ether ketone) (SPEEK) [66,67], sulfonated polysulfone (SPSf) [69-

71], and sulfonated poly(ether sulfone) (SPES) [72-75] are some of the examples. The structures of the sulfonated aromatic polymer are shown in Fig. 1.9.

The properties of the sulfonated polymers are mainly controlled by the degree of sulfonation (DS). The DS could be controlled by the reaction time, temperature, and amount of sulfonating agent (H_2SO_4, SO_3, chlorosulfonic acid) used in the reaction. Also, the simple sulfonation reaction procedure could be easily scaled up. The proton conductivity, water swelling, methanol permeability, and DMFC performance of these membranes have been investigated. All these sulfonated polymers with appropriate DS showed suppressed methanol permeability and decent proton conductivity in DMFC.

1.2.3.2.2 Polymerization reaction of sulfonated monomers.

Sulfonated aromatic polymers could also be synthesized through polymerization reaction from different monomers bearing sulfonic acid groups [76-82]. With this strategy, several proton exchange membranes with controllable chemical structures (degree of sulfonation and sulfonation sites) and well-refined microstructure have been investigated, *e.g.*, sulfonated polyimide (SPI) [83-85], sulfonated polyphenylene (SPPO) [86-88], sulfonated poly(aryl ether)s (SPAEs) [89,90], and sulfonated poly(ether ketone) (SPEK) [91,92]. By changing the monomers used in the polymerization reactions, the properties of the product polymers could be tuned, and some fundamental understanding of the structure-property-performance relationships have been achieved.

For example, Dr. Michael Guiver's group at the National Research Council of Canada investigated a serious of sulfonated poly(ether ketone) polymers with pendant phenyl structures as shown in Fig.1.10. The SPEK polymers exhibited several advantages in the synthesis and physical properties over the typical post-sulfonated polymers, such as rapid and mild reaction conditions, high molecular weights, site specificity, and easy control over IEC. The swelling stability, methanol permeability, and proton conductivity

of the SPEKs are tunable by changing the polymer structures. It was also found that to improve the osmotic and hydrolytic stability of the sulfonated polymers, the increasing hydrophilic-hydrophobic separation is desired by locating the sulfonic acid groups away from the polymer main chains [92].

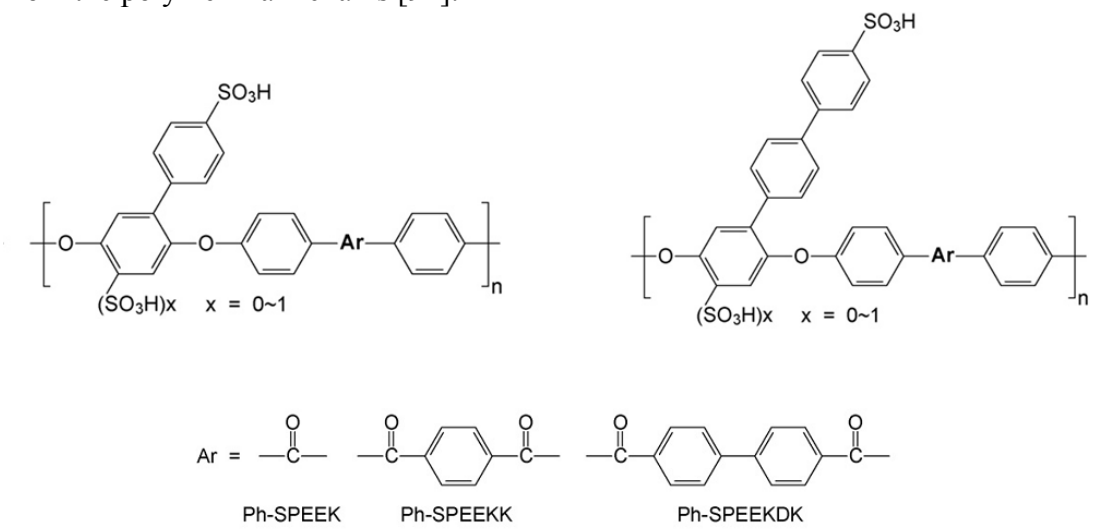

Figure 1.10: Structures of sulfonated poly(ether ketone) (SPEK) polymers [92].

Usually, the sulfonated aromatic polymers showed lower methanol crossover than the PFSA membranes due to their more rigid backbone compared to the PTFE backbone in Nafion type membranes. Using SPEEK as an example, based on the SAXS data and a microstructure model established by Keuer [93], the cluster size in SPEEK is smaller than that in Nafion membrane as shown in Fig. 1.11. The stronger confinement of water in the narrow channels of the aromatic polymers leads to a significantly lower dielectric constant of water, resulting in much lower methanol crossover compared to that with Nafion membrane.

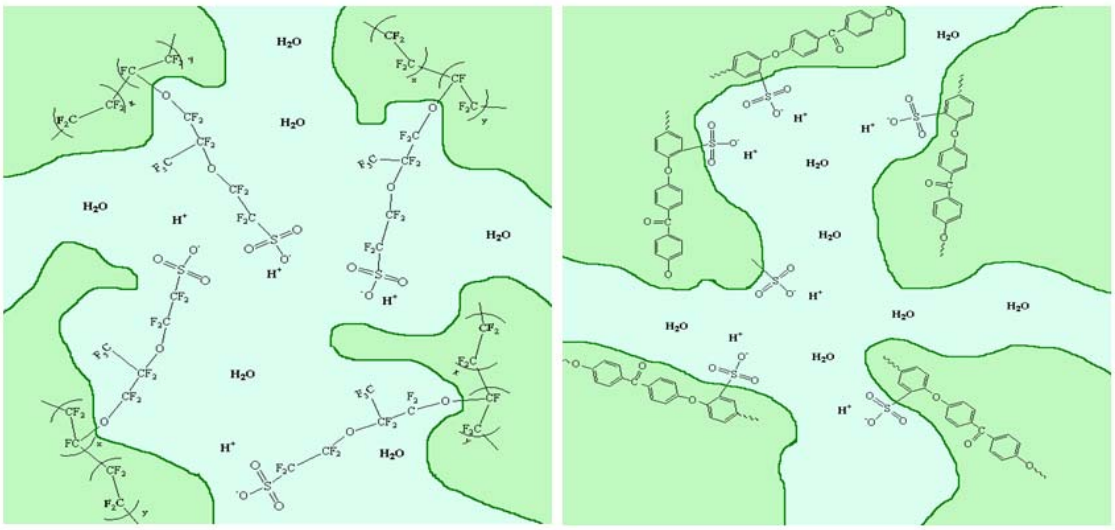

Figure 1.11: Schematic representation of the microstructures of (a) Nafion and (b) SPEEK membranes.

However, due to the lower acidity of the sulfonic acid groups in aromatic membranes (pKa ~ -1) compared to that in Nafion membranes (pKa ~ -6), the proton conductivity of these membranes is usually lower than that of Nafion. In order to maximize the proton conductivity, high degree of sulfonation (DS) is desired, which often leads to an increase in membrane swelling and degradation in mechanical stability.

1.2.3.3 Cross-Linked Polymer Membranes

Various strategies have been investigated in order to reduce the swelling of the sulfonated polymers with high DS. Covalent/ionic cross-linking is found to be an effective way to control the dimensional stability and suppress methanol crossover of the proton exchange membrane without scarifying the proton conductivity too much.

1.2.3.3.1 Covalent Cross-linked Membranes

Cross-linked sulfonated divinylbenzene polystyrene was synthesized and studied by D'Alelio in the 1940s [94]. However, the cross-linked polymer was found to have insufficient chemical stability due to easy attack by oxygen.

Later, covalent cross-linking procedure for SPSf was investigated through different synthesis strategies. Nolte [95] presented the synthesis approach to transfer part of the SO_3H groups to sulfonyl-N-imidazolide groups, followed by reaction with 4,4'-diaminodiphenylsulfone to form sulfonamide cross-linking bridges. Kerres' group [96-98] has also reported a novel cross-linking process consisting of the alkylation of sulfinate groups with α,ω-dihalogenoalkanes.

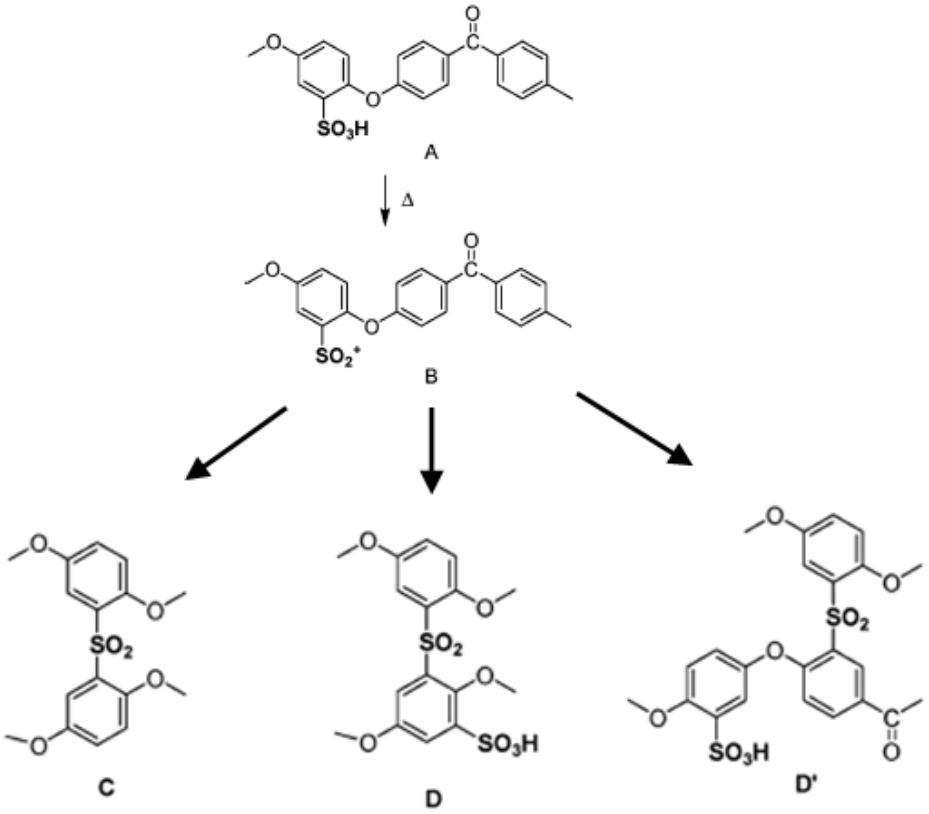

Figure 1.12: Schematic structures of the cross-linked SPEEK membranes [99].

Recently, other covalent cross-linked sulfonated aromatic polymers with high DS have also been reported [99-101]. For example, Vona et al. [99] studied the properties of the covalent cross-linked SPEEK with high DS (Fig. 1.12), and the resulting membrane showed much better swelling stability and lower methanol permeability compared to the uncross-linked polymers.

Usually, the thermal stability of these covalently cross-linked polymers is quite high (230 ~ 270 ^{o}C). However, the polymers with covalent cross-linking become brittle after drying, which is a critical problem for fuel cell applications. The brittleness is possibly caused by the inflexibility of the covalent networks. Because of this reason, more and more attention is being paid toward the development of ionomer networks containing ionic cross-links that are more flexible.

1.2.3.3.2 Ionic Cross-linked Membranes

Ionic cross-linked membranes were first investigated with anhydrous polymeric proton conductors like polybenzimidazole (PBI) as shown in Fig. 1.13 [102-104]. Unlike the polymers containing sulfonic acid groups, the nitrogen sites on the heterocylces in PBI act as proton donors and acceptors, which facilitate the protons transfer through Grotthuss-type mechanism. Due to the slow rate of the proton transfer facilitated by the Grotthuss-type mechanism at low temperature, usually the operation temperature of these kinds of membranes is higher than that of sulfonated polymers.

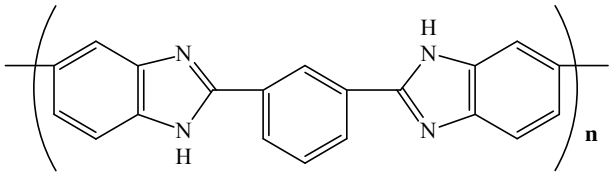

Figure 1.13: Structure of polybenzimidazole polymers (PBI).

In 1995, Wainright et al. [95] proposed a blend of PBI and phosphoric acid as the electrolyte for PEMFC and DMFC for the first time. The intrinsic property of phosphoric acid and ease in preparing the blends with a large variety of polymers drew more and more attention after this investigation [105-109]. In this type of acid-doped PBI membranes, nitrogen sites on the heterocylces exhibit basic properties, and they are also termed as acid-base blend membranes. The strong acid-base interactions and the hydrophobicity of the basic polymers could promote proton conduction and block methanol permeation through the membrane.

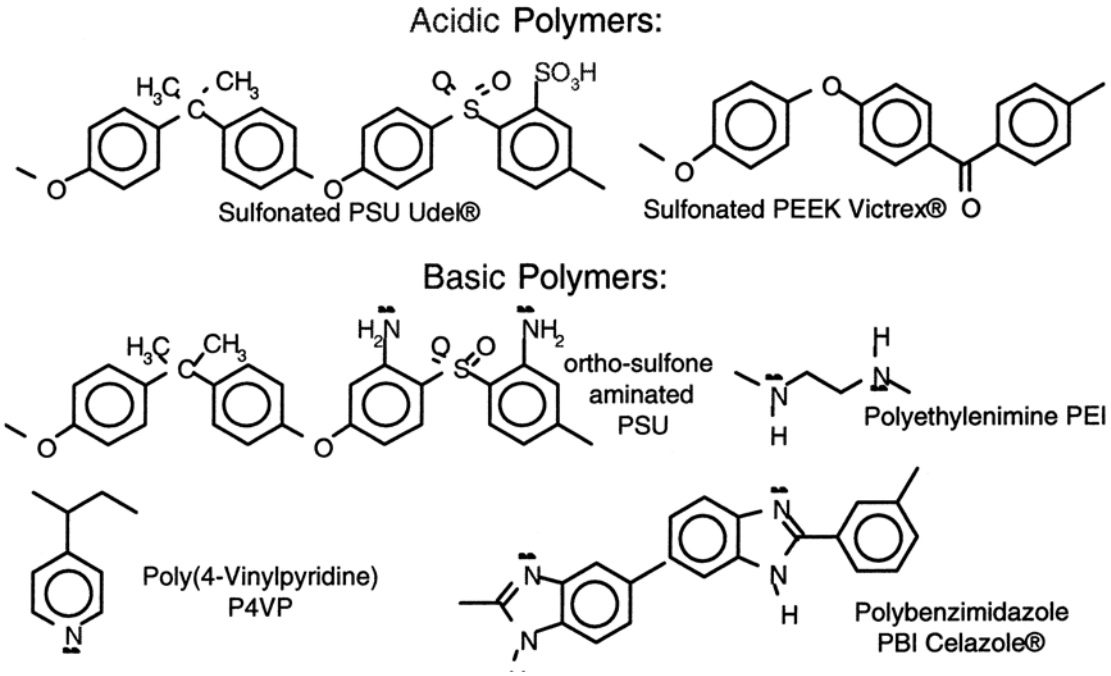

Figure 1.14: Some acidic and basic blends pursued in the literature [110].

Based on this approach, Schauer's group [111,112] has studied the acid-base blend membranes consisting of SPPO/PBI [SPPO refers to sulfonated poly(2,6-dimethyl-1,4-phenylene oxide)], which showed good thermal stability and flexibility as proton exchange membranes in fuel cells. Kerres' group [110,113-118] reported several ionic

cross-linked blend membrane systems based on acid-base interactions as shown in Fig. 1.14 (*e.g.*, sulfonated polysulfone (SPSf) / aminated PSf and SPEEK/PBI). All the blend membranes exhibit good flexibility, thermal stability, and lower methanol permeability in DMFC. However, the dimensional stability at T > 70°C is inadequate with some of the blend membranes.

Manthiram's group reported recently that blend membranes based on acid-base interactions between the sulfonic acid groups of SPEEK and the N-heterocycle groups tethered to polysulfone show suppressed methanol crossover and enhanced performance in DMFC. This blend membrane concept is based on industrially available, inexpensive polymer precursors like poly(ether ether ketone) and polysulfone that are compatible with each other due to similar aromatic backbons [51,119]. A part of this dissertation will focus on further investigation and a fundamental of understanding of this kind of blend membranes.

1.2.3.4 Inorganic Methanol Impermeable Membranes

Inorganic proton conductors were initially investigated as electrolyte materials for high temperature proton exchange membrane fuel cells. In this regard, solid acids such as $CsHSO_4$ [120, 121] and CsH_2PO_4 [122] were investigated since they can offer high-thermal stability (up to 250 ^oC) with anhydrous proton transport. For example, $CsHSO_4$ transforms at around 140 ^oC into a super ionic phase exhibiting proton conductivities of 10^{-3} - 10^{-2} S/cm. With an operating temperature of 150 - 200 ^oC, it can alleviate the poisoning of the Pt-based catalysts by CO and simplify the design of the fuel cell system without the need to have humidifiers as the proton conduction occurs in the absence of water.

The acceptor-doped perovskite oxides with general formula ABO_3 (A = Ba, B = Ce, Zr) have also attracted attention as potential proton conducting electrolyte materials.

These materials could provide proton conduction through the hydroxide defects that are produced by incorporation of water molecules into oxide ion vacancies in the crystal lattice [123-126]. Since these ceramic membranes are impermeable to methanol, zero methanol crossover could be achieved by using a thin ceramic membrane as the electrolyte in DMFC even with pure methanol as a fuel.

However, the low proton conductivity at low temperatures compared to the polymeric membranes and the difficulties to fabricate thin membranes with these inorganic ceramic proton conductors need to be addressed before they can get any practical use in DMFC applications. In addition, the chemical stability of these materials in the fuel cell environment needs to be fully assessed.

1.3 OBJECTIVE OF THIS DISSERTATION

The objective of this dissertation is to design and develop polymer proton exchange membranes and membrane-electrode assemblies (MEAs) that can overcome some of the problems encountered in DMFC. A few membrane systems are systematically investigated and their advantages and limitations compared to Nafion are presented. The primary membrane characteristics such as proton conductivity, thermal stability, swelling behavior, morphology and structural information, and proton conduction mechanism are investigated. The membranes are tested in practical fuel cells. The optimization of MEA fabrication with the alternative aromatic polymer membranes is also pursued. The knowledge gained can provide a better understanding of the proton conduction mechanisms and help in designing new membrane materials. Specifically, the following are investigated:

- With an aim to develop acid-base blend membranes, a series of heterocycle tethered basic polymers such as polysulfone bearing 4-nitro-benzimidazole (PSf-NBIm), polysulfone bearing 1*H*-Perimidine (PSf-PImd), and polysulfone bearing

5-amino-benzotriazole (PSf-BTraz)) are synthesized and the structures are carefully characterized. Blend membranes consisting of sulfonated poly(ether ether ketone) (SPEEK) and different basic polymers are investigated by measuring proton conductivity, liquid uptake, ion-exchange capacity, and electrochemical performance and methanol crossover in DMFC. Finally, the properties and performances of various blend membranes are compared and an understanding of the factors influencing the properties is developed.

- With an aim to investigate the methanol blocking effect of the heterocylces in acid-base blend membranes, a small molecule N,N-Bis-(1*H*-benzimidazol-2-yl) - isophthalamide (BBImIP) is synthesized and used as an additive in both sulfonated polysulfone (SPSf) and SPEEK membranes. The SPSf/BBImIP blend membranes are characterized by ion-exchange capacity and proton conductivity measurements as well as the electrochemical performance and methanol crossover measurements in DMFC. Similarly, the SPEEK/BBImIP blend membranes are also investigated by fuel cell performance and methanol crossover measurements.
- With an aim to investigate novel sulfonated copolymers containing pendant sulfonic acid groups, chemical and physical properties of copolymers based on poly(arylene ether sulfone) with different degrees of sulfonation are studied by NMR, FT-IR, TGA, DSC, water swelling, and proton conductivity measurements. With an aim to investigate the effect of these copolymers as a methanol barrier layer, a series of multilayer structures consisting of a thin SPS-DP center layer and two SPEEK outer layers on each side are fabricated and characterized by electrochemical performance and methanol crossover in DMFC. The SEM investigation of the structural stability of these tri-layer membranes is also presented.

- With an aim to overcome the incompatibility problem between the aromatic polymer membrane and the Nafion ionomer in the electrode, SPEEK is investigated as an ionomer in the catalyst layer in the electrode while employing SPEEK as the membrane to fabricate the MEAs for DMFC. The performances in DMFC, electrochemical active area, and limiting capacitance of the fabricated MEA are evaluated as a function of ion-exchange capacity (IEC) and content (wt. %) of the SPEEK monomer in the catalyst layer. The DMFC performance and methanol crossover of the MEA fabricated with SPEEK membrane and SPEEK ionomer (with optimum IEC value and SPEEK ionomer content) are compared with that fabricated with Nafion 115 membrane and Nafion ionomer.

CHAPTER 2

General Experimental Procedures

2.1 MATERIALS SYNTHESIS

Most of the chemical information, synthesis conditions, preparation procedures, and membrane fabrication processes will be presented in the specific chapters. This chapter presents only the general information adopted in this dissertation.

2.1.1 Chemical Information

Poly(ether ether ketone) (PEEK) was provided by Victrex (PEEK-450PF) and Evonik industry (Vestakeep® 2000 UFP 20). Nafion (Dupont) 115 and 117 membranes (sodium form) were purchased from G.C. Processing Inc.

Concentrated sulfuric aicd (98%), hydrogen peroxide (30 wt. %), 2-propanol (Certified ACS Plus), sodium hydroxide standard solution (0.05N) were purchased from Fisher Scientific. N,N-dimethylacetamide(DMAc) (98 wt.%) was purchased from Acros.

Nafion dispersion solution (5 wt. %) was purchased from Dupont. The 20, 40, and 60 wt. % (Johnson Mathew) platinum on Vulcan carbon was purchased from Alfa Aesar, and the 40 and 60 wt.% Pt-Ru (1:1 atom ratio) alloy on Vulcan carbon was purchased from E-TEK (BASF Fuel Cell).

All the chemicals used in this dissertation were used as-received without any further purification.

2.1.2 Sulfonation of Poly(ether ether ketone)

Concentrated sulfuric acid was used as both solvent and sulfonating agent in the sulfonation reaction [127]. 10 g of PEEK was dissolved in 150 mL of sulfuric acid at

room temperature in a flask equipped with a magnetic stirrer. The degree of sulfonation was controlled by changing the reaction time. After the sulfonation reaction, the solution was poured into ice-water mixture with vigorous stirring and the precipitated polymer was washed with de-ionized water for several times and dried at 100 ^{o}C in vacuum oven overnight. The typical sulfonation reaction time in this dissertation was ~ 48 h.

2.2 NAFION MEMBRANE PRE-TREATMENT

The commercially available Nafion membrane is usually in sodium form, so a pre-treatment of the membrane is needed before using it for further test. The as-received membranes were first cut into small pieces and washed with deionized water. The membranes were then boiled in 5 wt. % hydrogen peroxide solution for 1 h to remove the organic impurities, washed thoroughly several times with de-ionized water, and finally boiled in 0.5 M H_2SO_4 solution for another 1 h to exchange the Na^+ cations by H^+ ions in the membrane. After rinsing and boiling in deionized water for another 1 h, the pre-treated membranes were stored in deionized water before use.

2.3 MATERIALS ANALYSIS AND CHARACTERIZATION

2.3.1 Fourier Transform Infrared Spectroscopy (FT-IR)

The structures of the synthesized materials were characterized by Fourier Transform Infrared (FT-IR) Spectroscopy with a Perkin Elmer Spectrum BX FT-IR instrument in nitrogen atmosphere. The scanned wavenumber range was 4000 - 400 cm^{-1}, and 32 spectra were recorded and averaged to reduce the noise level.

2.3.2 Nuclear Magnetic Resonance (NMR)

^{1}H-NMR spectra were recorded on a Varian INOVA-500 spectrometer at room temperature by dissolving the synthesized materials in dimethylsulfoxide-d6 (DMSO-d6), with the chemical shifts δ being expressed in parts per million (ppm).

2.3.3 Thermogravimetric Analysis (TGA)

Mettler Toledo TGA/SDTA 851e was used to study the change in mass with temperature of the samples, especially the decomposition. Usually, the experiments were carried out at a heating rate of 5 ^{o}C/min in flowing nitrogen or air.

2.3.4 Differential Scanning Calorimetry (DSC)

A Perkin-Elmer series 7 differential scanning calorimeter (DSC) was used to study the thermal behaviors such as phase transition, decomposition, and melting point. Usually, the experiments were conducted with around 10 mg of sample in N_2 atmosphere at a heating rate of 10 ^{o}C/min.

2.3.5 Liquid Uptake of Membranes

The equilibrium liquid uptake (W_{uptake}) of the polymer membranes was calculated by the difference between the dry mass (W_{dry}) and wet mass (W_{wet}) of a membrane sample. The dry weight was measured after the sample was dried at 110 ^{o}C under vacuum for 24 h. To obtain the wet mass, the membrane was equilibrated with de-ionized water or methanol solution at different temperatures for 1 h. The wet membrane was then blotted carefully with a filter paper to remove surface water droplets before weighing. The percent liquid uptake was determined using the following formula:

$$W_{uptake} = \frac{W_{wet} - W_{dry}}{W_{dry}} \times 100\% \qquad (2.1)$$

2.3.6 Ion-Exchange Capacity (IEC) Measurement

The ion-exchange capacity (IEC) was determined by suspending 0.1 ~ 0.2 g of a specific membrane in 2.0 M NaCl solution (30 mL) for 24 h to liberate the H^+ ions and then titrating with standardized 0.05 N NaOH solution using phenolphthalein as an indicator. The IEC was calculated using the equation below:

$$IEC = \frac{0.05 \times V_{titration}}{W_{dry}} \times 1000 meq./g \qquad (2.2)$$

where $V_{titration}$ is the volume (mL) of the NaOH solution consumed during the titration.

2.3.7 Proton Conductivity Measurement

Proton conductivity values of the membranes were obtained from the impedance data, which were collected with a computer interfaced HP 4192 ALF Impedance Analyzer in the frequency range of 5 Hz to 10 kHz with an applied voltage of 10 mV. The conductivity of the membrane is calculated using the equation below:

$$\sigma = \frac{l}{R \cdot A} \qquad (2.3)$$

Where σ, l, R, and A are, respectively, the ionic conductivity, thickness, resistance, and area of the membrane.

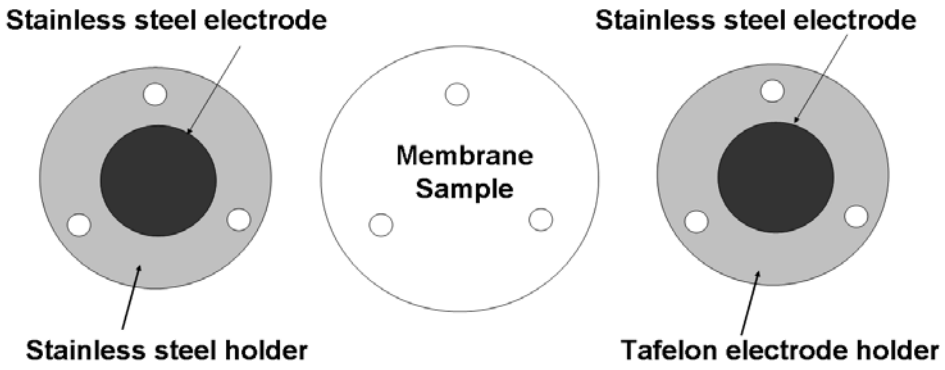

Figure 2.1: Schematic configurations of the cell components employed for dry membrane impedance measurement.

The proton conductivity values under anhydrous condition were obtained from the impedance data collected with a laboratory-made two-electrode setup and stainless steel as blocking electrodes in the transverse direction (*i.e.* through-plane) (Fig. 2.1). Before

the test, the membranes were dried overnight at 100 ^{o}C to remove the free water from the membrane, and the sample was maintained at a desired temperature without humidification for 30 minutes before each test.

The proton conductivity values under humidified conditions were obtained from the impedance data collected with an open window framed two platinum electrode cell (Fig.2.2) in the lateral direction (*i.e.* in-plane) by maintaining the membrane in a humidity chamber oven with water vapor at 100 % relative humidity (RH), and the details of the setup are available elsewhere [115].

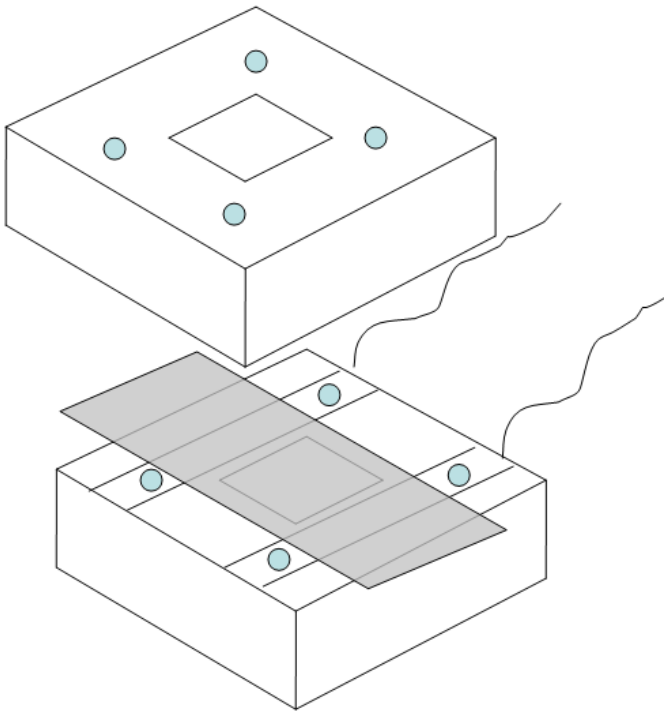

Figure 2.2: Schematic configurations of the cell components employed for wet membrane impedance measurement.

2.4 MEMBRANE-ELECTRODE ASSEMBLY (MEA) FABRICATION

2.4.1 Electrode Preparation

The electrodes (consisting of gas-diffusion and catalyst layers) for testing in DMFC were prepared as reported elsewhere [128]. The anode and cathode catalysts consisted of, respectively, commercial 40 or 60 wt. % Pt-Ru (1:1) on Vulcan carbon (E-TEK) and commercial 20, 40, or 60 wt. % Pt on Vulcan carbon (Alfa Aesar). The electrodes prepared were impregnated with Nafion solution (5 wt. % solution, DuPont Fluoro-products) by a spray technique and dried at 90 ºC under vacuum for 30 min. The loadings for cathodes (Pt) and anode (Pt-Ru) are presented in the specific chapters. The Nafion loading for both the anode and cathode catalysts was 0.35 mg/cm^2.

2.4.2 Membrane-electrode Assembly (MEA) Preparation

Figure 2.3: Bench Top Press (Carver Inc., Model 3851-0) used in this study to fabricate membrane-electrode assemblies (MEAs).

The membrane-electrode assembly (MEA) is a piece of membrane sandwiched between an anode and a cathode. To prepare the MEAs, the anode, membrane, and cathode were consequently arranged between two sheets of aluminum foils and hot pressed uniaxially using a Bench Top Press (Carver Inc., Model 3851-0) shown in Fig.2.3. For MEAs containing the Nafion membrane, the hot-pressing temperature was 140 ºC for 3 min with a pressure of 60 psi. For other MEAs containing aromatic polymer membranes, the hot-pressing temperature was 120 ^{o}C for 2 min with a pressure of 40 psi.

2.5 ELECTROCHEMICAL EVALUATION

The electrochemical evaluations of the membrane in DMFC were performed with a commercial fuel cell test system (890e Multi-range Fuel Cell Testing System, Scribner Associates Inc.) using a single cell fuel cell hardware (Fuel Cell Technologies) with serpentine flow field pattern having an active area of 5 cm^2.

2.5.1 Single Cell Fuel Cell Evaluation

About 1 liter methanol solution was stored in a glass flask, which was heated with a heating mantle (Electrothermal Engineering Ltd.), while the temperature of the flask was monitored and controlled. The flask had four ports at the top: one for a temperature probe, one for an outlet supplying methanol solution to the pump/cell, one for an air condenser, and one for the inlet return from the cell. Usually, the methanol solution with certain concentration (1 M or 2 M) was preheated to the same temperature as the cell operating temperature and was fed into the anode at a flow rate of 2.5 mL/min by controlling with a peristaltic pump without back pressurization. Oxygen was fed into the cathode side at a flow rate of 200 mL/min without back pressure, and the humidification temperature was same as the cell operating temperature.

Figure 2.4: Single cell test station used in this study (890e Multi-range Fuel Cell Testing System, Scribner Associates Inc.).

2.5.2 Methanol Crossover Evaluation

Methanol crossover was evaluated by a voltammetric method [129] in which methanol solution was fed at a flow rate of 2.5 mL/min into the anode side of the MEA while the cathode side was kept in an inert humidified N_2 atmosphere. By applying a positive potential at the cathode side, the flux rate of permeating methanol was determined by measuring the steady-state limiting current density resulting from the complete electro-oxidation at the membrane/Pt catalyst interface at the cathode side.

CHAPTER 3

Blend Membranes Based on Acid-base Interactions with Suppressed Methanol Crossover for Direct Methanol Fuel Cells

3.1 INTRODUCTION

Many effects have been made to develop fluorine-free polyelectrolyte membrane materials for DMFC due to the problems encountered with the Nafion membrane as discussed in Chapter 1. Sulfonated derivatives of poly(ether ether ketone) (SPEEK) [127, 130], polyphosphazene [131], polysulfone (PSf) [128, 132], and polyimide [133-135] as well as phosphoric acid doped polybenzimidazole (PBI) [136-138] are some examples of membrane materials investigated. These materials generally exhibit lower methanol crossover and are less expensive than Nafion. With an optimized degree of sulfonation, some of them show performance in DMFC comparable to that of Nafion. However, the high degrees of sulfonation necessary to maximize the proton conductivity often lead to an increase in membrane swelling and degradation in mechanical stability.

Covalent and ionic cross-linking in the membrane has been investigated as an effective approach to reduce the swelling of membranes. However, cross-linked polymers usually become brittle on drying as discussed in Chapter 1. Also, acid-base blends containing ionic cross-links have been found to exhibit lower methanol crossover in DMFC [139-142]. Unfortunately, they usually lead to a sacrifice in fuel cell performance, and microphase-separation is easy to occur in such blends due to the incompatibility between the acidic and basic (polybenzimidazole) polymer structures [143].

Recently, our group reported that polysulfone bearing benzimidazole (PSf-BIm) or amino-benzimidazole (PSf-ABIm) side groups could promote proton conduction in

SPEEK under anhydrous conditions through acid-base interactions between the sulfonic acid groups of the SPEEK and the nitrogen atoms of the benzimidazole groups tethered to similar aromatic backbones [144,145]. This blend membrane concept is based on industrially available, inexpensive polymer precursors that are compatible with each other due to similar aromatic backbones. In addition to SPEEK being known to exhibit lower methanol crossover compared to Nafion, the benzimidazole side groups tethered to the PSf backbone could also help to suppress methanol crossover further by inserting into the hydrophilic channels.

However, the pKa values of the N-heterocycles side groups in the basic polymers in the acid-base blend membranes play a significant role on the proton transfer between the acid and benzimidazole groups. With this perspective, we present here the tethering of 4-nitro-benzimidazole that has a lower pKa value than benzimidazole due to the substitution of electron-withdrawing nitro groups in the benzimidazole groups and an investigation of the blend membranes consisting of the basic polymer polysulfone-4-nitro-benzimidazole (PSf-NBIm) and the acidic polymer SPEEK. The ion-exchange capacity, proton conductivity, water uptake, and structural and microstructural characterizations of these blend membranes are presented in this chapter. In addition, the electrochemical performances in DMFC as a function of the PSf-NBIm content are compared with that of Nafion 115 membrane.

In order to investigate the size effect of the N-heterocycle side groups in the basic polymer, 1*H*-Perimidine (a tricyclic heterocycle consisting of a dihydri-pyrimidine ring ortho- and peri-fused to naphthalene) that has a larger size compared to benzimidazole is tethered to polysulfone by a condensation reaction between carboxylated polysulfone (CPSf) and 1,8-diaminonaphthalene. The ion-exchange capacity (IEC), proton conductivity, liquid uptake, microstructure, electrochemical performance in DMFC, and

methanol crossover properties of the blend membranes consisting of SPEEK and PSf-PImd as a function of PSf-PImd content and a comparison of the data with those of Nafion 115 membrane are presented here.

Additionally, the synthesis of polysulfone bearing 5-amino-benzotriazole (PSf-BTraz) via a condensation reaction between carboxylated polysulfone and 5-amino-benzotriazole as well as the investigation of blend membranes consisting of SPEEK and PSf-BTraz (with various BTraz contents) are presented. The 5-amino-benzotriazole (BTraz) group is larger in size compared to benzimidazole group, and the four nitrogen sites in the BTraz could facilitate proton transfer through Grotthuss-type mechanism more easily. The ion-exchange capacity (IEC), proton conductivity, liquid uptake, electrochemical performance in DMFC, and methanol crossover of the SPEEK/PSf-BTraz blend membranes with various PSf-BTraz contents are compared with those of plain SPEEK and Nafion membranes.

To have a better understanding of the effect of the pKa value and the size of the heterocycle group on the properties of the blend membranes, blend membranes consisting of SPEEK and different basic polymers (PSf-NBIm, PSf-PImd, PSf-BTraz, PSf-BIm, and PSf-ABIm) are prepared with the same [-SO_3H]/[BIm] ratio in the blend. A comparison of the microstructure, proton conductivity, electrochemical performance, and methanol crossover of these membranes is presented.

3.2 EXPERIMENTAL

3.2.1 Materials Synthesis

4-nitro-1,2-phenylenediamine (99%), 1,8-Diaminonaphthalene (97%) were purchased from Alfa Aesar. O-phenylenediamine (98%), 2-Amino-benzimidazole (99%),

5-Amino-benzotriazole (99+%), and Triphenylphosphite (TPP) (99 %) were purchased from Acros. All chemicals were used as-received.

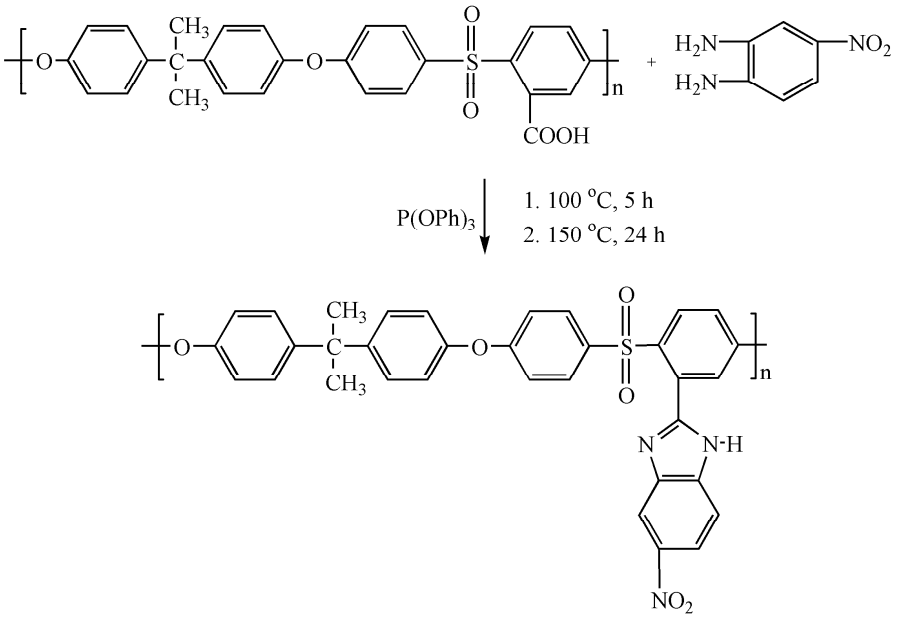

Figure 3.1: Synthesis scheme of polysulfone bearing 4-nitro-benzimidazole side group.

The synthesis of PSf-NBIm was carried out by a condensation reaction between carboxylated polysulfone (CPSf) and 4-nitro-1,2-phenylenediamine as shown in Fig. 3.1. The details of the synthesis of CPSf with different degrees of carboxylation per repeat unit are available elsewhere [146]. CPSf polymers with a degree of carboxylation of 1.03, 1.58 and 1.90 were used, and the PSf-NBIm polymers prepared with them are hereafter designated, respectively, as PSf-NBIm-103, PSf-NBIm-158, and PSf-NBIm-190. Fig. 3.1 shows the reaction between the carboxylated polysulfone and 4-nitro-1,2-phenylenediamine in presence of a dehydrating agent triphenylphosphite (TPP) to give polysulfone bearing 4-nitro-benzimidazole. For example, PSf-NBIm-158 was prepared by dissolving 0.5 g of CPSf with a degree of carboxylation of 1.58 (designated as CPSf-

158) and 0.236 g of 4-nitro-1,2-phenylenediamine in 30 mL of *N*,*N*-dimethylacetamide (DMAc) in a three-neck flask, followed by the addition of 2.9 mL of TPP into the flask. The solution was stirred at 100 ^{o}C for 5 h and then at 150 ^{o}C for 24 h under nitrogen atmosphere and poured into 1 L of methanol to precipitate the polymer. The precipitate was then filtered and washed with methanol and de-ionized water several times before drying the product in a vacuum oven at 100 ^{o}C overnight.

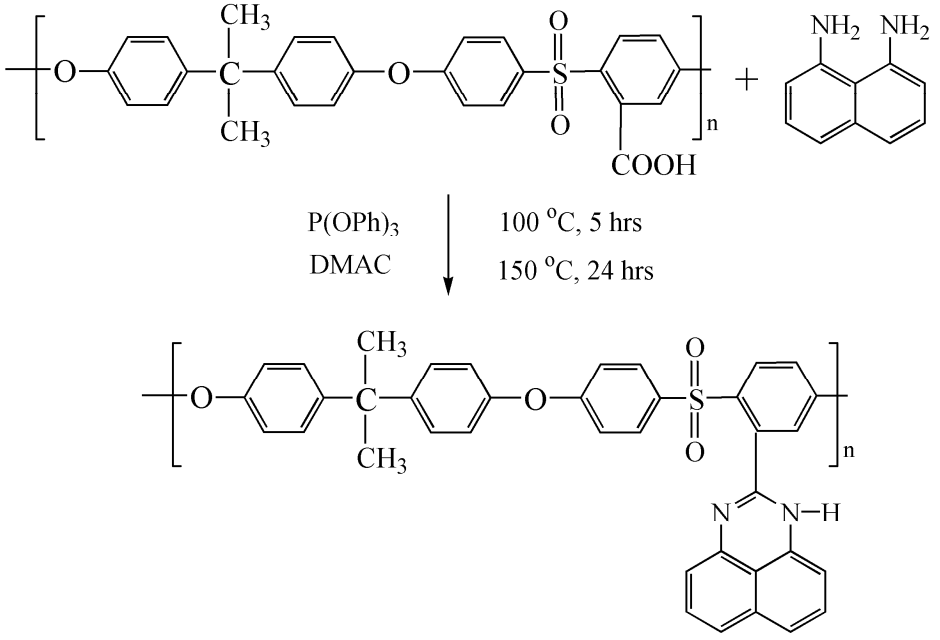

Figure 3.2: Synthesis scheme of polysulfone bearing 1*H*-Perimidine side group.

The PSf-PImd was also synthesized by a condensation reaction between carboxylated polysulfone (CPSf) and 1,8-Diaminonaphthalene (DANP) as shown in Fig. 3.2. CPSf with a degree of carboxylation of 1.03, 1.58, and 1.90 were used, and the PSf-PImd samples prepared with them are hereafter designated as, respectively, PSf-PImd-103, PSf-PImd-158, and PSf-PImd-190. For PSf-PImd-158, 0.5 g of CPSf with a degree of carboxylation of 1.58 and 0.244 g DANP were dissolved in 30 mL of DMAc in a

three-neck flask, followed by the addition of 2.9 mL of TPP into the flask. The solution was stirred at 100 ^{o}C for 5 h and then at 150 ^{o}C for 24 h under nitrogen atmosphere before pouring into 1 L of methanol to precipitate the polymer. The precipitate was then filtered and washed with methanol and de-ionized water several times before drying the product in a vacuum oven at 100 ^{o}C overnight.

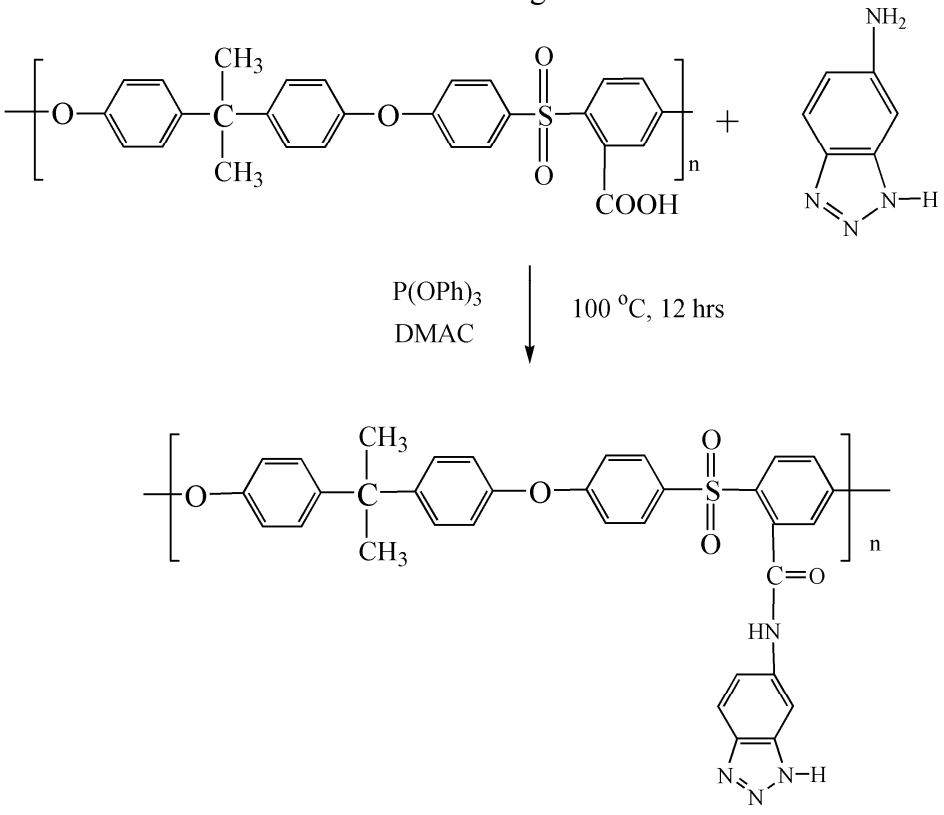

Figure 3.3: Synthesis scheme of polysulfone bearing 5-amino-benzotriazole side groups.

The PSf-BTraz polymer was synthesized by a condensation reaction between carboxylated polysulfone (CPSf) and 5-amino-benzotriazole (Acros) as shown in Fig. 3.3. CPSf with a degree of carboxylation of 1.03, 1.58, and 1.90 were used, and the PSf-BTraz samples prepared with them are hereafter designated as, respectively, PSf-BTraz-103, PSf–PImd-158, and PSf–PImd-190. Triphenylphosphite (TPP) and N,N-

dimethylacetamide (DMAc) were used, respectively, as dehydration agent and solvent in the reaction. The precipitated product polymer was washed and dried with a procedure similar to that reported elsewhere [144].

The syntheses of polysulfone bearing benzimidazole (PSf-BIm) and polysulfone bearing 2-amino-benzimidazole (PSf-ABIm) were carried out as reported before by our group [144, 145].

3.2.2 Membrane Preparation

Plain SPEEK membrane and blend membranes consisting of SPEEK and the basic polymers (PSf-NBIm, PSf-PImd, PSf-BTraz, PSf-BIm, and PSf-ABIm) were prepared by casting from DMAc solutions (~ 10 % w/w). The resulting membranes were dried at 90 ^{o}C overnight and at 130 ^{o}C for another 6 h, followed by washing thoroughly in boiled de-ionized water several times to remove the residual solvent. All the membranes were controlled to have a thickness of 60 ± 5 μm with an active area of 5 cm^2 for DMFC evaluation.

3.2.3 Small-angle X-ray Scattering (SAXS)

The SAXS experiments with the membranes were carried with 1.54 Å Cu Kα radiation and a multiwire gas-filled 2D detector (Molecular Metrology, Inc.). The experiments were typically carried out at room temperature for a duration of 90 min. In order to enhance the electron density contrast between the polymer matrix and the ionic cluster, all the membranes were neutralized with Cs^+ ions by soaking in 2 M CsCl solution for 24 h, washing with de-ionized water, and drying in an oven at 90 ^{o}C for 24 h before each test.

3.2.4 Scanning Transmission Electron Microscopy (STEM).

The morphological and cluster size distribution studies of the Nafion, SPEEK, and SPEEK/PSf-ABIm membranes were carried out with a Philips EM 208 transmission electron microscope (TEM) operated at 200 keV. The membranes were stained with silver to ion exchange the H^+ ions by Ag^+ ions in the sulfonic acid groups by immersing them overnight in 2 M $AgNO_3$ (Alfa Aesar) aqueous solution, followed by rinsing with water and drying at room temperature for 12 h. The stained membranes were embedded in epoxy resin and sectioned to 90 nm thick using a Leica microtome Ultracut UCT and placed on copper grids.

3.2.5 Membrane-electrode Assembly (MEA) Fabrication

The electrodes consisting of gas-diffusion and catalyst layers were prepared as discussed in Chapter 2. For the evaluation of SPEEK/PSf-NBIm blend membranes, the anode and cathode catalysts loadings were, respectively, 0.6 and 1.0 mg/cm^2 of 40 wt.% PtRu and 20 wt.% Pt. For the evaluation of SPEEK/PSf-PImd membranes, the anode and cathode catalysts loadings were, respectively, 1.0 mg/cm^2 of 40 wt.% PtRu and 20 wt.% Pt. For the evaluation of SPEEK/PSf-BTraz membranes and the comparison of different blend membranes, the anode and cathode catalysts loadings were, respectively, 2.5 mg/cm^2 of 60 wt.% PtRu/C and 2.5 mg/cm^2 60 wt.% Pt/C.

The MEA fabrication process used in this study can be found in Chapter 2.

3.3 RESULTS AND DISCUSSION

3.3.1 SPEEK/PSf-NBIm Membranes

3.3.1.1 Polymer Synthesis

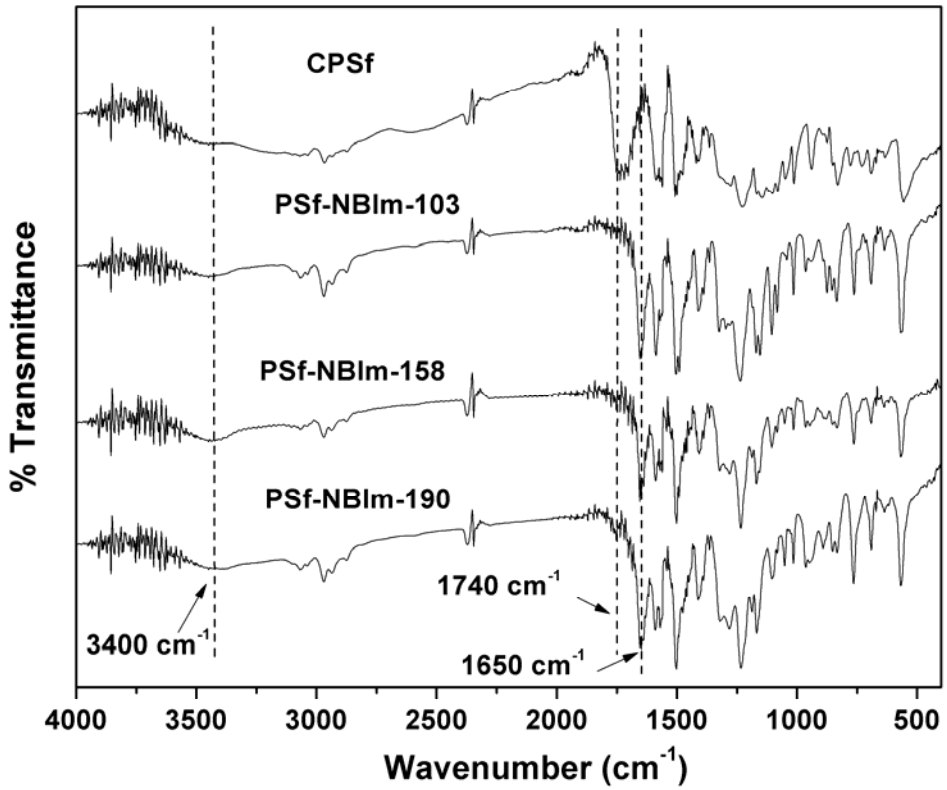

Figure 3.4: FT-IR spectra of carboxylated polysulfone and polysulfone bearing 4-nitro-benzimidazole side groups.

Fig. 3.4 shows the FTIR spectra of carboxylated polysulfone and PSf-NBIm with different degrees of carboxylation. The main absorption bands of PSf-NBIm indicating the presence of 4-nitro-benzimidazole are closely similar to those of PBI or poly(2,5-benzimidazole). The bands around 3400 cm^{-1} are attributed to the isolated N-H stretching. The strong absorption at 1740 cm^{-1} due to the C=O asymmetric stretching in CPSf almost disappeared in PSf-NBIm, indicating nearly the full conversion of the carboxylic acid

groups into 4-nitro-benzimidazole groups. More importantly, the C=N stretching at 1650 cm^{-1} clearly distinguishes the PSf-NBIm from CPSf. Thus, the spectral data confirm the formation of the 4-nitrobenzimidazole side groups on polysulfone. Although blend membranes containing SPEEK and PSf-NBIm synthesized from precursors having different degrees of carboxylation were prepared, only the data of the blend membrane containing PSf-NBIm-158 that was prepared with the carboxylic acid precursor having a degree of carboxylation of 1.58 are presented below, and the blend membrane is referred to hereafter as SPEEK/PSf-NBIm for convenience.

Fig. 3.5 shows the ^{1}H-NMR spectrum of the PSf-BIm-158 sample. From the integration value of the ^{1}H-NMR spectrum, useful information about the product polymer could be extracted. By setting first the integration value of the isopropylidene groups (CH_3-C-CH_3) at low frequencies (1.6 ppm) to be 6H, the integration of the ortho-sulfone proton signals at high frequencies (7.8 - 8.2 ppm) resulted in a value of 2.4 H as expected since the DS of PSf-COOH was close to 1.6 (1.58 to be exact). The rest of the aromatic proton signals should then integrate to:

(i) 12 H if no nitro-benzimidazole group is tethered (all COOH groups).

(ii) 15 H if one COOH is converted to nitro-benzimidazole group and 0.6 COOH still remain free

(iii) 16.8 H if all the COOH groups are converted to nitro-benzimidazole groups.

In Fig. 3.5, the rest of the aromatic signals integrate to 16.4 H, which corresponds to a tethering of approximately 1.5 (1.47 to be exact) nitro-benzimidazole groups per repeat unit and 91.8 % conversion of the COOH groups to nitro-benzimidazole groups.

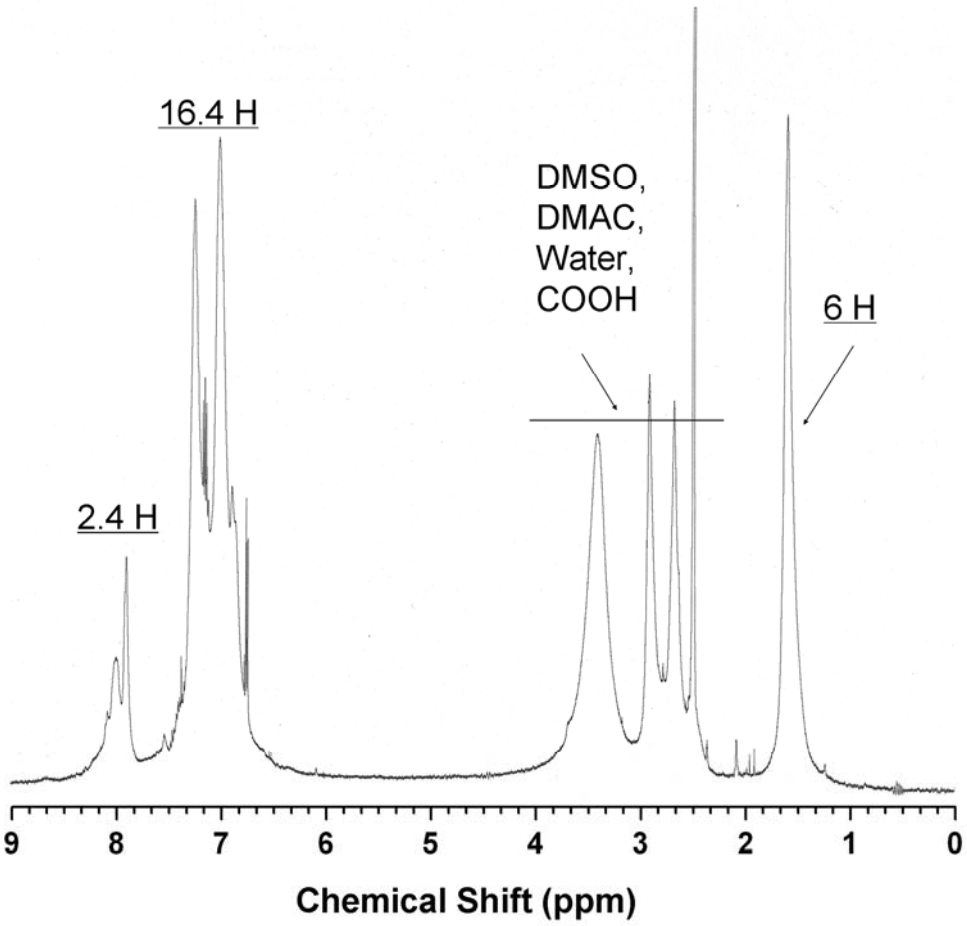

Figure 3.5: ^{1}H-NMR spectrum of the PSf-NBIm-158 sample.

3.3.1.2 Proton Conductivity and IEC

In order to study the effectiveness of the 4-nitrobenzimidazole side group as a proton transfer medium, blend membranes containing SPEEK and various PSf-NBIm contents were prepared. Fig. 3.6 compares the proton conductivities of the SPEEK/PSf-NBIm blend membranes with various PSf-NBIm contents and the plain SPEEK membrane under anhydrous conditions. It can be seen that the proton conductivity of the plain SPEEK membrane decreases with increasing temperature above 100 ^{o}C due to the decreasing amount of water, which is the proton transfer medium (vehicle). However, the

proton conductivity of the SPEEK/PSf-NBIm blend membranes increases with increasing temperature due to the presence of the nitro-benzimidazole groups tethered onto polysulfone. The nitrogen atoms on the benzimidazole ring can act as proton donors and acceptors and thereby help proton transfer under anhydrous conditions between the sulfonic acid groups of SPEEK by a hopping mechanism. This assertion is further supported by an increase in proton conductivity with increasing PSf-NBIm content in the blend membranes.

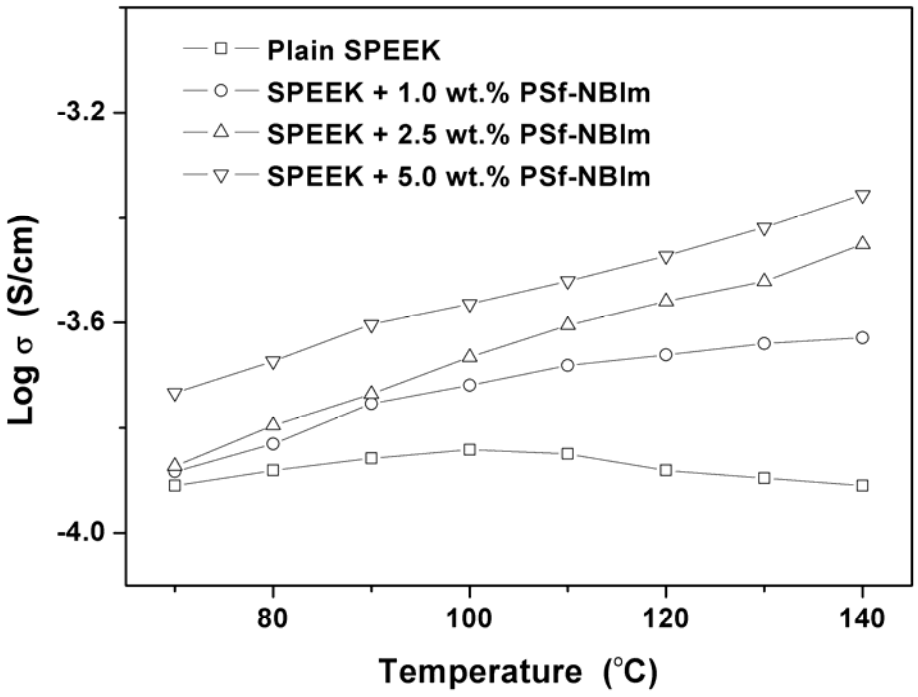

Figure 3.6: Variations with temperature of the proton conductivities of the plain SPEEK and SPEEK/PSf-NBIm (with various PSf-NBIm contents) blend membranes under anhydrous conditions.

Table 3.1 gives the ion-exchange capacity (IEC) values and the proton conductivity values measured under 100 % R.H. at 65 ^{o}C for various contents of PSf-NBIm (or [-SO_3H]/[NBIm] ratios) in the SPEEK/PSf-NBIm blend membranes. It can be

seen that the IEC values of the blend membranes are lower than that of plain SPEEK, indicating the occurrence of acid-base interactions in the blend membranes and the consequent reduction in the amount of H^+ ions dissociating from the sulfonic acid groups. Moreover, the IEC value decreases as the PSf-NBIm content increases due to an increase in the degree of acid-base interaction. At a given temperature, while the blend membrane with 1.0 wt.% PSf-NBIm shows proton conductivity similar to that of plain SPEEK, the blend membranes with 2.5 and 5.0 wt.% PSf-NBIm show higher proton conductivity than plain SPEEK membrane. The increase in proton conductivity is due to the assistance of proton transfer by the nitro-benzimidazole groups in PSf-NBIm through the acid-base interactions as illustrated in Fig. 3.7. The sulfonic acid groups of SPEEK can protonate the nitrogen site of nitro-benzimidazole, facilitating the hopping of the proton bound to the other nitrogen of the nitro-benzimidazole unit to the oxygen of another sulfonate anion group. However, the proton conductivity is maximum at an intermediate PSf-NBIm content of 2.5 wt.%, and decreases thereafter on going to 5 wt.% PSf-NBIm, suggesting that the proton conductivity is maximized at an optimum PSf-NBIm content.

Table 3.1: Ion-exchange capacity (IEC) and proton conductivity (σ) of plain SPEEK and SPEEK/PSf-NBIm blend membranes with various [-SO_3H]/[NBIm] mole ratios.

Membrane	[SO_3H]/[NBIm] mole ratio	IEC (meq./g)	σ at 100 % RH and 65 ºC (S/cm)
Plain SPEEK	--	1.36	6.9×10^{-2}
SPEEK + 1.0 wt.% PSf-NBIm	56.3	1.31	6.4×10^{-2}
SPEEK + 2.5 wt.% PSf-NBIm	22.1	1.26	9.2×10^{-2}
SPEEK + 5.0 wt.% PSf-NBIm	10.8	1.19	8.1×10^{-2}

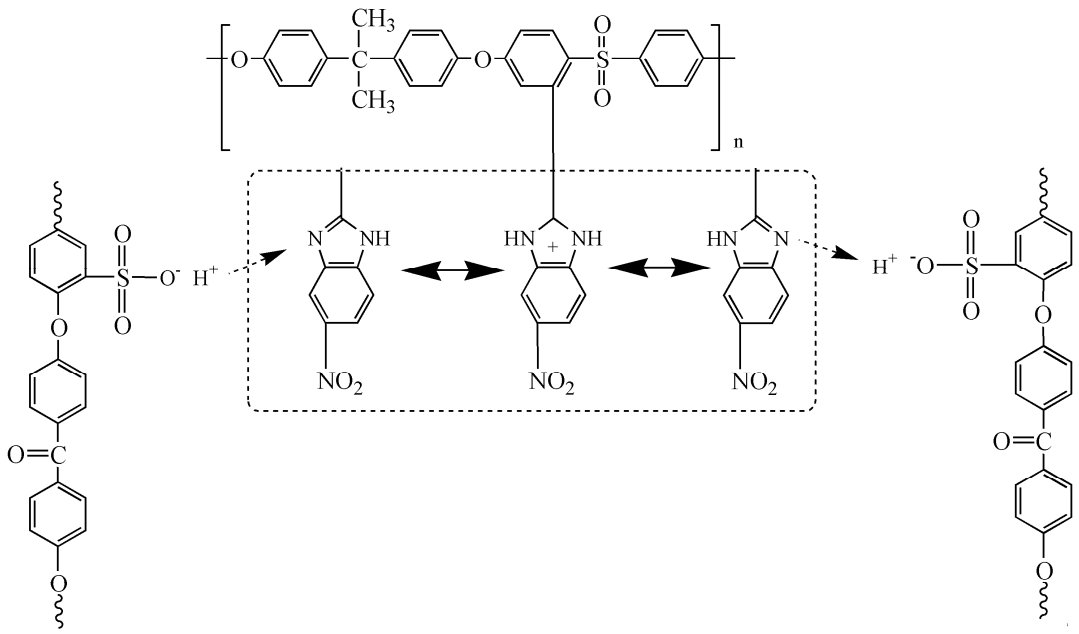

Figure 3.7. Illustration of the proton transfer mechanism involving acid-base interactions in the SPEEK/PSf-NBIm blend membrane.

Under humidified conditions, the vehicle-type mechanism for proton transfer is predominant due to the availability of a greater number of sulfonic acid groups compared to the nitro-benzimidazole groups in the blend membranes, while the Grotthuss-type mechanism involving the nitrogen atoms on the nitro-benzimidazoles could provide an enhancement in proton conduction. Moreover, the insertion of the nitro-benzimidazole side groups into the ionic channels of the sulfonic acid groups could expand the width of the ionic channels, enhancing the proton transfer by the vehicle-type mechanism (see below). However, if the nitro-benzimidazole content becomes too high as in the case of 5.0 wt.% PSf-NBIm with a [-SO_3H]/[NBIm] ratio of 10.8, then the presence of the hydrophobic nitro-benzimidazole groups within the ionic clusters could perturb the

proton conduction by the vehicle-type mechanism, resulting in an overall reduction in proton conductivity.

3.3.1.3 Ionic Cluster Size

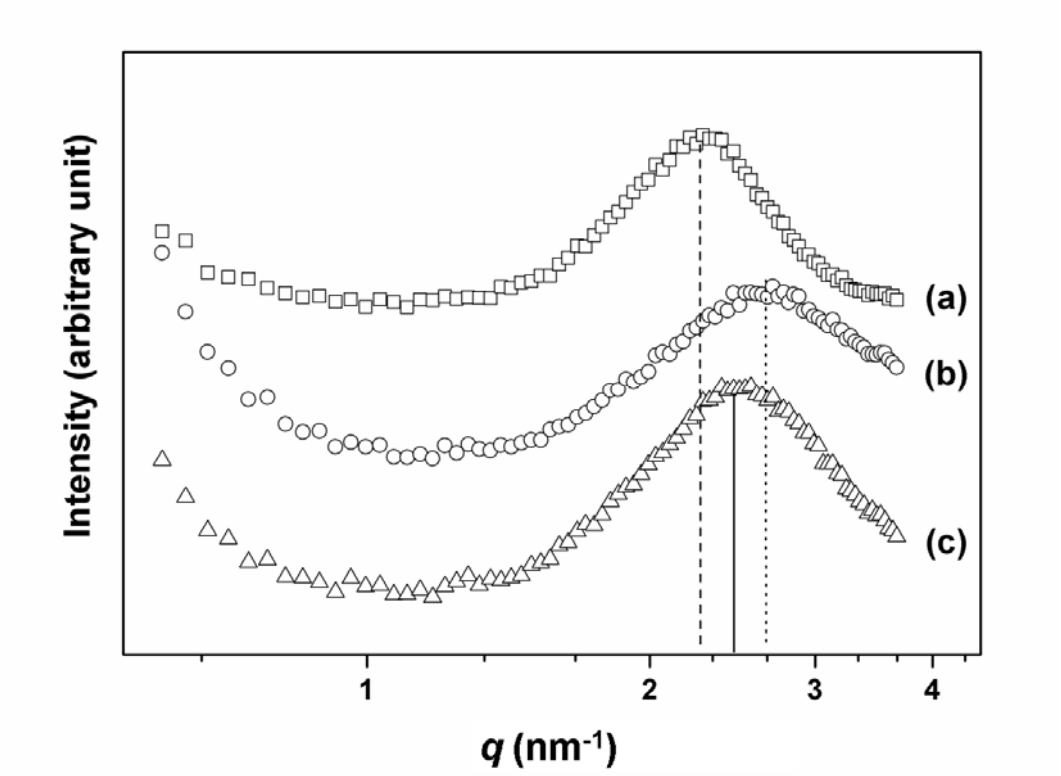

Figure 3.8: Comparison of the SAXS profiles of cesium-neutralized (a) Nafion, (b) plain SPEEK, and (c) SPEEK/PSf-NBIm (2.5 wt.% PSf-NBIm) blend membranes.

To study the microstructural differences among Nafion, plain SPEEK, and SPEEK/PSf-NBIm blend membranes, small angle X-ray scattering was performed with dry membranes after neutralizing with Cs^+. In the sulfonated ionomers like SPEEK and Nafion, the anion packing is determined by the counterion, but it is independent of the cation type [147,148]. By neutralizing with Cs^+ ions, the electron density contrast between the hydrocarbon PEEK polymer matrix and the ionic cluster should be

enhanced. Also, the neutralized dry SPEEK membranes with a degree of sulfonation < 50 % are known to show similar trends as that in water and methanol solutions [149].

Fig. 3.8 compares the SAXS profiles of the Nafion 115, plain SPEEK, and SPEEK/PSf-NBIm membranes after neutralizing with Cs^+ ions. It can be seen that both the plain SPEEK and SPEEK/PSf-NBIm membranes show the ionomer peak with a higher *q*-value compared to Nafion 115, indicating that the plain and blend SPEEK membranes exhibit a smaller Bragg distance (center-to-center distance of clusters) and ionic cluster size compared to Nafion 115 due to the high rigidity of the PEEK backbone to which the $-SO_3H$ groups are attached. The smaller free volume resulting from a smaller ionic cluster size leads to lower methanol/water permeability and suppressed methanol crossover in DMFC (see later). Moreover, even though the degree of sulfonation of the plain and blend SPEEK membranes are the same, the SPEEK/PSf-NBIm blend membrane shows slightly larger Bragg distance compared to plain SPEEK, indicating the expansion of the ionic cluster size due to the insertion of the nitro-benzimidazole side groups into the cluster formed by the sulfonic acid groups in SPEEK.

3.3.1.4 Liquid Uptake

Membrane swelling is a critical issue for MEA stability in fuel cells, and it generally trends with liquid uptake. Table 3.2 compares the percent liquid uptake at different temperatures in water and in 1 M methanol solution for various PSf-NBIm contents of the SPEEK/PSf-NBIm blend membranes. The liquid uptake increases as the temperature or the concentration of methanol increases at a given PSf-NBIm content, and decreases with increasing PSf-NBIm content at a given temperature or methanol concentration. The lower liquid uptake of the SPEEK/PSf-NBIm blend membrane is believed to be due to the increase in both the hydrophobicity of PSf-NBIm and the acid-base interaction between and sulfonic acid and nitro-benzimidazole groups in the blend

membrane. The lower liquid uptake could also help to lower the methanol crossover in DMFC as the crossover is known to have a similar trend as the liquid uptake in the SPEEK membrane.

Table 3.2: Comparison of the liquid uptake in water and 1 M methanol solution for plain SPEEK and SPEEK/PSf-NBIm-158 blend membranes.

Membrane	Liquid Uptake			
	Water (wt.%)		1 M Methanol Solution (wt.%)	
	25 ºC	65 ºC	25 ºC	65 ºC
Plain SPEEK	34.3	45.3	47.5	59.3
SPEEK + 1.0 wt.% PSf-NBIm	32.8	43.2	44.1	57.3
SPEEK + 2.5 wt.% PSf-NBIm	30.1	41.6	41.7	54.2
SPEEK + 5.0 wt.% PSf-NBIm	27.1	39.1	38.9	47.8

3.3.1.5 Electrochemical Stability

Although the SPEEK/PSf-NBIm blend membrane shows higher proton conductivity and lower water uptake compared to the plain SPEEK, there is a possibility that the nitro-benzimidazole with a nitro-group could poison the Pt catalyst like imidazole in fuel cells. To investigate the poisoning effect, cyclic voltammetry was performed with imidazole and 4-nitro-benzimidazole in $N(n\text{-}C_4H_9)_4PF_6$-CH_3CN solution in the presence of Pt catalyst, and Fig. 3.9 compares the voltammograms. While a large irreversible oxidation peak is seen in the voltammogram of imidazole as reported in the literature [150], no obvious oxidation peaks are found in the case of 4-nitro-benzimidazole in the potential range of 0 to +1.8 V, indicating that 4-nitro-benzimidazole exhibits better electrochemical stability than imidazole under fuel cell operating conditions. This is

further confirmed by the electrochemical performance measurements in fuel cell as presented below.

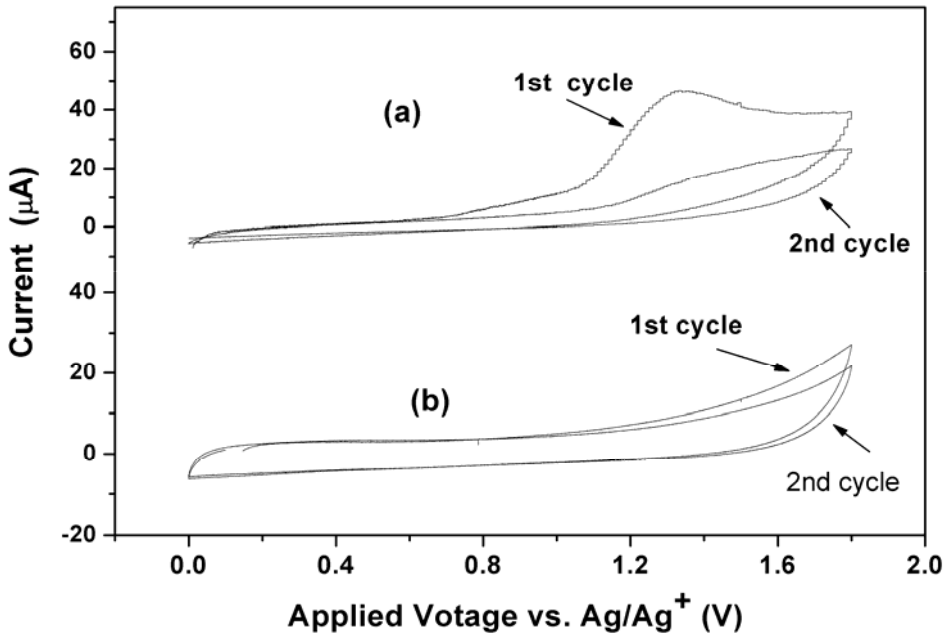

Figure 3.9: Cyclic voltammograms (first two cycles) of Pt/C catalysts in (a) imidazole and (b) 4-nitro-benzimidazole solution at 25 ºC. The experiments were carried out with an acetonitrile (CH_3CN) solution consisting of 5×10^{-3} mol/dm^3 imidazole or 4-nitro-benzimidazole and 0.1 mol/dm3 tetra-n-butylammonium hexafluorophosphate [$N(n\text{-}C_4H_9)_4PF_6$] at room temperature with a potential sweep rate of 50 mV/s using a glassy carbon electrode, a platinum auxiliary electrode, and an Ag/AgCl reference electrode.

3.3.1.6 Fuel Cell Performance and Methanol Crossover

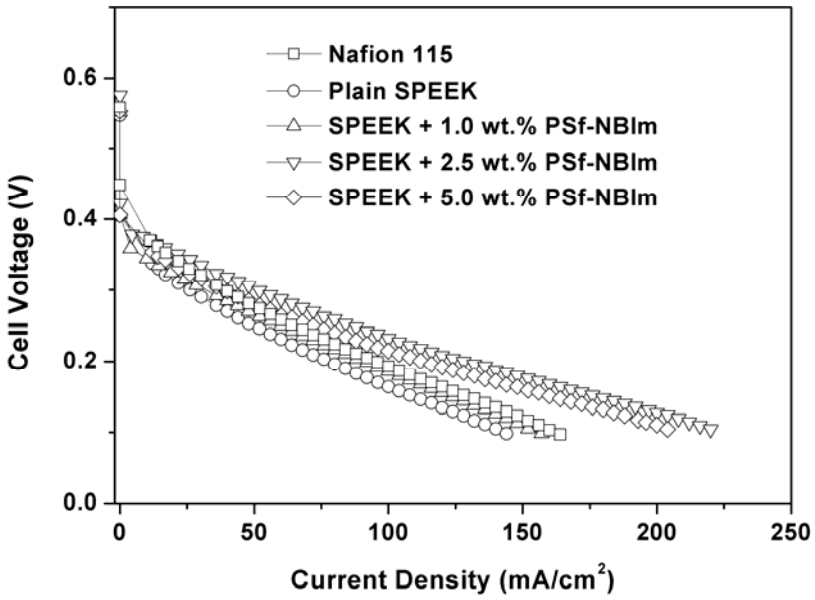

Figure 3.10: Comparison of the polarization curves recorded with Nafion-115, plain SPEEK, and SPEEK/PSf-NBIm (with various PSf-NBIm contents) blend membranes in DMFC. Methanol concentration: 1 M, cell temperature: 65 ^{o}C.

Fig. 3.10 compares the polarization curves of the SPEEK/PSf-NBIm blend membranes containing various PSf-NBIm contents (1.0 to 5.0 wt.%) with those of plain SPEEK and Nafion 115 membranes at 65 ^{o}C. The SPEEK/PSf-NBIm blend membranes show higher fuel cell performance than plain SPEEK membrane, which is consistent with the higher proton conductivity values seen in Table 3.2. More importantly, although the plain SPEEK membrane shows lower performance than Nafion 115 membrane due to the lower proton conductivity, the SPEEK/PSf-NBIm blend membranes with PSf-NBIm contents of 2.5 and 5.0 wt.% exhibit higher performance than Nafion 115, confirming the assistance of PSf-NBIm in enhancing the proton conduction. The higher performance is also due to the lower methanol crossover in the blend membrane compared to that in

Nafion 115 membrane (see below). Interestingly, the performance of the SPEEK/PSf-NBIm blend membrane containing the nitro-benzimidazole groups is higher than that of the SPEEK/PSf-BIm blend membrane containing the benzimidazole groups with similar [-SO_3]/[BIm] ratio in the blend membranes, which is due to a higher proton conductivity measured with the former. We believe this is because the nitro-benzimidazole groups with a lower pKa value than the benzimidazole groups facilitate faster proton conduction in the acidic environment.

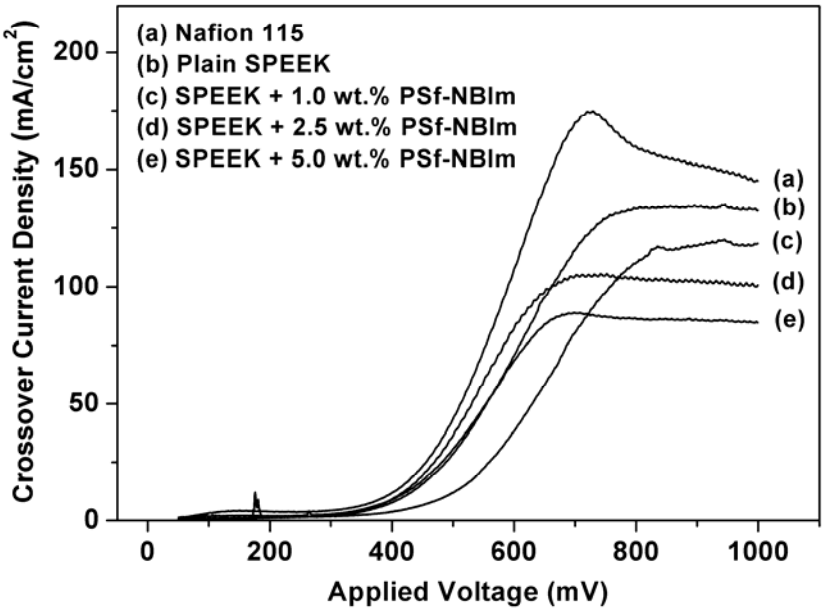

Figure 3.11: Comparison of the polarization curves and power densities recorded with Nafion-115, plain SPEEK, and SPEEK/PSf-NBIm (with various PSf-NBIm contents) blend membranes in DMFC. Methanol concentration: 1 M, cell temperature: 80 ^{o}C.

Methanol crossover is a critical parameter for long-term DMFC operation. Fig. 3.10 compares the methanol crossover current density of the SPEEK/PSf-NBIm blend membranes containing various PSf-NBIm contents with those of plain SPEEK and

Nafion 115 membranes. The plain SPEEK membrane shows lower methanol crossover than Nafion 115 although it is much thinner (~ 60 μm) than Nafion 115 (125 μm) due to the narrower hydrophilic regions and smaller ionic cluster size in SPEEK. Interestingly, even though the SPEEK/PSf-NBIm blend membrane shows slightly larger cluster size compared to the plain SPEEK as seen in Fig. 3.8, it shows much lower methanol crossover than plain SPEEK, indicating the effectiveness of PSf-NBIm in blocking methanol crossover by the insertion of the side groups into the hydrophilic region. The lower methanol crossover in the blend membrane could also help to lower the Pt catalyst loading at the cathode.

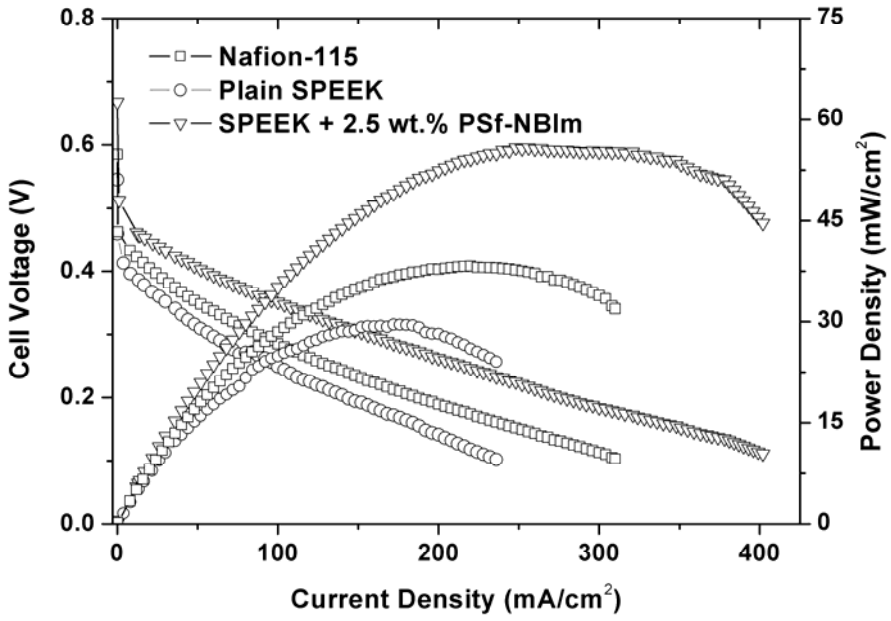

Figure 3.12: Comparison of the methanol crossover current densities for the Nafion-115, plain SPEEK, and SPEEK/PSf-NBIm (with various PSf-NBIm contents) membranes in DMFC. Methanol concentration: 1 M, cell temperature: 65 ^{o}C.

Fig. 3.12 compares the polarization curves and power density of the plain SPEEK, SPEEK/PSf-NBIm (2.5 wt.%), and Nafion 115 membrane at 80 ^{o}C with 1 M methanol solution. The power density value of the blend membrane is higher than those of both plain SPEEK and Nafion 115 membrane. The maximum powder density of the blend membrane (56 mW/cm^2) is 1.5 times higher than that of Nafion 115 (37 mW/cm^2).

3.3.2 SPEEK/PSf-PImd Blend Membranes

3.3.2.1 FTIR Characterization of Basic Polymer

Fig. 3.13 compares the FTIR spectra of the PSf-PImd samples with that of the carboxylated precursor. The C=N stretching (~ 1650 cm^{-1}) and N-H stretching (~ 3400 cm^{-1}) bands in the PSf-PImd samples clearly indicate the tethering of the heterocycle side groups onto polysulfone. Moreover, the almost complete disappearance of the C=O asymmetric stretching band (~ 1740 cm^{-1}) in the PSf-PImd samples distinguishes it from the CPSf precursor, suggesting a nearly full conversion of the carboxylic acid groups into 1H-Perimidine groups. The PSf-PImd-158, prepared by employing the CPSf with a degree of carboxylation of 1.58, was then blended with SPEEK to obtain the blend membrane, which is hereafter referred to as SPEEK/PSf-PImd for convenience.

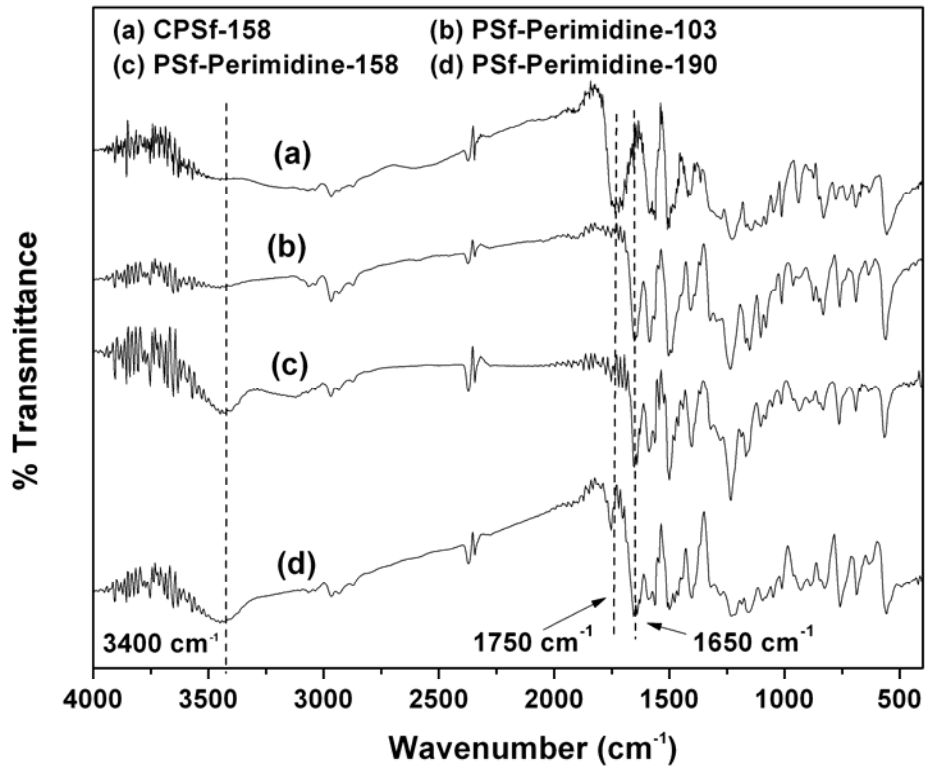

Figure 3.13: FTIR spectra of carboxylated polysulfone and polysulfone bearing 1*H*-Perimidine side group.

3.3.2.2 Proton Conductivity, IEC, and Liquid Uptake

In order to study the effectiveness of the 1*H*-Perimidine side group as a proton transfer medium, the proton conductivity under anhydrous conditions of the blend membranes consisting of SPEEK and various PSf-PImd contents was measured with increasing temperature as seen in Fig. 3.14 In SPEEK, water acts as a proton transfer medium (vehicle) and the water content plays an important role on the proton conduction. Thus, the proton conductivity of the plain SPEEK membrane decreases with increasing temperature above 100 ^{o}C due to the decreasing amount of water. However, in the SPEEK/PSf-PImd blend membranes, the nitrogen atoms on the PImd side groups can act

as proton donors and acceptors and facilitate proton transfer under anhydrous conditions between the sulfonic acid groups of SPEEK by a Grotthuss (hopping) mechanism, so the proton conductivity of the blend membranes increases with increasing temperature. This assertion is further supported by an increase in proton conductivity with increasing PSf-PImd content in the blend membranes.

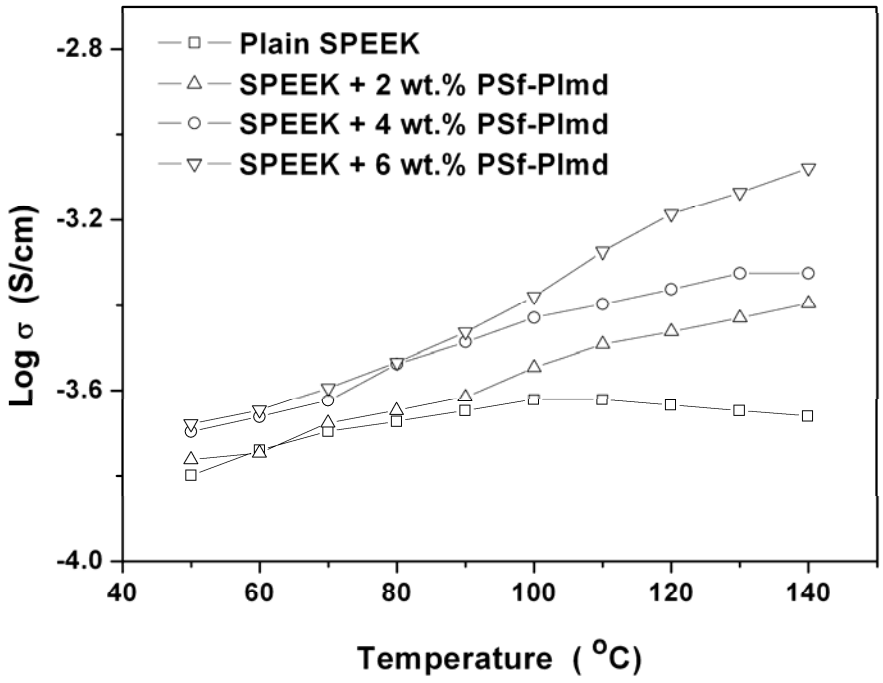

Figure 3.14: Comparison of the proton conductivities of the plain SPEEK and SPEEK/PSf-PImd (with various PSf-PImd contents) blend membranes under anhydrous conditions at various temperatures.

Table 3.3 summarizes the proton conductivities, liquid uptake, and ion-exchange capacities of the plain SPEEK and SPEEK/PSf-PImd membranes along with those of Nafion 115 membrane. As the acid-base interaction between the sulfonic acid and heterocycle group reduces the number of dissociable H^+ ions from the sulfonic acid groups, all the blend membranes show lower IEC values than the plain SPEEK

membrane. Moreover, as the PSf-PImd content increases, the IEC value decreases due to an increase in the degree of acid-base interaction, confirming the occurrence of acid-base interactions in the blend membranes.

Table 3.3: Comparison of the ion-exchange capacity (IEC), liquid uptake, and proton conductivity σ (under 100% relative humidity conditions at 25 ^{o}C) of plain SPEEK and SPEEK/PSf-PImd blend membranes with various amounts of PSf-PImd.

Membrane	IEC (meq./ g)	[SO_3H] / [PImd] ratios	Liquid uptake (wt.%)				σ (S/cm)
			water		1 M methanol solution		
			25 ^{o}C	65 ^{o}C	25 ^{o}C	65 ^{o}C	
Plain SPEEK	1.51	--	34.9	49.5	37.3	62.6	0.036
SPEEK + 2 wt.% PSf-PImd	1.42	37.5	29.7	45.2	34.1	56.3	0.039
SPEEK+ 4 wt.% PSf- PImd	1.29	16.9	27.4	38.4	30.4	49.1	0.043
SPEEK + 6 wt.% PSf-PImd	1.18	11.2	22.1	30.4	23.5	43.9	0.041
Nafion 115	0.89	--	30.8	39.2	36.4	41.2	0.091

Regarding the proton conductivity under humidity conditions, the blend membranes show an increase in conductivity with increasing PSf-PImd content up to 4.0 wt.% and then show a decrease in conductivity with further increase in the PSf-PImd content. As the blend membranes have a greater number of sulfonic acid groups compared to the number of heterocycle groups ([-SO_3H] / [PImd] = 37.5 to 16.9 for PImd contents of 2 to 4 wt. %), the predominant proton transfer mechanism could be vehicle-type, while the Grotthuss-type mechanism involving the nitrogen atoms on the heterocycles could provide an enhancement in proton conduction. Moreover, the expansion of the ionic channels (confirmed by the SAXS measurements presented later) with increasing PImd content could also enhance the proton transfer by vehicle-type

mechanism. However, when the [-SO_3H] / [PImd] ratio reaches 11.2 at 6.0 wt. % PImd, the presence of the hydrophobic 1*H*-Perimidine groups within the ionic clusters could perturb the proton conduction by the vehicle-type mechanism, resulting in an overall reduction in proton conductivity.

Table 3.3 also compares the percent liquid uptake at different temperatures and methanol concentrations for various PSf-PImd contents. Although the membranes show an increase in liquid uptake with increasing temperature and methanol concentration, all the blend membranes show lower liquid uptake compared to the plain SPEEK due to both the acid-base interaction and the lower hydrophilicity of the PSf-PImd polymer. Moreover, at a given temperature or methanol concentration, the liquid uptake of the blend membrane decreases with increasing PSf-PImd content. Lower liquid uptake can lead to reduced swelling and better MEA stability during fuel cell operation.

3.3.2.3 Small Angle X-ray Scattering

To study the microstructural differences among Nafion, plain SPEEK, and SPEEK/PSf-PImd blend membranes, small angle X-ray scattering (SAXS) was performed after neutralizing the membranes with Cs^+. Figure 3.15 compares the SAXS profiles of the Nafion 115, plain SPEEK, and SPEEK/PSf-PImd membranes. As seen, both the plain SPEEK and SPEEK/PSf-PImd membranes show ionomer peaks with higher q values compared to Nafion, suggesting a smaller Bragg distance (center-to-center distance of clusters) and ionic cluster size than in Nafion 115. This is due to the higher rigidity of the aromatic backbone in PEEK compared to that of the fluorocarbon aliphatic backbone in Nafion. The smaller free volume resulting from a smaller ionic cluster size in SPEEK and SPEEK/PSf-PImd blend membranes leads to lower methanol/water permeability and suppressed methanol crossover in DMFC. Moreover, the slightly larger Bragg distance in the SPEEK/PSf-PImd blend membrane compared to

that in the plain SPEEK membrane indicate a widening of the ionic cluster size due to the insertion of the basic PImd side groups into the ionic cluster in SPEEK due to acid-base interactions.

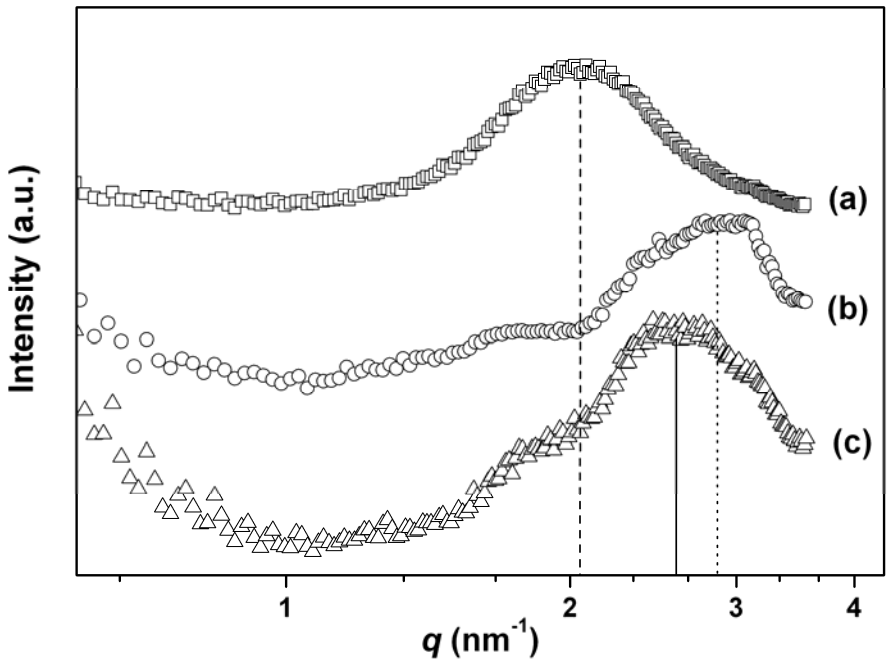

Figure 3.15: Comparison of the SAXS profiles of cesium-neutralized (a) Nafion, (b) plain SPEEK, and (c) SPEEK/PSf-PImd (6.0 wt. % PSf-PImd) blend membranes.

3.3.2.4 Electrochemical Evaluation in DMFC

The polarization curves of the SPEEK/PSf-PImd blend membranes containing various amounts of PSf-PImd (2.0 – 6.0 wt. %) in DMFC are compared in Fig. 3.16 with those of plain SPEEK and Nafion 115 membranes at 65 ^{o}C. The blend membranes show better performance in DMFC than plain SPEEK membrane due to higher proton conductivity (Table 6.3) and lower methanol crossover (see below). More interestingly,

although the plain SPEEK membrane shows lower performance than Nafion 115 membrane due to the lower proton conductivity, the blend membranes with PSf-PImd contents of 4 and 6 wt. % exhibit better performance than Nafion 115, confirming the assistance of PSf-PImd in enhancing the proton conduction.

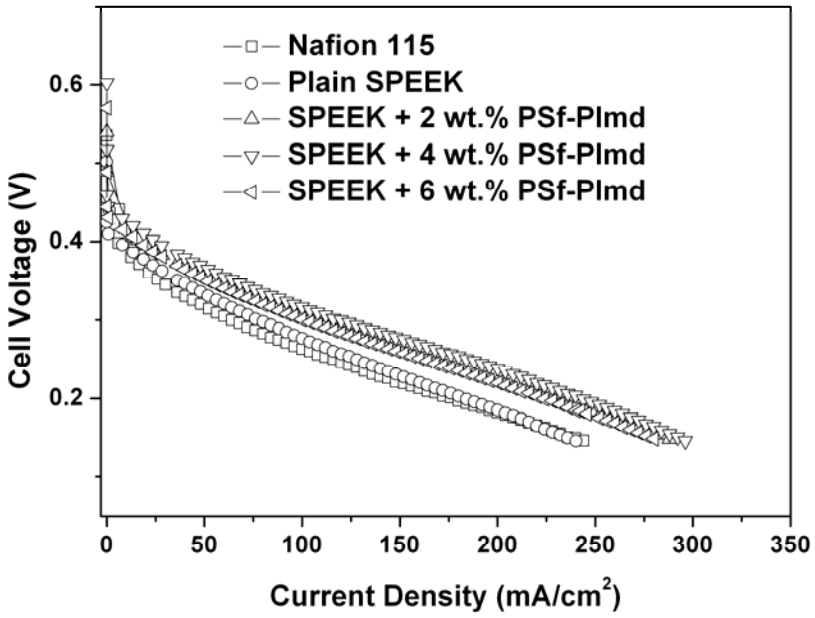

Figure 3.16: Comparison of the polarization curves of Nafion-115, plain SPEEK, and SPEEK/PSf-PImd (with various PSf-PImd contents) blend membranes in DMFC. Methanol concentration: 1 M, cell temperature: 65 ^{o}C.

Fig. 3.17 compares the methanol crossover current density of the SPEEK/PSf-PImd blend membranes containing various amounts of PSf-PImd with those of plain SPEEK and Nafion 115 membranes. As reported elsewhere, the plain SPEEK membrane shows lower methanol crossover than Nafion 115 although it is much thinner (~ 60 μm) than Nafion 115 (125 μm) due to the narrower hydrophilic regions and smaller ionic cluster size in SPEEK. Interestingly, even though the SPEEK/PSf-PImd blend membrane shows slightly larger cluster size compared to the plain SPEEK as seen in Fig. 3.15, it

shows much lower methanol crossover than plain SPEEK, indicating the effectiveness of PSf-PImd in blocking methanol crossover by the insertion of the hydrophobic PImd groups into the hydrophilic region as supported by the SAXS data. The lower methanol crossover in the blend membrane could not only help to lower the Pt catalyst loading at the cathode but also lead to a better long-term stability and performance. Moreover, the lower methanol crossover of the blend membranes containing the 1*H*-Perimidine groups compared to those containing the benzimidazole groups [144] suggests that the size of the tethered N-heterocycle groups may play a critical role in tuning the methanol permeability property of this type of acid-base blend membranes.

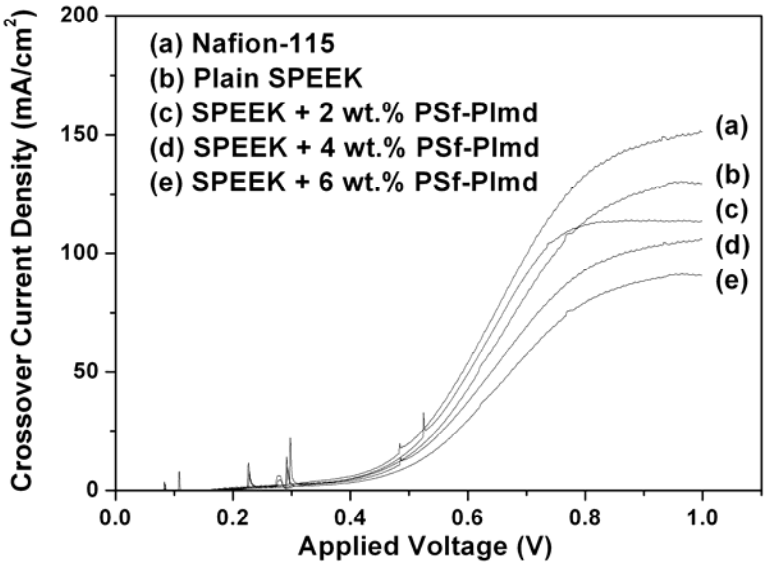

Figure 3.17: Comparison of the methanol crossover current density obtained with Nafion-115, plain SPEEK, and SPEEK/PSf-PImd (with various PSf-PImd contents) blend membranes in DMFC. Methanol concentration: 1 M, cell temperature: 65 ^{o}C.

3.3.3 SPEEK/PSf-BTraz Blend Membranes

3.3.3.1 Structure of the PSf-BTraz Polymers

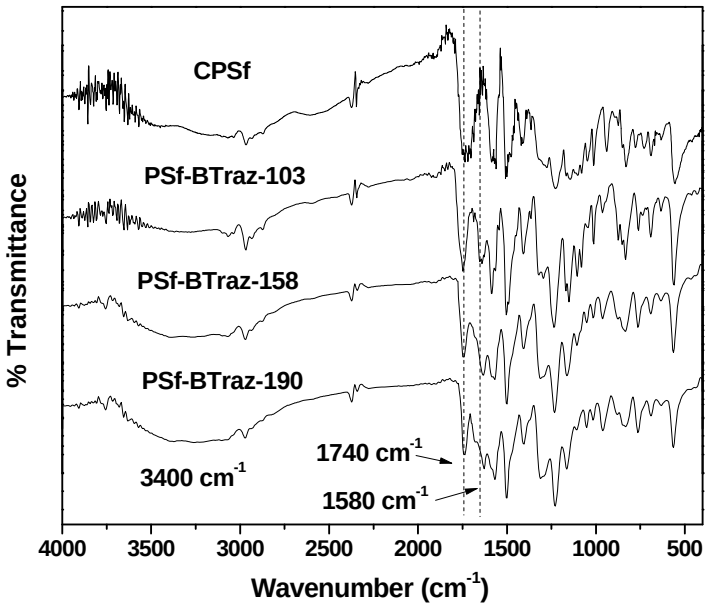

Figure 3.18: Comparison of the FTIR spectra of carboxylated polysulfone (CPSf) and polysulfone tethered with 5-amino-benzotriazole (PSf-BTraz).

Fig. 3.18 shows the FTIR spectra of the PSf-BTraz polymers synthesized using the CPSf precursor with various degrees of carboxylation. The strong absorption band of C=N stretching at 1580 cm^{-1} and the broad absorption of isolated N-H stretching around 3400 cm^{-1} distinguish PSf-BTraz from the CPSf precursor, indicating the attachment of amino-benzotriazole onto polysulfone. The asymmetric C=O absorption band at 1740 cm^{-1} indicates that the 5-amino-benzotriazole is tethered to the carboxyl group.

3.3.3.2 Liqui Uptake, IEC, Proton Conductivity under Humidity Condition

Table 3.4 compares the liquid uptake, IEC, and proton conductivity of SPEEK, Nafion 115, and SPEEK/PSf-BTraz blend membranes. All the blend membranes show lower IEC values than plain SPEEK membrane since the acid-base interaction between

the sulfonic acid and heterocycle groups reduces the number of dissociable H^+ ions from the sulfonic acid groups. Moreover, as the basic polymer content increases, the IEC value decreases due to an increase in the degree of acid-base interaction, which further confirms the occurrence of acid-base interactions in the blend membranes.

Table 3.4: Comparison of the ion-exchange capacity (IEC), [-SO_3H]/[BTraz] ratios, and proton conductivity (σ) of Nafion 115, plain SPEEK, and SPEEK/PSf-BTraz blend membranes with various contents of PSf-BTraz-158.

Membranes	IEC (meq./g)	[–SO_3H] /[BTraz] ratio	σ (S/cm)*
Plain SPEEK	1.42	--	0.039
SPEEK + 3 wt.% of PSf-BTraz	1.31	20.2	0.044
SPEEK+ 5 wt.% of PSf-BTraz	1.27	11.9	0.054
SPEEK + 8 wt.% of PSf-BTraz	1.22	7.2	0.049
Nafion 115	0.89	--	0.091

* 100% relative humidity condition at 25 ^oC

The comparison of the proton conductivity under humidity condition in Table 3.4 also shows the effect of the acid-base interactions in the blend membrane. The blend membrane shows an increase in conductivity with increasing PSf-BTraz content up to 5.0 wt. % and all the blend membranes exhibit higher proton conductivity than plain SPEEK membrane. Since there is more number of sulfonic acid groups compared to the number of heterocycle groups in the blend membranes (Table 3.4), the vehicle-type proton conduction mechanism is predominant and the Grotthuss-type mechanism involving the nitrogen atoms on the heterocycles may provide an enhancement in the proton conduction by providing extra proton transfer "bridge." Moreover, the insertion of the heterocycles into the ionic clusters formed by the sulfonic acid groups could broaden the proton transfer channels, resulting in an enhancement in the vehicle mechanism. The longer side

chains of PSf-BTraz and the more number of nitrogen sites (four) in the 5-amino-benzotriazole groups may make the proton hopping much easier in the SPEEK/PSf-BTraz blend membranes compared to that in SPEEK/PSf-BIm (BIm refers to benzimidazole); in fact, the latter exhibits lower proton conductivity compared to the former with the same [-SO_3H] / [BIm] ratio.

Table 3.5 compares the liquid uptake of different membranes in water and methanol solution at 25 and 65 ^oC. Although all the membranes exhibit an increase in liquid uptake with increasing temperature and methanol concentration, all blend membranes show lower liquid uptake compared to plain SPEEK due to the acid-base interactions and lower hydrophilicity of the PSf-BTraz polymer. Moreover, at a given temperature or methanol concentration, the liquid uptake of the blend membrane decreases with increasing PSf-BTraz content, which further confirms the occurrence of acid-base interactions in the blend membranes.

Table 3.5: Comparison of the liquid uptake in water and methanol solution of Nafion 115, plain SPEEK, and SPEEK/PSf-BTraz blend membranes with various contents of PSf-BTraz-158.

Membranes	In water (%)		In methanol solution (%)			
			1 M		2M	
	25 ^oC	65 ^oC	25 ^oC	65 ^oC	25 ^oC	65 ^oC
Plain SPEEK	26.2	32.7	31.1	37.8	43.8	51.5
SPEEK + 3 wt.% of PSf-BTraz	23.8	30.7	30.5	35.4	39.5	42.7
SPEEK+ 5 wt.% of PSf-BTraz	21.4	27.2	25.7	32.3	30.8	35.8
SPEEK + 8 wt.% of PSf-BTraz	18.6	23.4	22.3	28.6	26.8	30.3
Nafion 115	30.8	39.2	36.4	41.2	42.1	48.7

3.3.3.3 Proton Conductivity under Anhydrous Condition

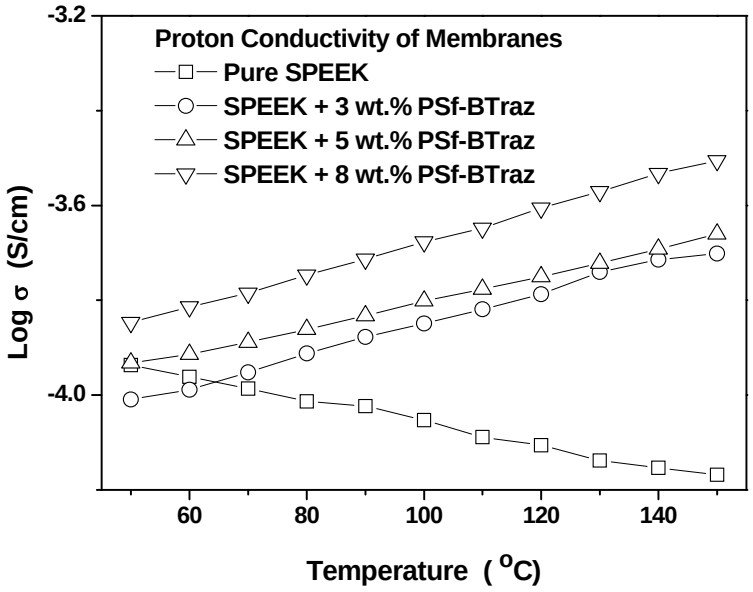

Figure 3.19: Comparison of the proton conductivities of the plain SPEEK and SPEEK/PSf-BTraz (with various PSf-BTraz-158 contents) blend membranes under anhydrous condition at various temperatures.

Fig. 3.19 compares the temperature dependence of the proton conductivity under anhydrous condition of the SPEEK and its blend membranes with various PSf-BTraz contents. While the proton conductivity of SPEEK decreases with increasing temperature due to the decreasing amount of proton carriers (water), the proton conductivities of SPEEK/PSf-BTraz blend membranes increase. The nitrogen sites on amino-benzotriazole side groups play an important role in this phenomenon, since the nitrogen could act as proton donor and acceptor, facilitating proton transfer between the sulfonic acid groups through Grotthuss-type mechanism under anhydrous conditions. The increase in proton conductivity with increasing BTraz content confirms the assistance of the BTraz groups in the proton transfer under anhydrous condition.

3.3.3.4 Methanol Crossover and Fuel Cell Performance Evaluation

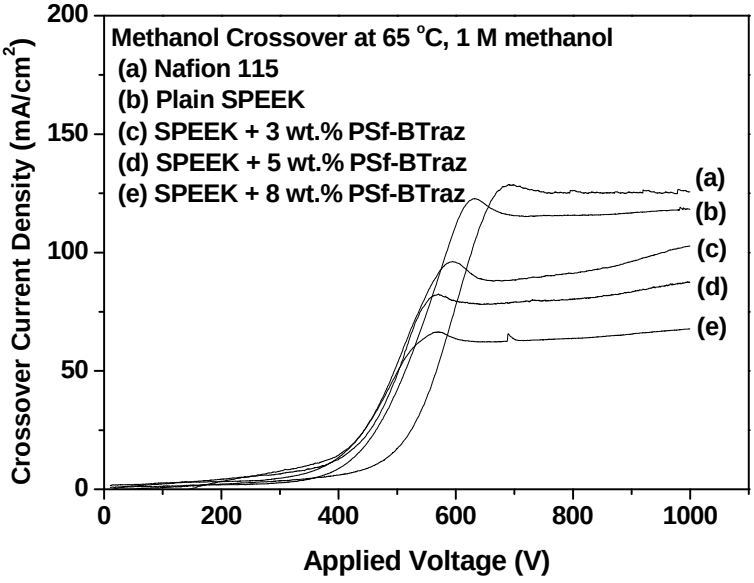

Figure 3.20: Comparison of the methanol crossover current density of Nafion 115, plain SPEEK, and SPEEK/PSf-BTraz (with various PSf-BTraz-158 contents) blend membranes in DMFC. Methanol concentration: 1 M, cell temperature: 65 ^{o}C.

Fig. 3.20 compares the methanol crossover current density of the SPEEK/PSf-BTraz blend membranes containing various amounts of PSf-BTraz (3.0 – 8.0 wt. %) in DMFC with those of plain SPEEK and Nafion 115 membranes at 65 ^{o}C with 1 M methanol solution. The thin blend membranes (~ 60 μm) shows much lower methanol crossover than plain SPEEK (~ 60 μm) and Nafion (125 μm) membrane, indicating the effectiveness of PSf-BTraz in blocking methanol permeation by the insertion of the hydrophobic heterocycle groups into the hydrophilic region. The lower methanol crossover in the blend membrane could not only help to lower the Pt catalyst loading at the cathode but also lead to a better long-term stability and performance. Moreover, the lower methanol crossover of the blend membranes containing the amino-benzotriazole

groups compared to those containing the benzimidazole groups suggests that the size of the tethered N-heterocycle groups may play a critical role in tuning the methanol permeability property of this type of acid-base blend membranes.

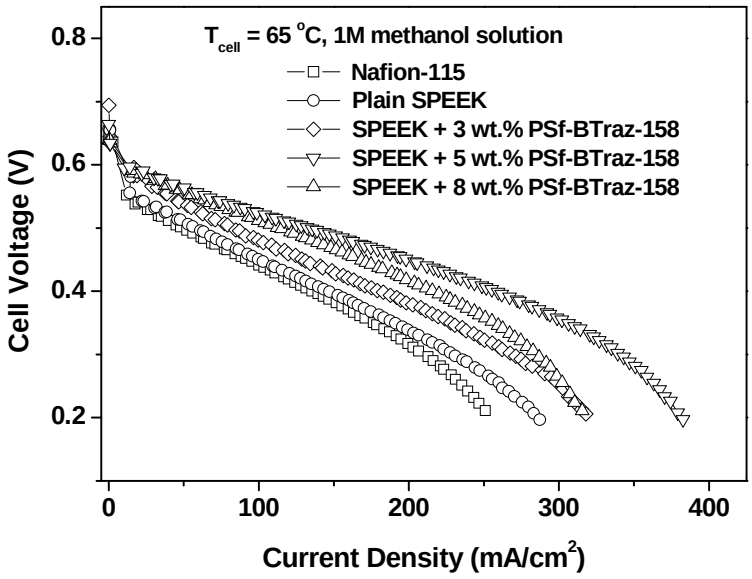

Figure 3.21: Comparison of the polarization curves of Nafion 115, plain SPEEK, and SPEEK/PSf-BTraz (with various PSf-BTraz-158 contents) blend membranes in DMFC. Methanol concentration: 1 M, cell temperature: 65 ^{o}C.

Fig. 3.21 compares the polarization curves of the SPEEK/PSf-BTraz blend membranes containing various amounts of PSf-BTraz (3.0 – 8.0 wt. %) in DMFC with those of plain SPEEK and Nafion 115 membranes at 65 ^{o}C. The blend membranes show better performance in DMFC than plain SPEEK membrane due to higher proton conductivity (Table 3.4) and lower methanol crossover. More interestingly, although the plain SPEEK membrane shows similar performance to Nafion 115 membrane due to the lower proton conductivity, the blend membranes exhibit much better performance than

Nafion 115, confirming the assistance of PSf-BTraz in enhancing the proton conduction and blocking methanol crossover.

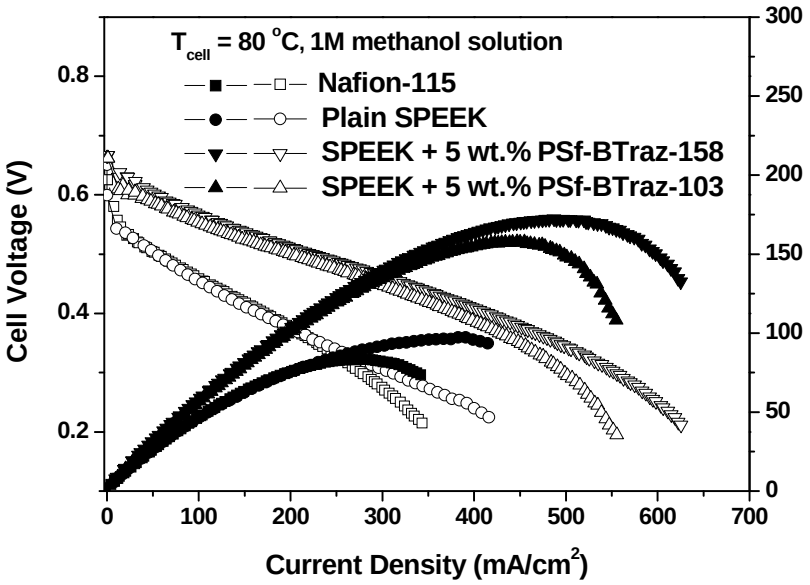

Figure 3.22: Comparison of the polarization curves and power density of Nafion 115, plain SPEEK, SPEEK/5wt.% PSf-BTraz-158, and SPEEK/5wt.% PSf-BTraz-103 blend membranes in DMFC. Methanol concentration: 1 M, cell temperature: 80 ^{o}C.

Fig. 3.22 compares the fuel cell performance and power density of the blend membranes (SPEEK + 5 wt.% PSf-BTraz-158 and SPEEK + 5 wt.% PSf-BTraz-103), plain SPEEK membrane, and Nafion 115 membranes at 80 ^{o}C. With the same basic polymer weight content, the blend membrane containing PSf-BTraz-158 shows higher fuel cell performance than that containing PSf-BTraz-103. Use of PSf-BTraz synthesized with CPSf precursors having a higher degree of carboxylation could further enhance proton conductivity and suppress methanol crossover through a stronger acid-base interactions. With optimized basic polymer contents, the maximum power density offered by the SPEEK/PSf-BTraz-158 blend membrane (174 mW/cm^2) is twice of that of Nafion

115 (84 mW/cm^2) membrane and 1.8 times of that of SPEEK membrane (97 mW/cm^2) at 80 ^{o}C with 1 M methanol solution.

3.3.4 Comparison of Blend Membranes Consisting of Different Basic Polymers

As discussed in the previous sections (sections 3.3.1 – 3.3.3) in this chapter, polysulfone was tethered with different N-heterocycles and the resulting basic polymers were blended with SPEEK. However, the IEC of the SPEEK used and the catalyst loading in each section were different. In order to further understand the effect of the size of the hetrocycles and the pKa values on the properties of the blend membranes based on acid-base interactions, blend membranes consisting of the SPEEK and different basic polymers (shown in Fig. 3.23) with the same [-SO_3H]/[BIm] ratio were prepared and characterized. The properties of these membranes are and discussed below.

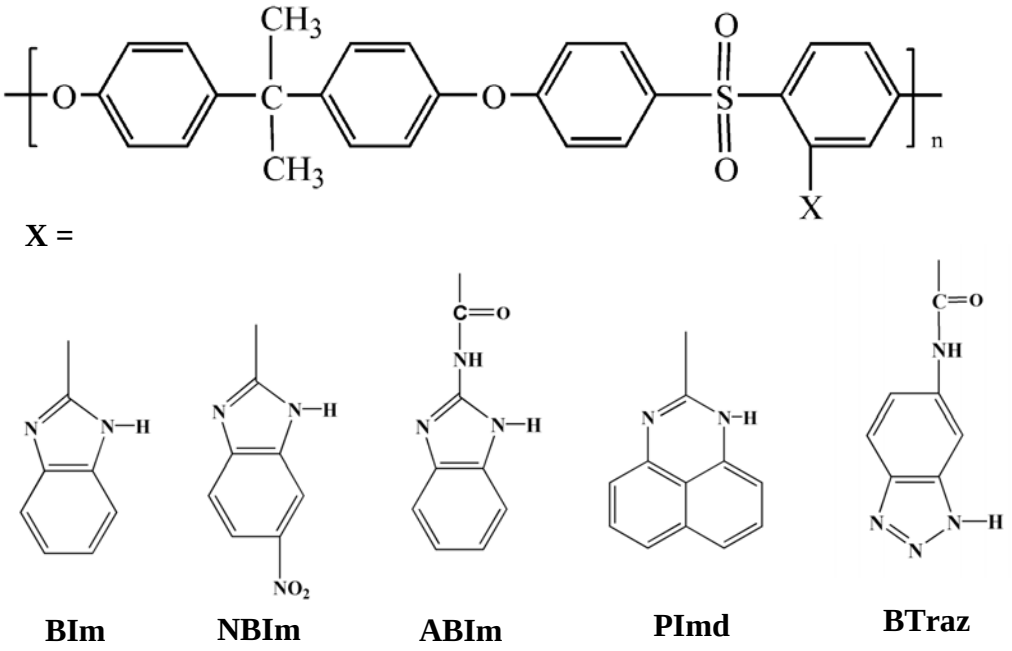

Figure 3.23: Structures of the various basic polymers used in obtaining the blend membranes with SPEEK. BIm: benzimidazole; NBIm: nitro-benzimidazole; ABIm: 2-amino-benzimidazole; PImd: 1*H*-Perimidine; and BTraz: 5-amino-benzotriazole.

3.3.4.1 Comparison of the Microstructures of the Blend Membranes

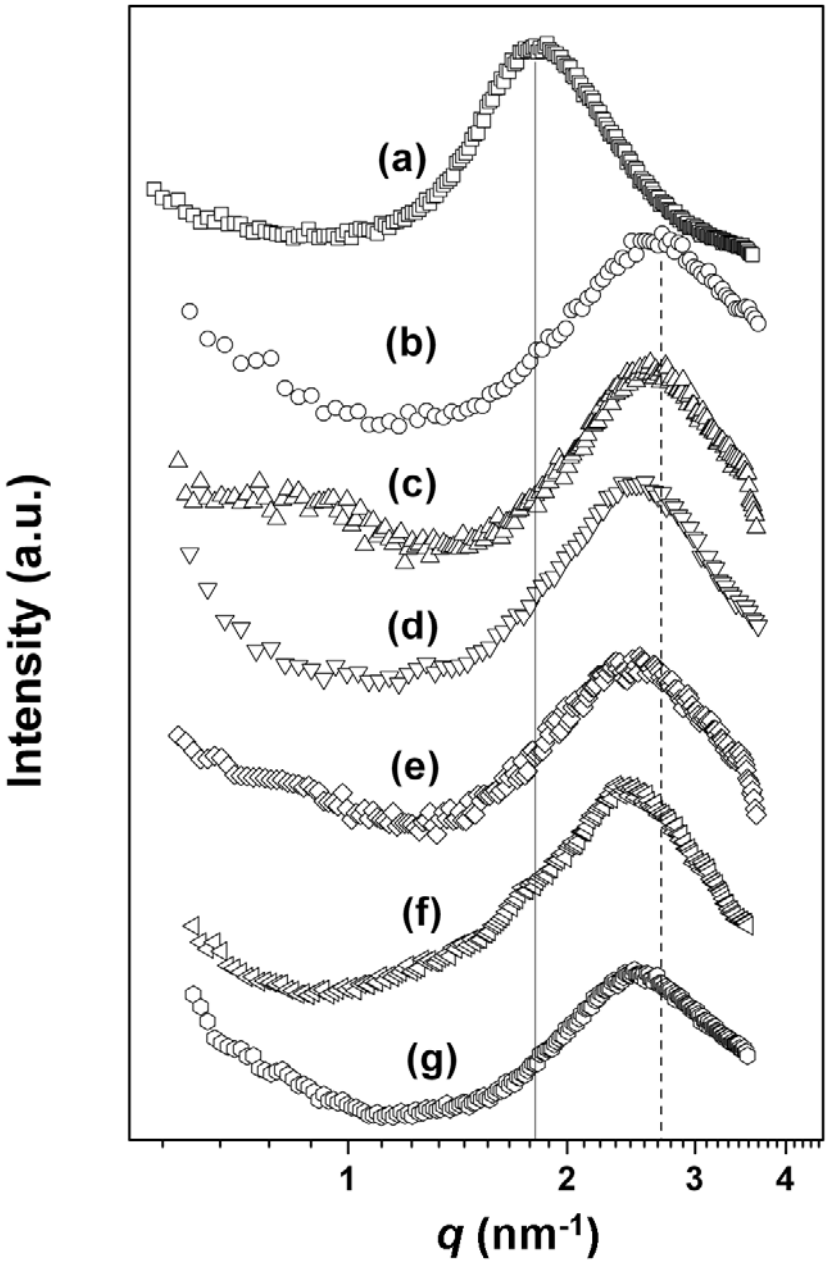

Figure 3.24: Comparison of the SAXS profiles of cesium-neutralized (a) Nafion, (b) plain SPEEK, (c) SPEEK/PSf-BIm, (d) SPEEK/PSf-NBIm, (e) SPEEK/PSf-ABIm, (f) SPEEK/PSf-PImd, and (g) SPEEK/PSf-BTraz.

To study the micro-structural differences among Nafion, plain SPEEK, and different blend membranes, small angle X-ray scattering (SAXS) was performed after neutralizing the membranes with Cs^+. Fig. 3.24 compares the SAXS profiles of these membranes. As seen, the plain SPEEK and all blend membranes show ionomer peaks with higher q values compared to that of Nafion, suggesting a smaller Bragg distance and ionic cluster size than that in Nafion 115. This is due to the higher rigidity of the aromatic backbones in these polymers compared to that of the PTFE backbone in Nafion. The smaller free volume resulting from a smaller ionic cluster size in the SPEEK and blend membranes also leads to lower methanol/water permeability and suppressed methanol crossover in DMFC.

Another interesting result is that the Bragg distance of the blend membranes increase slowly with increasing size of the heterocycle side groups in the basic polymers. When comparing the peak positions of the SPEEK/PSf-BIm and SPEEK/PSf-PImd blend membranes, a shift from right to left could be clearly seen. Since the concentration of the heterocycles in the blend membranes are almost the same in these two samples, the shift could only be due to the difference in the size of the different heterocycles in the blend membranes. Although the larger size of the heterocycles could block the methanol permeation more effectively, it leads to a decrease in the proton conductivity of the blend membranes.

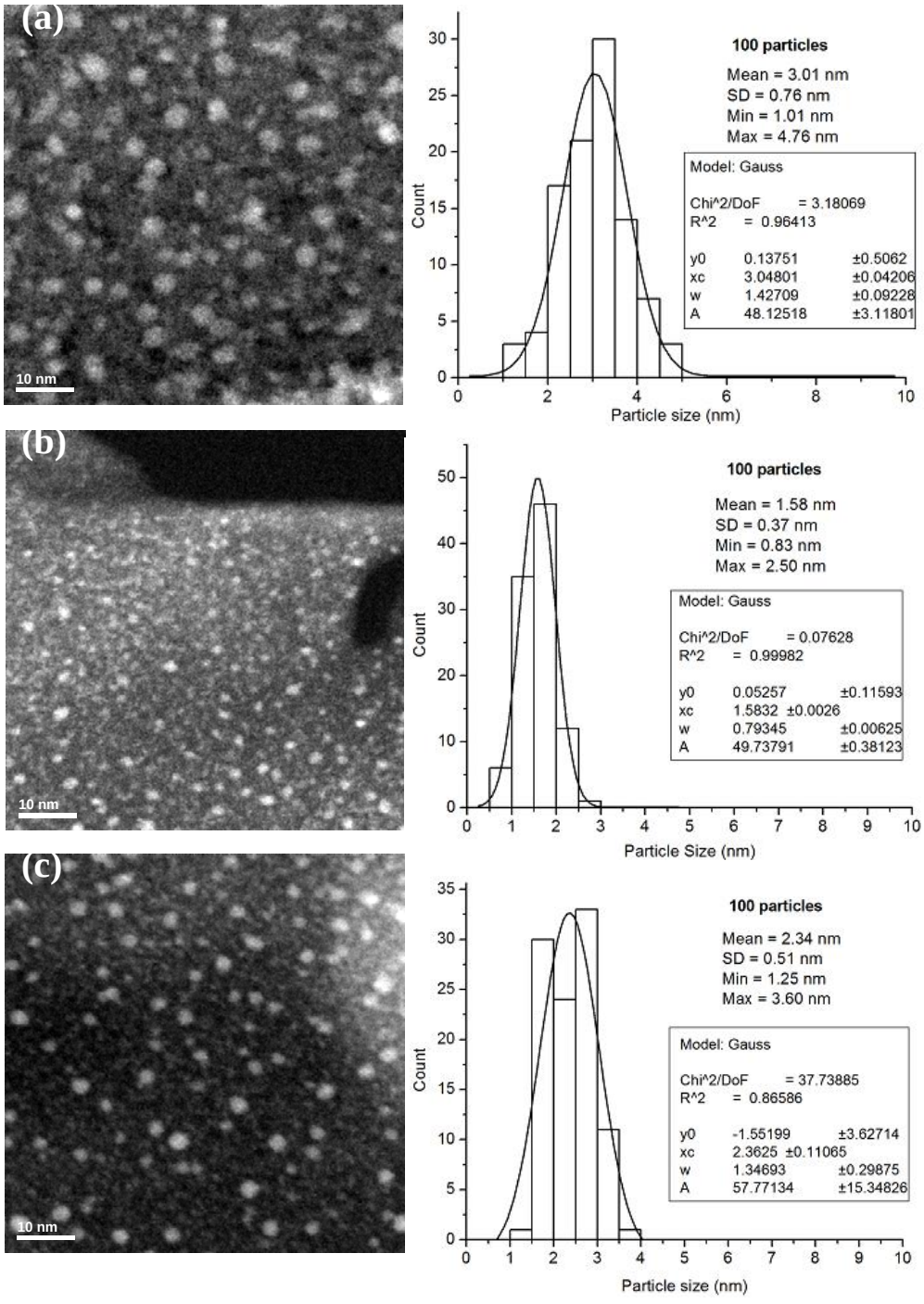

Figure 3.25: TEM images and cluster size statistical count of silver-stained (a) Nafion, (b) plain SPEEK, and (c) SPEEK/PSf-ABIm membranes (in collaboration with Dr. Karalee Jarvis).

High-angle annular dark field scanning transmission electron microscopy (HAADF/STEM) was used to investigate the morphologies of the different membranes. This technique allows the formation of pure mass-thickness contrast images, so it is ideal for the observation of regions where different compositions may exist. However, in Nafion and SPEEK based membranes, the hydrophilic and hydrophobic regions of the polymer showed no contrast due to their similar atomic weight. After substituting the protons by silver ions in the membrane, the contrast between the hydrophobic and hydrophilic regions is increased. In the STEM images, the dark areas represent the hydrophilic (ionic) domain and the brighter areas represent the hydrophobic domain. Figure 3.25 shows the STEM images for Nafion, SPEEK, and the SPEEK/PSf-ABIm polymer blends and the corresponding hydrophilic cluster size distribution. Clearly, Nafion has the largest size distribution, followed by the SPEEK/PSf-ABIm blend and SPEEK which has the smallest cluster size. This trend is consistent with the small angle x-ray scattering data discussed above.

3.3.4.2 Comparison of the Electrochemical Performance of the Blend Membranes

Table 3.6 and Fig. 3.26 compare the proton conductivity, electrochemical performance, and methanol crossover in DMFC of the Naifon, plain SPEEK, and various SPEEK blend membranes.

In Fig. 3.26, all the blend membranes show higher fuel cell performance than plain SPEEK, which is consistent with the higher proton conductivity values in Table 3.6, which were measured at the same temperature. More importantly, although the plain SPEEK membrane shows performance similar to Nafion 115 membrane due to lower proton conductivity, all the blend membranes exhibit higher performance than Nafion 115, confirming the assistance of the heterocycles in enhancing the proton conduction. Since the longer side chain and the more nitrogen sites (four) in amino-benzotriazole may

make the proton hopping much easier in the blend membranes consisting of SPEEK and PSf-BTraz compared to those consisting of other N-heterocycles, the SPEEK/PSf-BTraz membrane shows the highest proton conductivity among these blend membranes.

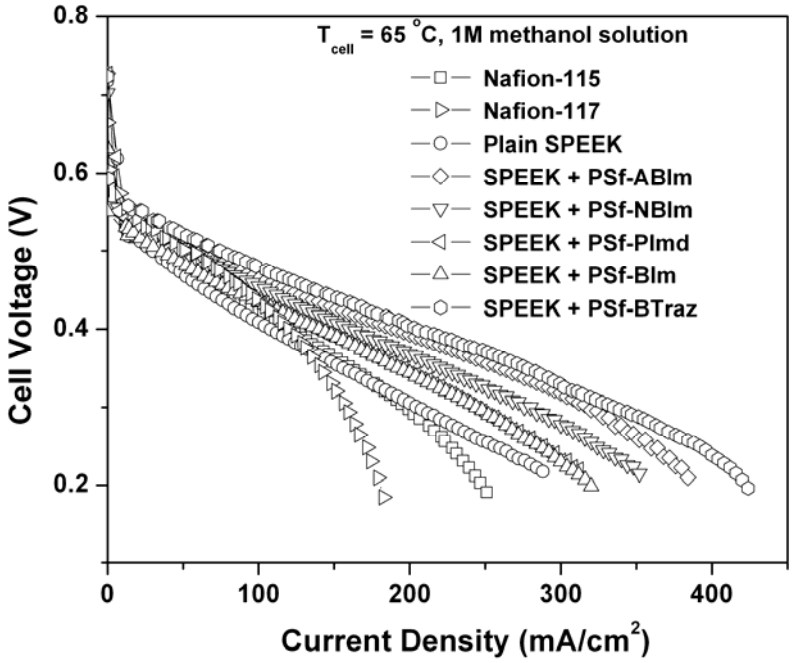

Figure3.26: Comparison of the polarization curves of Nafion-115, Nafion-117, plain SPEEK, and blend membranes consisting of SPEEK and various basic polymers in DMFC. Methanol concentration: 1 M, cell temperature: 65 ^{o}C.

Also, the higher performance could be due to the lower methanol crossover in the blend membranes compared to that in Nafion 115 and plain SPEEK as seen in Table 3.6. Methanol crossover is a critical parameter for long-term DMFC operation and has a significant effect on the overall performance of DMFC. Among the blend membranes studied, the SPEEK/PSf-PImd blend membranes show the lowest methanol crossover due to the largest size of the 1*H*-Perimidine side groups in the basic polymers. This conclusion is also supported by the observed open-circuit voltage (OCV) of DMFC at the

steady-state. The lower methanol crossover could suppress the cathode catalyst poisoning and lower the mixed potential at cathode, resulting in an increase of the OCV at steady-state. When comparing the OCV of the SPEEK/PImd with that of the plain SPEEK and Nafion membranes, the blend membrane shows 0.05 and 0.11 V higher than, respectively, plain SPEEK and Nafion 115 membranes. More interestingly, even though the blend membranes show larger ionic cluster size than plain SPEEK, they exhibit lower methanol crossover, indicating the effectiveness of the basic polymers in blocking methanol permeation by the insertion of the heterocycle side groups into the hydrophilic region that are formed by the sulfonic acid groups of the SPEEK polymer. Since the blend membranes show increased proton conductivity and suppressed methanol crossover than plain SPEEK, they all show higher maximum power density in DMFC compared to plain SPEEK and Nafion 115 membranes.

Table 3.6: Comparison of the proton conductivity (σ), open-circuit voltage (OCV), maximum power density, and methanol crossover current density in DMFC of plain SPEEK, Nafion-115, Nafion-117, and blend membranes consisting of various basic polymers. For DMFC operation, methanol concentration was 1 M and the cell temperature was 65 ^{o}C.

Membranes	OCV (V)	Maximum power density (mW/cm^2)	Methanol crossover current density (mA/cm^2)	σ 65 ^{o}C, 100% R.H. (mS/cm)
Nafion-115	0.63	59	122	144
Nafion-117	0.71	49	86	143
SPEEK	0.69	64	115	69
SPEEK / PSf-ABIm	0.71	95	95	93
SPEEK / PSf-NBIm	0.73	84	87	87
SPEEK / PSf-BIm	0.72	73	91	79
SPEEK / PSf-PImd	0.74	73	77	73
SPEEK / PSf-BTraz	0.72	101	87	96

3.4 CONCLUSIONS

Polysulfone bearing 4-nitro-benzimidazole (PSf-NBIm), 1*H*-Perimidine (PSf-PImd), and 5-amino-benzotriazole (PSf-BTraz) have been synthesized by a condensation reaction between carboxylated polysulfone and appropriate N-containing precursors. Blend membranes consisting of sulfonated poly(ether ether ketone) (SPEEK) (an acidic polymer) and various contents (0 - 8.0 wt.%) of PSf-NBIm, PSf-PImd, or PSf-BTraz (a basic polymer) have been characterized by ion-exchange capacity, liquid uptake, proton conductivity, ionic cluster size, methanol crossover, and fuel cell performance measurements. The blend membranes exhibit higher proton conductivity, lower liquid uptake in water and methanol solution, lower methanol crossover, and better performance in DMFC compared to plain SPEEK membrane. The SAXS and TEM data show that all the SPEEK based membranes exhibit smaller ionic cluster size compared to Nafion membrane due to the more rigid backbone of the aromatic polymers. However, all the blend membranes show larger ionic cluster size than plain SPEEK due to the insertion of the heterocycle side groups into the ionic cluster formed by the sulfonic acid groups of SPEEK. Also, the scattering peaks of SAXS profile shift to lower q value with increasing N-heterocycle size in the blend membranes, resulting in an increase in the ionic cluster size. Despite the increase in ionic cluster size, the blend membranes exhibit lower liquid uptake in water and methanol/water solutions and reduced methanol crossover due to the hydrophobicity and methanol blocking effect of the hetrocycle groups. The blend membranes with an optimized hetrocycle-tethered polysulfone content show better electrochemical performance in DMFC than plain SPEEK due to an enhancement in proton conductivity through the acid-base interactions and a reduction in methanol crossover.

The size and pKa values of the tethered N-heterocycle groups play a critical role in tuning the methanol permeability property of this type of acid-base blend membranes. Among the various blend membranes studied, the SPEEK/PSf-PImd blend membrane shows the lowest methanol crossover among all the blend systems studied due to the largest size of the 1*H*-perimidien group. The SPEEK/PSf-BTraz blend membrane shows the highest proton conductivity and electrochemical performance due to the easiest proton transfer through the 5-amino-benzotriazole groups. For example, the blend membrane consisting of SPEEK and 5 wt. % PSf-BTraz exihibit 2 and 1.8 times maximum power density than, respectively, Nafion 115 and plain SPEEK membranes at 80 ^{o}C with 1 M methanol feed. The blend membrane strategy presented in this chapter represents as an effective way to increase proton conductivity and lower the methanol crossover of the aromatic polymer membranes for DMFC applications.

CHAPTER 4

N, N'-Bis-(1H-benzimidazol-2-yl)-isophthalamide as an Additive in Sulfonated Polymer Membranes for Direct Methanol Fuel Cells

4.1 INTRODUCTION

In Chapter 3, blend membranes based on acid-base interactions were presented, and the N-heterocycle tethered polysulfone polymers were found to be effective in suppressing methanol crossover in the SPEEK-based blend membranes. To further investigate the methanol-blocking effect of the heterocycles in blend membranes, *N*,*N*'-Bis-(1H-benzimidazol-2-yl)-isophthalamide (BBImIP) [151], which contains two amino-benzimidazole groups bonded to a phenyl ring, is synthesized and investigated in this chapter as an additive to sulfonated polymers. With two 2-amino-benzimidazole groups, which could greatly increase the proton transfer sites, and three phenyl rings, which are compatible with the aromatic polymers, BBImIP is appealing as an additive to aromatic polymers like SPSf or SPEEK for use in DMFC. Also, the similarities in the structural features of polysulfone and SPEEK offer good compatibility and mechanical stability. With these perspectives, the blending of BBImIP with SPSf and SPEEK and their effects on the ion-exchange capacity, proton conductivity, cell performance in DMFC, and methanol crossover are presented.

4.2 EXPERIMENTAL

4.2.1 Materials

Isophthalic acid (IPA, 99%) and 2-amino-benzimidazole (99%) were purchased from Acros Organics. The methanesulfonic acid (MSA, 99%) and phosphorus pentoxide

were purchased from Fisher Scientific. Trimethylsilyl chlorosulfonate (TMCS) (98 wt.%) was purchased from Aldrich. Polysulfone (Udel-1700) was provided by Udel. All chemicals were used as-received without further purification. The sulfonation procedure of poly(ether ether ketone) is presented in Chapter 2. SPEEK with a degree of sulfonation of 42 % and IEC of 1.31 meq./g was used.

4.2.2 Sulfonation of Polysulfone

The sulfonation reaction was carried out in a 150 mL three-neck flask equipped with a nitrogen inlet and a magnetic stirrer. In a typical reaction, 5 g of polysulfone was dissolved in 100 mL of chloroform at room temperature and treated with TMCS to produce a silyl sulfonate polysulfone intermediate. The amount of the intermediate produced depended on the mole ratio x of the sulfonating agent to the polymer-repeat units (x = 3.2). After holding the reaction at room temperature for 24 h, a slight excess of sodium methoxide was added to the solution and kept for 2 h to cleave the silyl sulfonate intermediates and to produce the final sulfonated product. The solution was later poured into 800 mL methanol to participate the polymer, followed by filtering and washing thoroughly with methanol, rinsing several times with de-ionized water, and drying in a vacuum oven at 110 ºC for 24 h. The sulfonated polysulfone (SPSf) with an IEC of 0.86 meq../g and DS of 42 % was used in this study.

4.2.3 Synthesis of *N*,*N*'-Bis-(1H-benzimidazol-2-yl)-isophthalamide

N,*N*'-Bis-(1H-benzimidazol-2-yl)-isophthalamide (BBImIP) was synthesized by using phosphorus pentoxide-methanesulfonic acid (PPMA) as a dehydration agent, as shown in Fig. 4.1. Phosphorus pentoxide (2.5 g, 16 mmol) was dissolved in methanesulfonic acid (25 mL, 385 mmol) at 60 ^{o}C while purging with nitrogen gas in a three-necked flask to prepare PPMA. Isophthalic acid (0.456 g, 2.8 mmol) and 2-amino-

benzimidzole (0.731 g, 5.5 mmol) were then added to PPMA and the mixture was stirred at 100 ^{o}C for 5 h. After the reaction was complete, the mixture was poured into de-ionized water to precipitate the product from the PPMA solution. The precipitate was then filtered and the solid was neutralized with 20 % NaOH solution (500 mL) overnight, followed by filtering and washing with de-ionized water before drying the product in a vacuum oven at 100 ^{o}C for overnight.

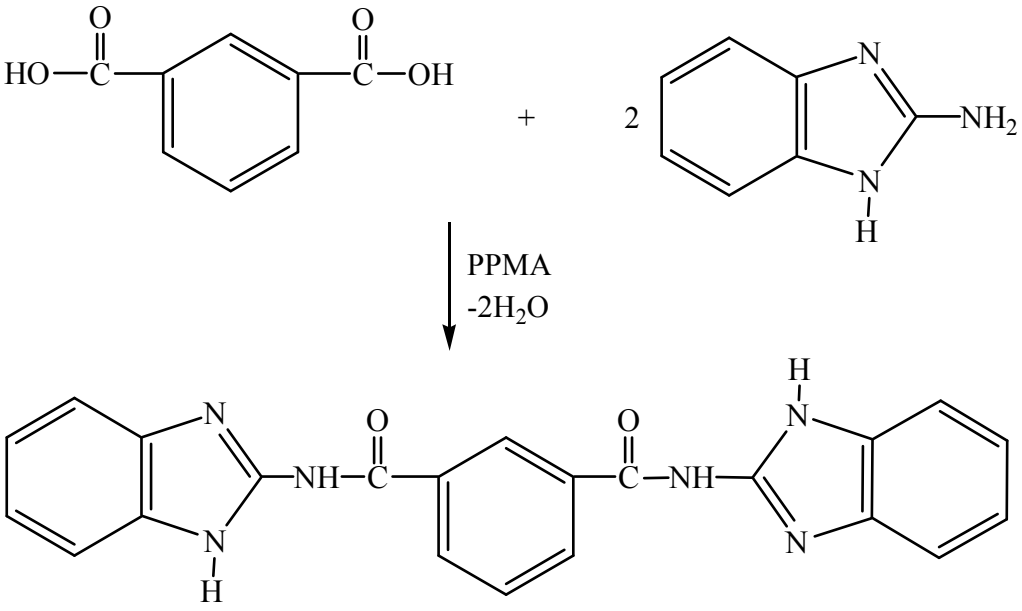

Figure 4.1: Synthesis scheme of *N,N'*-Bis-(1H-benzimidazol-2-yl)-isophthalamide by PPMA.

4.2.4 Membrane Preparation

Plain SPSf or SPEEK membrane and their blend membranes with BBImIP were prepared by a casting method, employing a *N,N'*-dimethylacetamide (DMAc) solution. All membranes were dried at 90 ^{o}C overnight, followed by holding in a vacuum oven at 130 ^{o}C for 6 h. The membranes were washed thoroughly with boiled de-ionized water several times to remove the residual solvent. The thickness of the membrane was

controlled by changing the amount of SPSf or SPEEK and BBImIP in the solution, and all the membranes in this study had a thickness of 50 ±5 μm with an active area for DMFC evaluation of 5 cm^2.

4.2.5 Membrane-electrode Assembly (MEAs) Fabrication

The electrodes (consisting of gas-diffusion and catalyst layers) for testing in DMFC were prepared as discussed in Chapter 2. The anode and cathode catalysts consisted of, respectively, commercial 40 wt.% Pt-Ru (1:1) on Vulcan carbon (E-TEK) and commercial 20 wt.% Pt on Vulcan carbon (Alfa Aesar). The electrodes prepared were impregnated with Nafion solution (5 wt.% solution, DuPont Fluoro-products) by a spray technique and dried at 90 ºC under vacuum for 30 min. The loadings for cathodes (Pt) and anode (Pt-Ru) were 1.0 and 0.6 mg/cm^2, respectively, and the Nafion loading for both the anode and cathode catalysts was 0.35 mg/cm^2. The membrane-electrode assemblies (MEAs) were fabricated by uniaxially hot-pressing the anode and cathode onto a membrane at 140 ºC for 3 min. The electrochemical performances in DMFC of the MEAs thus fabricated were evaluated with a single-cell fixture having an active area of 5 cm^2 and feeding a preheated methanol solution into the anode at a flow rate of 2.0 mL/min by a peristaltic pump without back pressurization and humidified oxygen into the cathode at a flow rate of 200 mL/min with a back pressure of 20 psi.

4.3 RESULTS AND DISCUSSION

4.3.1 Structure Characterization of BBImIP

Fig. 4.2 shows the FTIR spectra of 2-amino-benzimidazole, isophthalic acid, and BBImIP. The C=O asymmetric stretching (1680 cm^{-1}) in isophthalic acid and the C=N asymmetric stretching (1650 cm^{-1}) in 2-amino-benzimidazole are both present in BBImIP, indicating that the amino-benzimidazole groups are tethered to the carboxylic

acid group. The absorption peak of N-H at 3400 cm^{-1} in the BBImIP further confirms the formation of the aimed product.

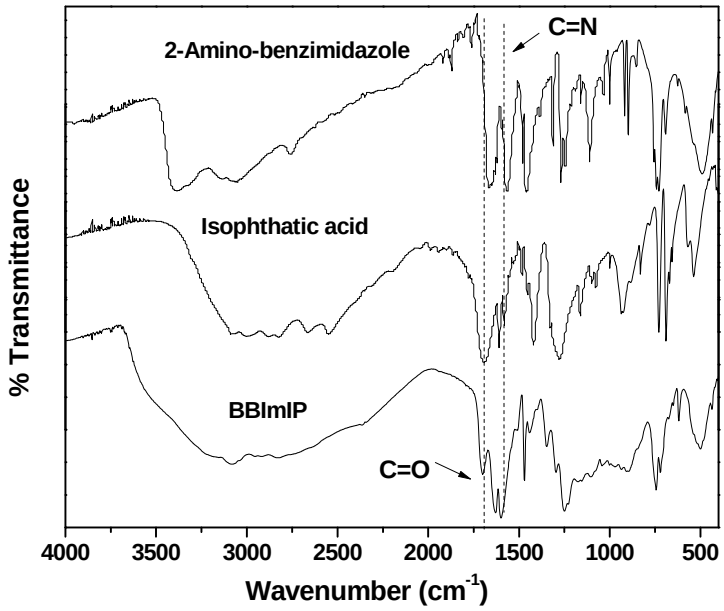

Figure 4.2: FTIR spectra of 2-Amino-benzimidazole, IPA, and BBImIP.

Fig. 4.3 shows the ^{1}H-NMR spectrum of the synthesized BBImIP. It shows ^{1}H NMR (in DMSO-d_6) peaks with chemical shift values of 8.93 (1H), 8.30 (2H), 7.69 (1H), 7.50 (4H), and 7.21 (4H). Based on the NMR results, the yield was calculated to be 90 %.

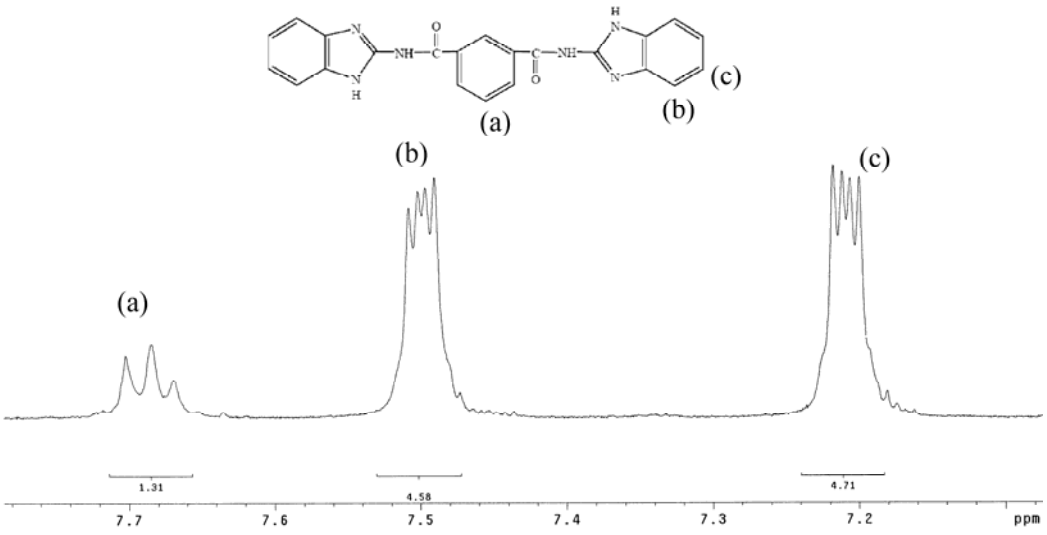

Figure 4.3: ^{1}H-NMR spectrum of the synthesiszed N,N'-Bis-(1H-benzimidazol-2-yl)-isophthalamide (BBImIP).

4.3.2 IEC and Proton Conductivity of the SPSf/BBImIP Blend Membranes

In order to study the effect of BBImIP on proton transfer in the SPSf/BBImIP blend membranes, proton conductivity was measured under anhydrous conditions. Fig. 4.4 compares the proton conductivities of the SPSf/BBImIP blend membranes with various contents of BBImIP and plain SPSf membrane. Proton conduction under anhydrous conditions can be considered to be mainly due to the hopping of proton between the sulfonic acid groups of SPSf and the nitrogen atoms of BBImIP. The 2-amino-benzimidazole (ABIm) in BBImIP contains six nitrogen atoms, which could act as proton acceptors and donors and help proton hopping under anhydrous conditions.

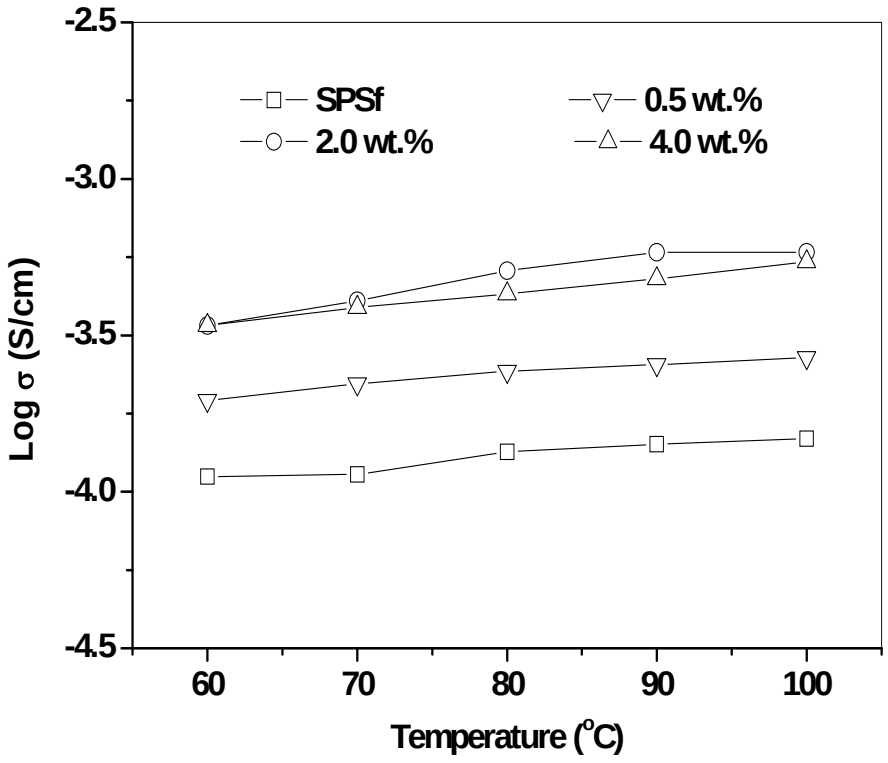

Figure 4.4: Variations of the proton conductivities of the plain SPSf and SPSf/BBImIP blend membranes under anhydrous conditions with temperature. The wt.% values refer to the BBImIP content.

As seen in Fig. 4.4, all the blend membranes show higher conductivities than plain SPSf at a given temperature due to the presence of BBImIP and the hopping of protons through it. However, the proton conductivity is highest at 0.5 – 2 wt.% BBImIP ([-SO_3H]/[ABIm] ratio = 33.9 to 8.3), and it decreases as the content of BBImIP increases to 4.0 wt.% ([-SO_3H]/[ABIm] ratio = 4.1), suggesting that the proton conductivity is maximized at an optimum content of BBImIP in this kind of blend membranes. At higher BBImIP content, the increasing possibility of crosslinking between

sulfonic acid and 2-amino-benzimidazole groups results in a lowering of proton conductivity.

Table 4.1: Ion-exchange capacity (IEC) and proton conductivity (σ) of plain SPSf and SPSf/BBImIP blend membranes with various [-SO_3H]/[ABIm] (ABIm = 2-amino-benzimidazole) molar ratios

Membrane	[-SO_3H]/[ABIm] Ratio	IEC (meq./g)	σ at 100 % RH (S/cm)	
			65ºC	80ºC
Plain SPSf	-	0.86	3.1×10^{-2}	3.4×10^{-2}
SPSf + 0.5 wt.% of BBImIP	33.9	0.76	2.3×10^{-2}	2.6×10^{-2}
SPSf + 2.0 wt.% of BBImIP	8.3	0.57	2.7×10^{-2}	2.9×10^{-2}
SPSf + 4.0 wt.% of BBImIP	4.1	0.43	1.3×10^{-2}	1.7×10^{-2}

Table 4.1 compares values of ion-exchange capacity and proton conductivity measured under 100 % relative humidity (RH) at 65 and 80 ^oC for various contents of BBImIP (or [-SO_3H]/[ABIm] ratios) in the SPSf/BBImIP blend membranes. It can be seen that the IEC values of the blend membranes are lower than that of plain SPSf, indicating the occurrence of acid-base interactions in the blend membranes and the consequent reduction in the amount of H^+ ions dissociating from sulfonic acid groups. Moreover, the IEC value decreases as the content of BBImIP increases due to an increase in the degree of acid-base interaction. The proton conductivities of the blend membranes are also lower than the plain SPSf membrane. In the SPSf/BBImIP blend membranes, all the 2-amino-benzimidazole groups may be protonated due to the excess sulfonic acid groups present (see the [-SO_3H]/[ABIm] ratio in Table 4.1). The protonated 2-amino-benzimidazole groups can help proton transfer by hopping. Therefore, it can be anticipated that proton conduction may occur by both vehicle-type and hopping mechanisms under humidified conditions. The vehicle-type mechanism could occur in the hydrophilic regions formed by the clustering of the sulfonic acid groups, while the

hopping mechanism could occur in the regions where the 2-amino-benzimidazole of BBImIP may insert into the hydrophilic regions formed by the sulfonic acid group cluster due to acid-base interaction. Thus, the vehicle-type mechanism may be predominant in both the plain SPSf membrane and the SPSf/BBImIP blend membranes under humidified conditions, resulting in a lower proton conductivity values for the blend membranes compared to the plain SPSf since proton transfer through 2-amino-benzimidazole by the hopping mechanism could be more sluggish than that by the vehicle-type mechanism. Also, the proton conductivity values measured under hydrous condition were much higher than those measured under anhydrous condition, suggesting that the vehicle-type mechanism is predominant in the blend membranes under 100 % humidified condition.

4.3.3 Electrochemical Performance and Methanol Crossover of SPSf/BBImIP Blend Membranes in DMFC.

Fig. 4.5 compares the polarization curves of the SPSf/BBImIP blend membranes with various contents of BBImIP at 65 ^{o}C, recorded with 1 M methanol solution as the fuel. The fuel cell performances of blend membranes are lower than that of plain SPSf membrane due to their lower proton conductivities under humidified conditions as seen in Table 4.1. Also, as the content of BBImIP increases, the fuel cell performance decreases. For the SPSf/BBImIP blend membrane with 2.0 wt.% BBImIP, the slope in the linear part of the polarization curve, which is reflective of the bulk resistance of the membrane, is smaller than those of the other two blend membranes due to the higher proton conductivity. In addition, all the SPSf/BBImIP blend membranes show higher open circuit voltages (OCVs) than the plain SPSf membrane, which could be related to the lower methanol crossover through the blend membranes and a reduced poisoning of the cathode catalyst by methanol [34].

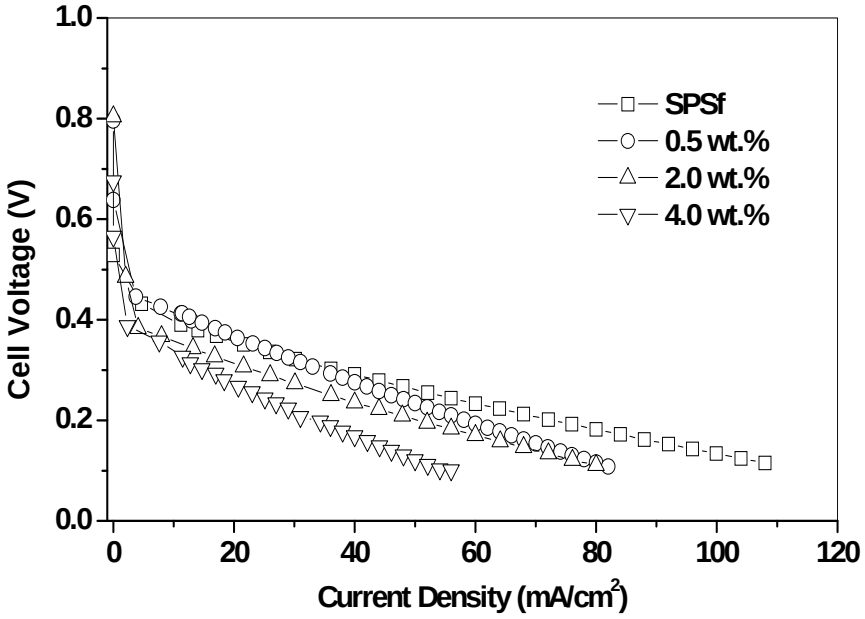

Figure 4.5: Comparison of the polarization curves of the plain SPSf and SPSf/BBImIP blend membranes in DMFC. The wt. % values refer to the BBImIP content. Methanol concentration: 1 M, cell temperature: 65 ^{o}C.

Fig. 4.6 compares the methanol crossover current densities of the SPSf/BBImIP blend membranes with various contents of BBImIP. It is well known that SPSf membrane usually exhibits lower methanol crossover than Nafion membrane due to its narrow water/methanol pathway. It can be seen that the SPSf/BBImIP blend membranes exhibit even much lower methanol crossover than the plain SPSf, indicating the effectiveness of BBImIP in blocking methanol crossover by inserting into the hydrophilic regions formed by the sulfonic acid groups. While the protonated 2-amino-benzimidazole could help proton transfer by hopping, it could block methanol permeability through the hydrophilic region. The lower methanol crossover in the SPSf/BBImIP blend membrane could help to

lower the Pt catalyst loading at the cathode in addition to lowering the methanol fuel waste.

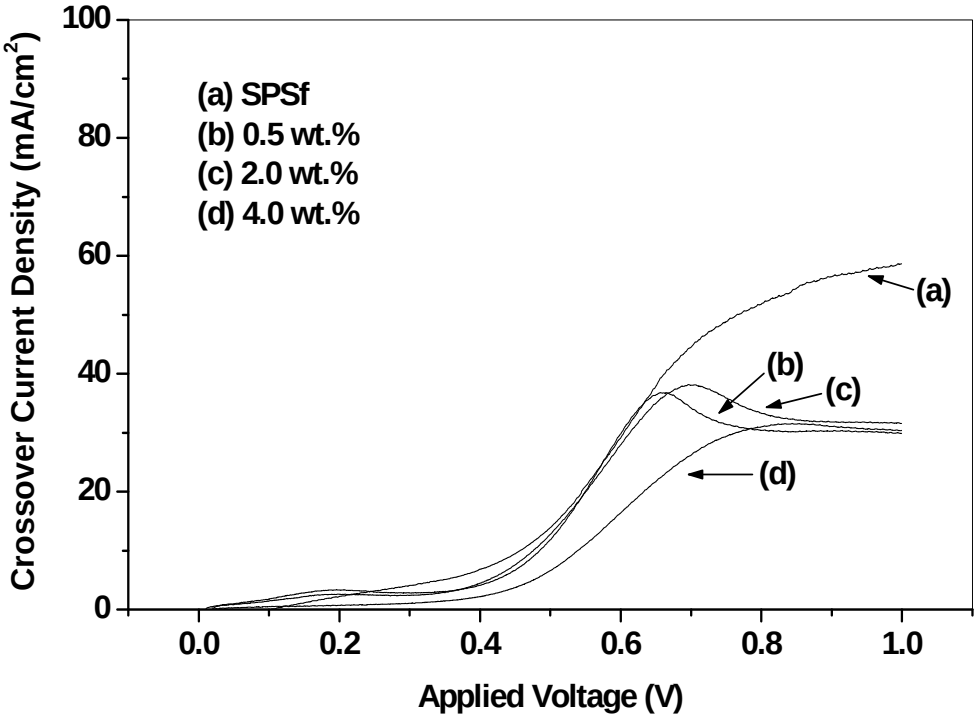

Figure 4.6: Comparison of the variations of the methanol crossover current density for the plain SPSf and SPSf/BBImIP blend membranes in DMFC. The wt. % values refer to the BBImIP content. Methanol concentration: 1 M, cell temperature: 65 ^{o}C.

4.3.4 DMFC Evaluation of SPEEK/BBImIP Membranes

To study the effect of BBImIP in other sulfonated polymer systems, fuel cell performances and methanol crossover values of the SPEEK/BBImIP blend membranes were also measured and compared with those of plain SPEEK membrane. For SPEEK membranes, the degree of sulfonation has a profound effect on the ion-exchange capacity (IEC), proton conductivity, and water uptake. Although the proton conductivity of

SPEEK increases with increasing degree of sulfonation, SPEEK membranes with degree of sulfonation higher than 60% exhibit high water uptake and methanol permeability, which could degrade the mechanical stability and increase the methanol crossover during fuel cell operation. Generally, SPEEK membranes with degree of sulfonation between 40 and 55 % show reasonable proton conductivity, low solubility, and good mechanical stability. With this perspective, we chose SPEEK with a degree of sulfonation of 42 % and IEC of 1.31 meq./g for studying the effect of BBImIP.

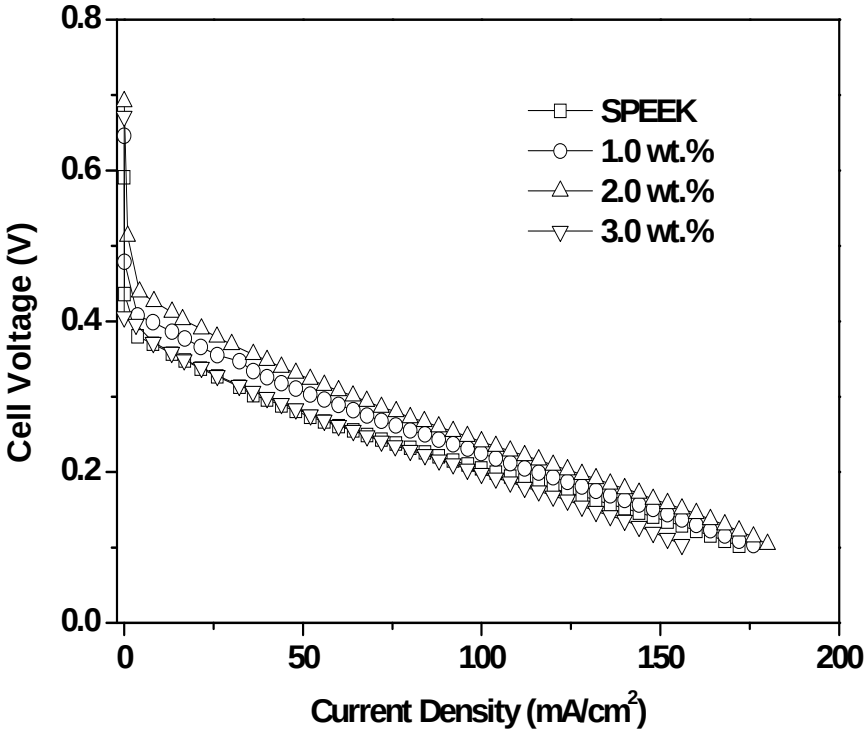

Figure 4.7: Comparison of the polarization curves of the plain SPEEK and SPEEK/BBImIP blend membranes in DMFC. The wt. % values refer to the BBImIP content. Methanol concentration: 1 M, cell temperature: 65 ^{o}C.

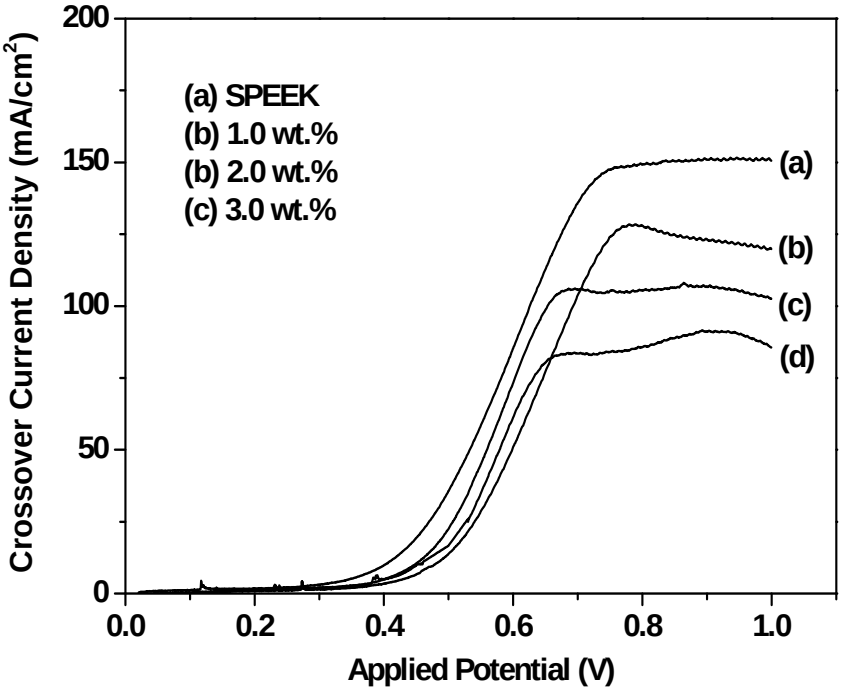

Figure 4.8: Comparison of the variations of the methanol crossover current density for the plain SPEEK and SPEEK/BBImIP blend membranes in DMFC. The wt.% values refer to the BBImIP content. Methanol concentration: 1 M, cell temperature: 65 ^{o}C.

Fig. 4.7 compares the polarization curves of the SPEEK/BBImIP blend membranes with various contents of BBImIP (1.0, 2.0, and 3.0 wt.%) at 65 ^{o}C, recorded with 1 M methanol solution as the fuel. As seen, the SPEEK/BBImIP blend membrane with 1.0 and 2.0 wt.% BBImIP show higher fuel cell performances than the plain SPEEK membrane. However, as the content of BBImIP increases to 3.0 wt.%, the fuel cell performance of the blend membrane decreases slightly lower than that of the plain SPEEK membrane. Also, the blend membranes show higher OCVs than the plain SPEEK membrane due to a suppression of methanol crossover. The higher fuel cell performance of the SPEEK/BBImIP blend membranes with certain compositions compared to that of

plain SPEEK, which is in contrast to that found with the SPSf/BBImIP blend membranes in Fig. 4.5, may be related to the stronger acidity of the sulfonic acid groups in SPEEK. The sulfonated phenyl ring in SPEEK is more electron withdrawing than that in SPSf, which leads to strong acidity. The stronger acidity of the sulfonic acid groups in SPEEK could help to enhance the proton conduction by the hopping mechanism in the SPEEK/BBImIP blend membranes, resulting in improved fuel cell performance.

Fig. 4.8 compares the methanol crossover current densities of the SPEEK/BBImIP blend membranes with various contents of BBImIP. As seen, BBImIP in the SPEEK/BBImIP blend membrane lowers methanol crossover similar to that in the SPSf/BBImIP blend membranes. In addition, the methanol crossover decreases gradually as the content of BBImIP in the SPEEK/BBImIP blend membranes increases.

4.4 CONCLUSION

N,*N*'-Bis-(1H-benzimidazol-2-yl)-isophthalamide (BBImIP) has been synthesized and explored as an additive, for the first time, in sulfonated aromatic polymer membranes like sulfonated polysulfone (SPSf) and sulfonated poly(ether ether ketone) (SPEEK) for use in DMFC. While the SPEEK/BBImIP blend membranes with 1.0 – 3.0 wt.% BBImIP exhibit performance in DMFC similar to better than that of plain SPEEK membrane, the SPSf/BBImIP blend membranes with 0.5 – 4.0 wt.% BBImIP show lower performance than plain SPSf in DMFC. Nevertheless, both the blend membranes offer an important advantage of suppressed methanol crossover in DMFC compared to their plain counterparts SPEEK or SPSf. The reduced methanol crossover of the SPSf/BBImIP or SPEEK/BBImIP blend membranes in DMFC could result in better long-term performance and lower cathode catalyst loading. The study demonstrates that blend membranes based on acid-base interactions between acidic and basic aromatic polymers may offer an attractive strategy to develop high performance membranes for DMFC.

CHAPTER 5

Novel Sulfonated Poly(arylene ether sulfone) as a Methanol Barrier in Multilayer Membranes for Direct Methanol Fuel Cells

5.1 INTRODUCTION

As discussed in the previous chapters, sulfonated aromatic polymers like SPEEK and SPSf have been found to show lower methanol crossover compared to Nafion membrane in DMFC. The degree of sulfonation (DS) with these membranes could be controlled by the reaction time and the amount of sulfonating agent (H_2SO_4, SO_3) used in the reaction. Also sulfonated aromatic polymers could be synthesized through the polymerization reactions of different sulfonated monomers. With this strategy, several proton exchange membranes with controllable chemical structures (controllable degree of sulfonation and sulfonation sites) and well-defined microstructures have been investigated. It has been found that to improve the osmotic and hydrolytic stability of the sulfonated polymers, an increasing hydrophilic-hydrophobic separation is desired by locating the sulfonic acid groups away from the polymer main chains [152-155].

With this perspective, our group reported recently novel sulfonated copolymers consisting of pendant sulfonic acid groups, which were synthesized by a nucleophilic displacement polymerization reaction, employing 4,4'-difluorodiphenylsulfone (DHNS) and a hydroxyl terminated monomer like hydroquinone, 4,4-diphenol, and 4,4-thiodiphenol in presence of potassium carbonate as shown in Fig. 5.1 [156]. The resulting product copolymers were designated, respectively, as SPS-HQ, SPS-DP, and SPS-TDP. These polymers showed low methanol permeability and liquid uptake in water and methanol solutions as shown in Fig. 5.2 and Fig. 5.3.

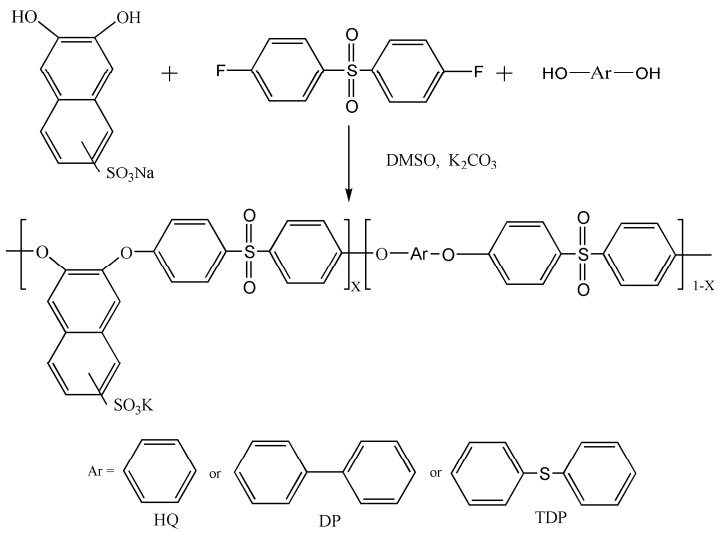

SPS-HQ: Ar = HQ and 50 mol% DHNS
SPS-DP: Ar = DP and 60 mol% DHNS
SPS-TDP: Ar = TDP and 60 mol% DHNS

Figure 5.1: Synthesis scheme of the SPS-HQ, SPS-DP, and SPS-TDP polymers.

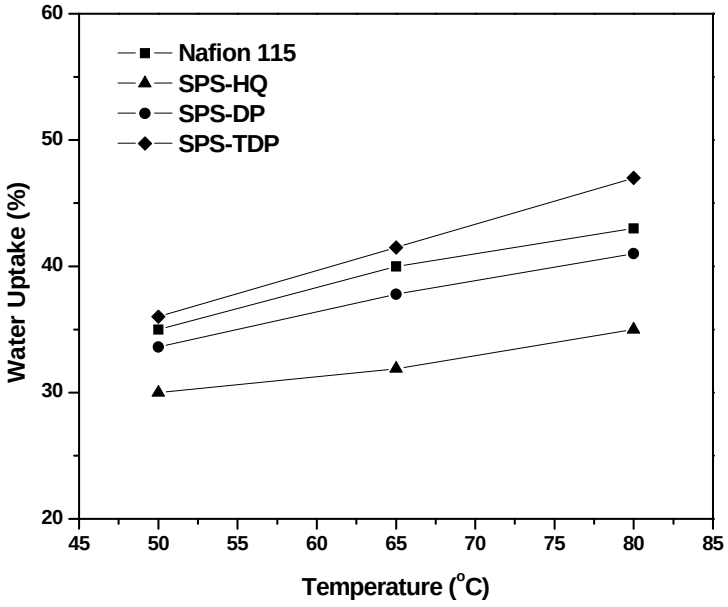

Figure 5.2: Comparison of the water uptakes of the SPS-HQ, SPS-DP, and SPS-TDP polymers.

Even though the SPS-DP copolymer showed the highest proton conductivity among these copolymers, the value is still low compared to other sulfonated aromatic polymers such as SPEEK and SPSf. Due to the low proton conductivity of the copolymer, thinner membranes compared to SPEEK or Nafion are needed for DMFC operation to achieve low cell resistance. Unfortunately, very thin membranes will sacrifice the mechanical property and generate issues related to membrane-electrode assembly (MEA) fabrication since brittle thin membranes tend to break during the hot-pressing process.

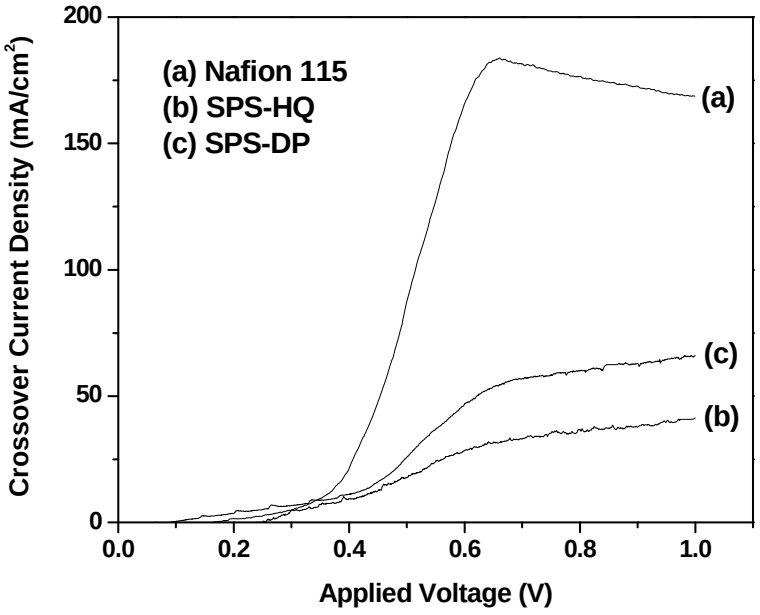

Figure 5.3: Comparison of the methanol crossover current densities of the MEAs fabricated with the (a) Nafion 115, (b) SPS-HQ, and (c) SPS-DP membranes. The cell temperature was 80 ^{o}C and the methanol concentration was 1 M.

One approach to make use of the low methanol permeability of the membranes without introducing too big a cell resistance is to adopt a multilayer membrane approach [157-159] in which a thin layer of the low methanol permeability polymer forms the center layer and a relatively high proton conducting polymer forms the outer layers. For

example, our group [160] reported that multilayer membranes with SPEEK as the methanol-barrier center layer and recast Nafion as the proton conducting outer layers increase the overall cell performance significantly because of the suppressed methanol crossover. Si et al. [161] also reported the use of a Nafion/PVDf/ Nafion (PVDf refers to polyvinylidene fluoride) tri-layer membrane in DMFC, but PVDf is a proton insulator. Jiang et al. [162] reported that SPEEK with different degrees of sulfonation could also be used to fabricate the tri-layer membranes, but the proton conductivity of the methanol-barrier SPEEK is still too low when low methanol permeability is desired.

We present here a further investigation of the chemical and thermal properties of the SPS-DP polymers with different degrees of sulfonation and the fabrication and characterization of tri-layer membranes consisting of a thin inner layer of SPS-DP and two outer layers of SPEEK. The low methanol permeability of the thin SPS-DP layer is expected to suppress the methanol crossover significantly without adversely increasing the cell resistance. The multilayer membranes could also offer good mechanical strength with long-term stability due to the similar backbone structures of SPEEK and SPS-DP polymers. The electrochemical performance, methanol crossover in DMFC, and the structural stability of the multilayer membranes with different thicknesses of the methanol-barrier center layer are presented here.

5.2 EXPERIMENTAL

5.2.1 Materials Synthesis

4,4-difluorodiphenylsulfone (DFDPS, 99 %), 4,4-diphenol (DP, 97 %), anhydrous dimethyl sulfoxide (DMSO, 99.7 %), potassium carbonate (anhydrous), and N,N′-dimethylacetamide (DMAc, 99+%,) were purchased from Acros organics. 6,7-dihydroxy-2-naphthalenesulfonate (DHNS, 98%, sodium form) was purchased from Rintech, Inc.

Poly(ether ether ketone) (PEEK450 PF) was obtained from Victrex. All chemicals were used as-received.

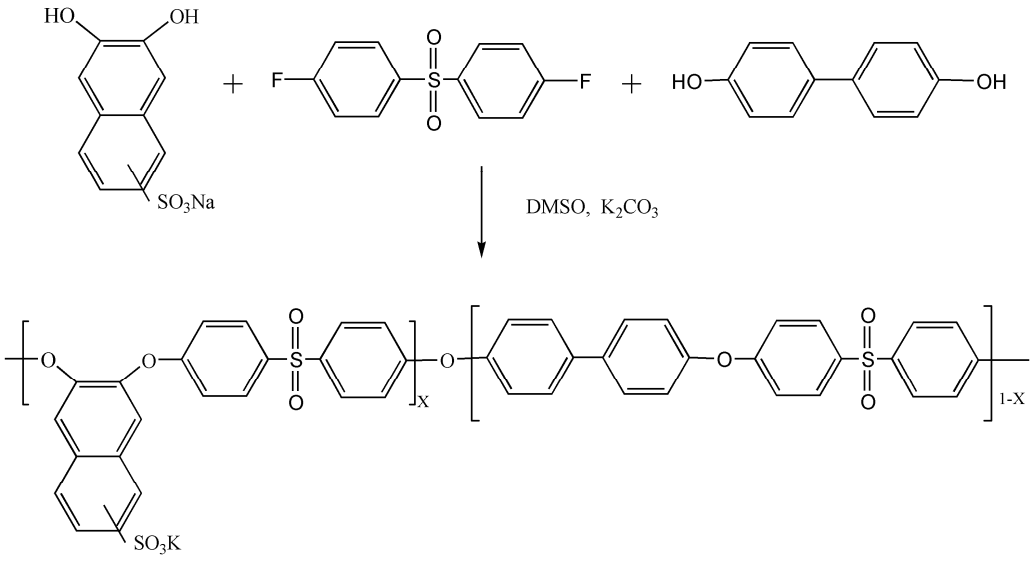

Figure 5.4: Synthesis scheme of the SPS-DP copolymers.

Sulfonated poly(arylene ether sulfone) copolymers were synthesized by an aromatic substitution polymerization reaction as shown in Fig l. In a typical reaction, 5 mmol of DFDPS, 2 mmol of DP, 3 mmol of DHNS, and 12 mL of DMSO were added into a 50 mL three-neck flask equipped with a nitrogen inlet, reflux condenser, and a magnetic stirrer. After the dissolution of the monomer in DMSO, 10 mmol of anhydrous potassium carbonate was added, the solution was heated gradually up to 160 ^{o}C, and maintained at 160 ^{o}C for 72 h. After cooling to room temperature, the dark brown solution was poured into 400 mL of ethanol. The precipitated polymer was then filtered, washed with water thoroughly, and dried in a vacuum oven at 90 ^{o}C overnight. The product polymer thus obtained is designed as SPS-DP-60.

The sulfonated poly(ether ether ketone) (SPEEK) was synthesized by sulfonating PEEK with concentrated sulfuric acid for certain amount of time to get the desired degree of sulfonation. SPEEK with an ion-exchange capacity (IEC) of 1.56 and a degree of sulfonation (DS) of 51 % was used in this study [163].

5.2.2 Membrane Preparation

The plain SPEEK, SPS-DP, and the multilayer membranes were prepared by a solution casting method employing SPEEK/DMAc (10 % w/w) or SPS-DP/DMAc (10 % w/w) solutions. For the multilayer membranes, a thin SPS-DP-60 membrane with various thickness values (5~30 μm) was first casted, followed by casting two layers of SPEEK membrane on each surface. After casting all the layers, the membranes obtained were hot-pressed at 130 ^{o}C and 20 psi for 2 min. All the plain and multilayer membranes were dried at 90 ^{o}C overnight, held in a vacuum oven at 130 ^{o}C for 6 h, and washed thoroughly with boiled de-ionized water several times to remove the residual solvent. The thickness of the membrane was controlled by changing the amount of SPS-DP or SPEEK during the casting process, and all the membranes in this study had the same total thickness of 60 μm with 5 cm^2 active area.

5.2.3 The Membrane-Electrode Assemblies (MEAs) Fabrication

The electrodes (consisting of gas-diffusion and catalyst layers) for testing in DMFC were prepared as reported in Chapter 2. The anode and cathode catalysts consisted of, respectively, commercial 60 wt.% Pt-Ru (1:1) alloy on Vulcan carbon (E-TEK) and 60 wt.% Pt on Vulcan carbon (Alfa Aesar). The loadings for cathodes (Pt) and anode (Pt-Ru) were 2.5 mg/cm^2 on both sides, and the Nafion loading for both the anode and cathode catalysts was 0.45 mg/cm^2. After the catalyst layers were deposited onto the

gas diffusion layers (A-6 ELAT/SS/NC/ V2 carbon cloth, E-TEK), the resultant anode and cathode electrodes were hot pressed onto the membrane at 120 ^{o}C, 40 psi for 2 min.

5.2.4 Membrane Cross Sectional Characterization.

Before and after the DMFC durability evaluation, the cross-sectional structure of the multilayer membrane was studied with a JEOL JSM-5610 scanning electron microscope (SEM). The samples were prepared by freezing the membrane in liquid nitrogen followed by breaking the frozen membrane with forceps.

5.3 RESULTS AND DISCUSSION

5.3.1 FTIR and NMR Characterization

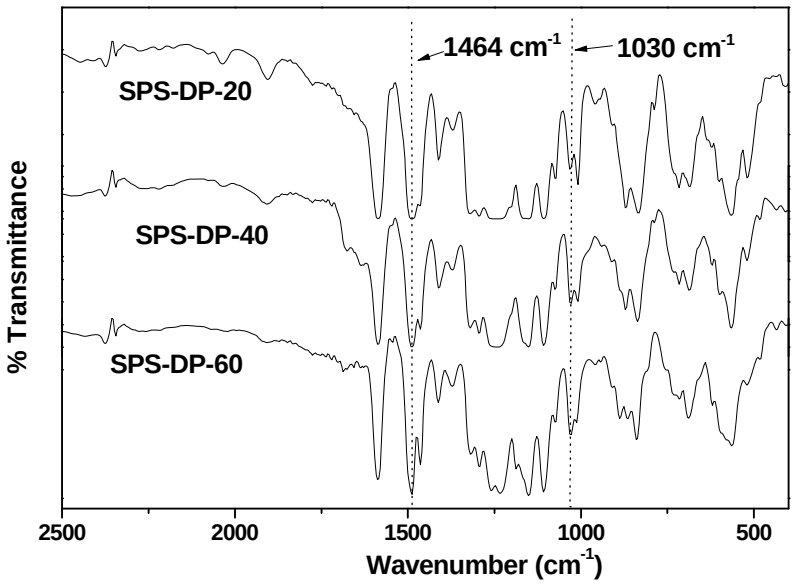

Figure 5.5: FTIR spectra of the SPS-DP copolymers.

The chemical structure of the sulfonated polymers (in acid form) was characterized by FTIR and ^{1}H NMR spectroscopies (Figs. 5.5 and 5.6). Fig. 5.5 compares the FTIR spectra of the sulfonated copolymers obtained with different acid monomer contents. The absorption band at 1030 cm^{-1} corresponds to the aromatic sulfonic acid group in the SPS-DP copolymer. The intensity of this characteristic absorption increases with increasing sulfonated monomer content. The bands at 1230 and 1260 cm^{-1} are assigned to the phenoxy groups. The band at 1464 cm^{-1} is assigned to the phenyl ring and the band at 1588 cm^{-1} is attributed to the C=C stretching vibrations, which are consistent with the literature data reported for other polymers with similar structures [164].

Fig. 5.6 compares the ^{1}H NMR spectra of the SPS-DP copolymers with different degrees of sulfonation. The chemical shifts of the protons in the polymer main chains could be readily assigned since the DFDPS as well as the DP monomer are commonly used in the literature for the synthesis of proton conducting polymers [156,165,166]. The increasing intensities of the hydrogen at H4 position on the naphthalenesulfonate containing units reflect the increasing sulfonated monomer content. Interestingly, by comparing the intensities of the H4 (1H) signal with the H8 (4H) signal of the diphenol segment, we can calculate the degree of sulfonation of the products. For example, the intensity ratio of the H8 (4H) to H4 (1H) proton signal for SPS-DP-40 was 6.68, implying 0.63 diphenol units and hence 0.37 DHNS units containing the sulfonic acid groups. All the IEC values calculated from the NMR data are listed in Table 5.1 with other properties of the copolymers.

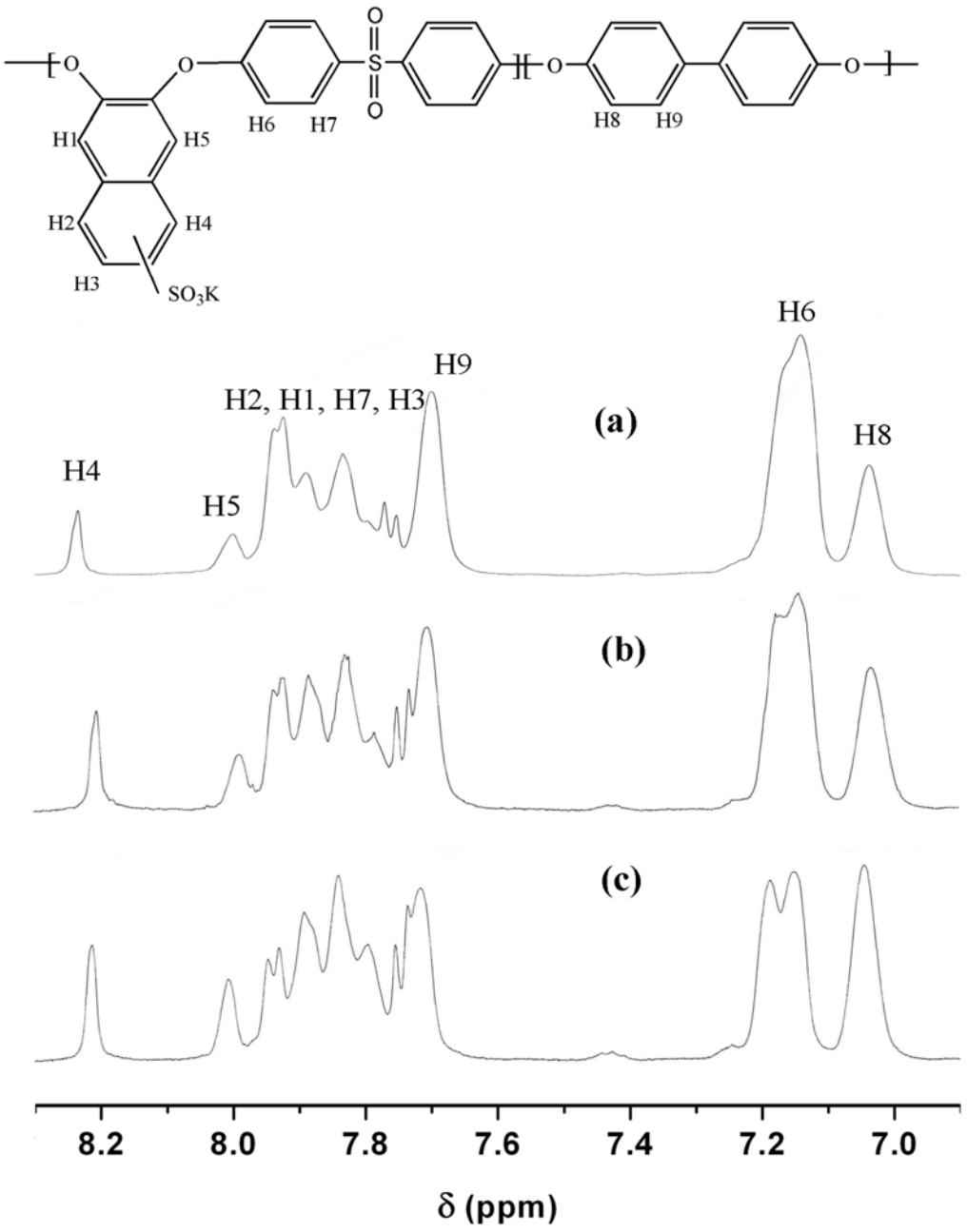

Figure 5.6: ^{1}H NMR spectra of the SPS-DP copolymers with different sulfonated monomer content in DMSO-d6: (a) SPS-DP-20, (b) SPS-DP-40, and (c) SPS-DP-60. The numbers 20, 40, and 60 refer to the sulfonated monomer content used to synthesize the polymer.

5.3.2 Thermal Stability Data

The thermal properties of the copolymers were investigated by TGA and DSC analyses. As seen in Fig. 5.7, all the copolymers show sufficient thermal stabilities in air. The initial weight loss seen at < 100 ^{o}C is attributed to the removal of residual water bonded to the sulfonic acid groups in the polymer. The weight loss related to the decomposition of the sulfonic acid groups from the polymers is in the temperature range of 250 – 450 ^{o}C, which is much higher compared to the DMFC operation temperature (<100 ^{o}C). With increasing degree of sulfonation, the weight loss corresponding to the loss of sulfonic acid groups increases, and the decomposition temperature shifts to lower temperatures. The weight loss seen above 450 ^{o}C is due to the main-chain degradation.

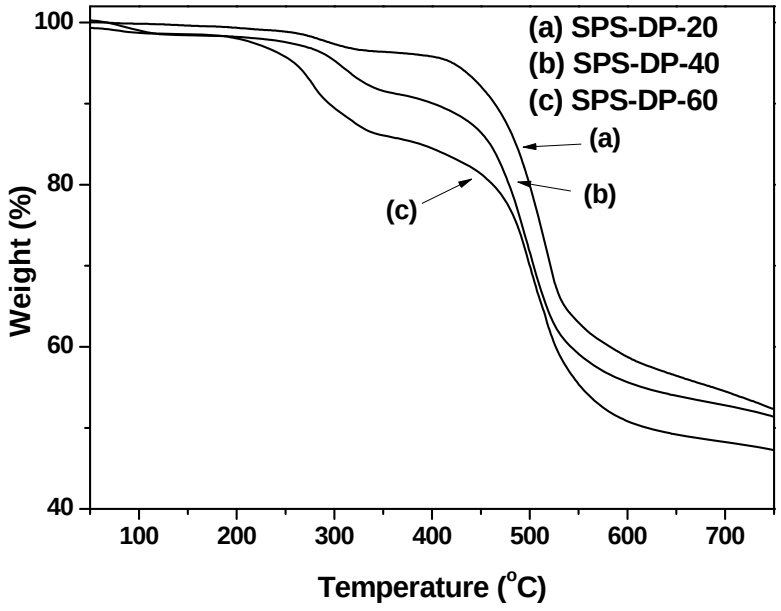

Figure 5.7: TGA plots of the SPS-DP copolymers recorded in flowing air.

For DSC measurements, all the copolymers were first pre-heated at 10 ^{o}C/min to a temperature below their decomposition temperatures, which were derived from the TGA curves collected in nitrogen atmosphere. After cooling down, they were heated again at a rate of 10 ^{o}C/min to their decomposition temperatures, and the data from the second scan are compared in Fig. 5.8. The copolymers show an increase in the glass transition temperature T_g with increasing degree of sulfonation (as seen in Fig. 5.7), which is consistent with other copolymers synthesized from the same sulfonated monomer.

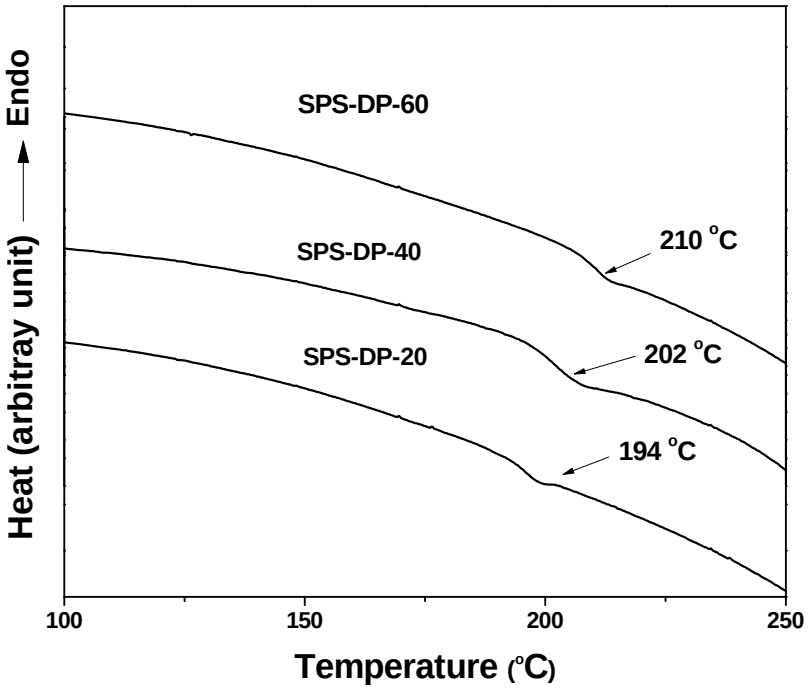

Figure 5.8: DSC plots of the SPS-DP copolymers recorded in flowing nitrogen.

5.3.3 IEC and Liquid Uptake and Proton Conductivity

Table 5.1 gives the ion-exchange capacity (IEC) values, liquid uptake in water and methanol solution, and the proton conductivity values measured under 100 % R.H. at

25 ^{o}C for the sulfonated copolymers with different degrees of sulfonation as well as those of the SPEEK (DS = 51 %) membrane.

Table 5.1: Ion-exchange Capacity (IEC), liquid uptake, and proton conductivity (σ) of SPEEK and SPS-DP membranes with different degrees of sulfonation.

Polymer	IEC from titration (meq./g)	IEC from NMR (meq./g)	Theoretical IEC (meq./g)	Liquid uptake				σ* (mS/cm)
				In water (%)		In 1 M methanol solution (%)		
				25 ^{o}C	65 ^{o}C	25 ^{o}C	65 ^{o}C	
SPS-DP-20	0.46	0.47	0.48	4.9	5.2	5.9	6.2	11
SPS-DP-40	0.89	0.90	0.94	13.1	16.5	16.7	17.3	18
SPS-DP-60	1.31	1.32	1.36	17.6	27.8	18.2	30.9	31
SPEEK	1.56	-	-	32.9	47.5	36.3	58.6	45

* 100 % RH at 25 ^{o}C

The SPS-DP copolymers show IEC values in the range of 0.46 to 1.32 with increasing degree of sulfonation. The IEC values obtained from the titration data are reasonably close to those calculated from the ^{1}H NMR results. The close agreement between the IEC values obtained by the two methods also confirms that the observed degrees of sulfonation are close to the expected values. When considering the liquid uptake, even though the sulfonated polymers show an increase in the liquid uptake with increasing temperature and methanol concentration, the values are much lower than those found with the SPEEK membrane at a given temperature and methanol concentration. This is not only due to the low IEC values of the SPS-DP copolymer compared to that of SPEEK, but also due to the more rigid backbone structure of SPS-DP compared to that of the SPEEK membrane [157].

The proton conductivity values determined with the copolymer films range from 0.011 to 0.031 S/cm at room temperature depending on the sulfonic acid content. Even

though the sulfonated copolymers show lower proton conductivities compared to that of the SPEEK membrane (0.045 S/cm), all of them show better dimensional stability. As reported before, the copolymers also show much suppressed methanol permeability compared to Nafion membrane, suggesting that the SPS-DP-60 copolymers are promising for DMFC applications.

5.3.4 Effect of the Center-layer Thickness on Methanol Crossover and Membrane Resistance

In order to maintain a low cell resistance, the SPS-DP layer needs to be thin in the multilayer membrane, but too thin a layer could result in poor mechanical properties. With this perspective, a series of multilayer membranes were fabricated for DMFC as shown in Fig. 5.9. The SPS-DP-60 copolymer with a lower methanol permeability was used as the methanol-barrier center layer, while SPEEK with an IEC of 1.56 and higher proton conductivity was used as the outer layer on either side of the inner layer. While the total membrane thickness was maintained constant at 60 μm, the thickness of the inner layer was varied from 5 to 30 μm.

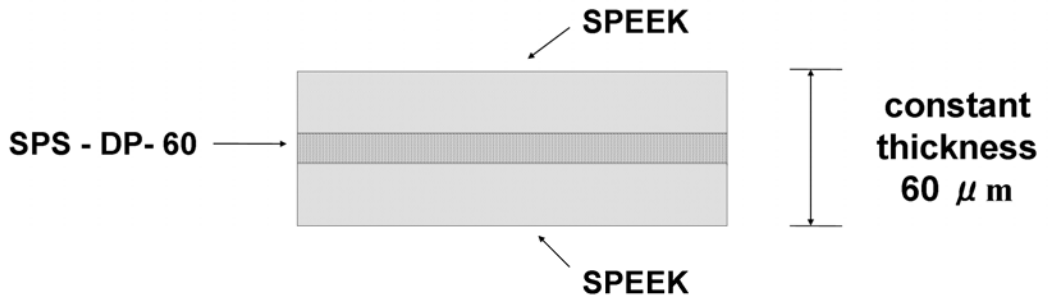

Figure 5.9: Schematics of the multilayer membrane structure.

Fig. 5.10 shows variations of methanol crossover current density and membrane resistance with the thickness of the methanol-barrier center layer. As seen, at 65 ^{o}C with

1 M methanol solution, the methanol crossover current density of the SPS-DP-60 membrane (35 mA/cm^2) is only 30 % of that of the plain SPEEK membrane (115 mA/cm^2) with the same membrane thickness. Due to the methanol blocking effect of the SPS-DP copolymer, the methanol crossover of the multilayer membranes is significantly reduced. The methanol crossover is only 66 and 42 % of that of plain SPEEK with, respectively, 5 and 15 μm thick methanol-barrier center layers. On increasing the center-layer thickness to 30 μm, the methanol crossover is further reduced to 37 %, which is very close to that of the SPS-DP copolymer. However, the resistance of the multilayer membrane increased significantly with increasing thickness of the center layer. For example, the resistances of the multilayer SPEEK/SPS-DP/SPEEK membranes with 5 and 15 μm center-layer thicknesses are, respectively, 13 and 20 mΩ. However, the resistance of the multilayer membrane with 30 μm thick center layer is almost 3 times higher than that of plain SPEEK membrane. When considering the trade-off between methanol crossover and membrane resistance, the optimized thickness for the center layer is ~ 15 μm. With a thickness of 15 μm for the SPS-DP methanol-barrier center layer, the methanol crossover is 42 % of that of plain SPEEK with a small increase in membrane resistance compared to that for plain SPEEK. Similarly, at a given methanol concentration and temperature, the methanol crossover for the multilayer membrane is 39 % of that for Nafion 115 membrane without much difference in the membrane resistance, indicating a better selectivity with the multilayer membrane in DMFC.

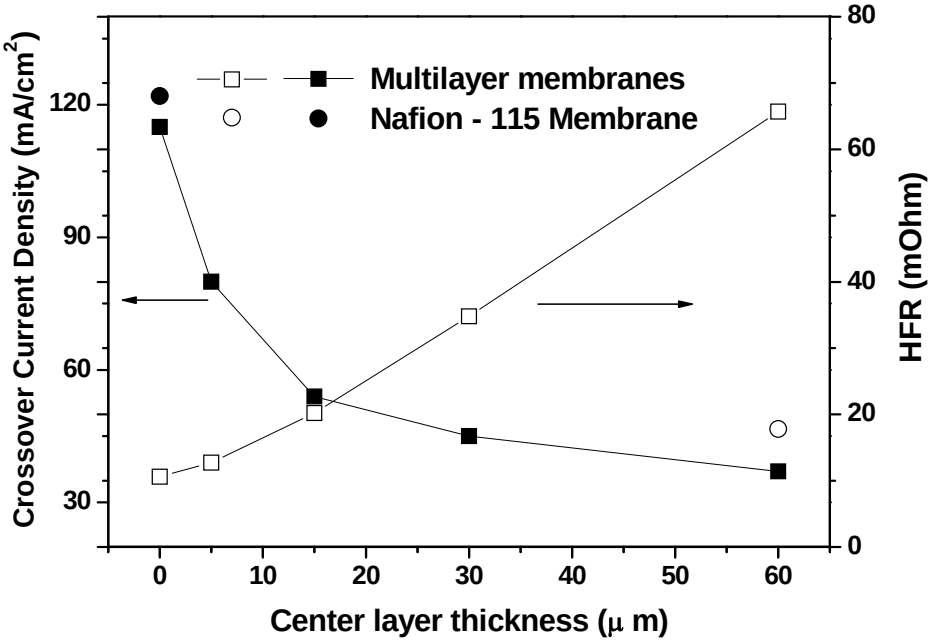

Figure 5.10: Methanol crossover current density and high frequency resistance (HFR) of the 60 μm thick SPEEK/SPS-DP-60/SPEEK multilayer membrane with different SPS-DP-60 center-layer thickness.

5.3.5 Fuel Cell Performance

Fig. 5.11 compares the polarization curves of the multilayer membranes (with different SPS-DP methanol-barrier center layer thickness) in DMFC with those of the plain SPEEK, SPS-DP-60 copolymer, and Nafion-115 membranes at 65 ^{o}C with 1 M methanol solution. The multilayer membranes with 5 and 15 μm center layer thickness exhibit higher performance in DMFC than plain SPEEK membrane despite a higher membrane resistance mainly due to the much suppressed methanol crossover through the multilayer membrane (Fig. 5.10). However, with a much larger thickness (> 30 μm) of the SPS-DP methanol-barrier center layer, the membrane resistance increases

significantly while the methanol crossover is limited by the properties of the center layer polymer, resulting in a decrease in the overall fuel cell performance.

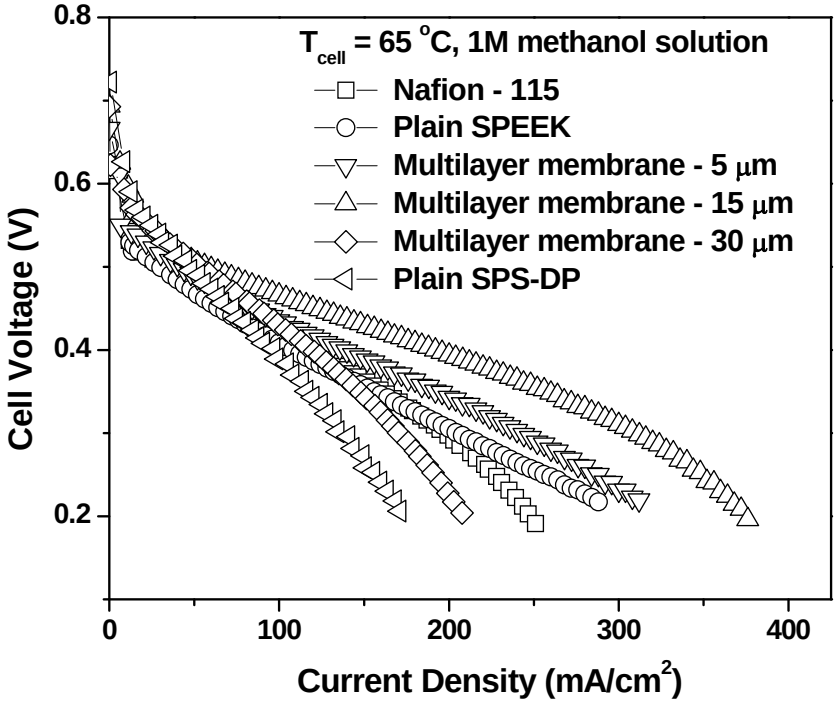

Figure 5.11: Comparison of the polarization curves recorded with Nafion 115, plain SPEEK, plain SPS-DP-60, and SPEEK/SPS-DP-60/SPEEK multilayer (with different SPS-DP-60 center-layer thickness) membranes in DMFC. Methanol concentration: 1 M, cell temperature: 65 °C. The thickness values indicated in μm with the multilayer membranes refer to the center layer thickness.

Fig. 5.12 compares the polarization curves and power density of the plain SPEEK membrane, multilayer SPEEK/SPS-DP-60/SPEEK membrane with an optimized center layer thickness of 15 μm, and Nafion 115 membrane at 80 °C with 1 M methanol solution. The power density value of the multilayer membrane is much higher than those of both the plain SPEEK and Nafion 115 membranes. The maximum power density of

the multilayer membrane (140 mW/cm^2) is 1.4 times higher than that of the plain SPEEK membrane (96 mW/cm^2) and 1.7 times higher than that of the Nafion 115 membrane (82 mW/cm^2).

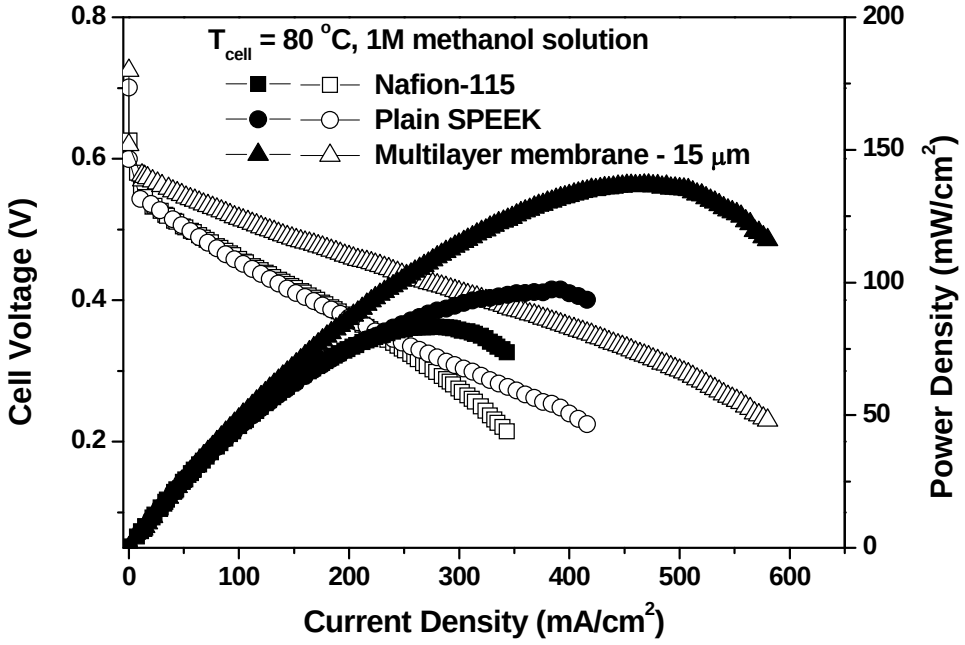

Figure 5.12: Comparison of the polarization curves and power density recorded with Nafion 115, plain SPEEK, and SPEEK/SDPS-DP-60/SPEEK (15 μm SPS-DP-60 central-layer thickness) membranes in DMFC. Methanol concentration: 1 M, cell temperature: 80 °C.

5.3.6 MEAs Cross-sectional Characterization Using SEM

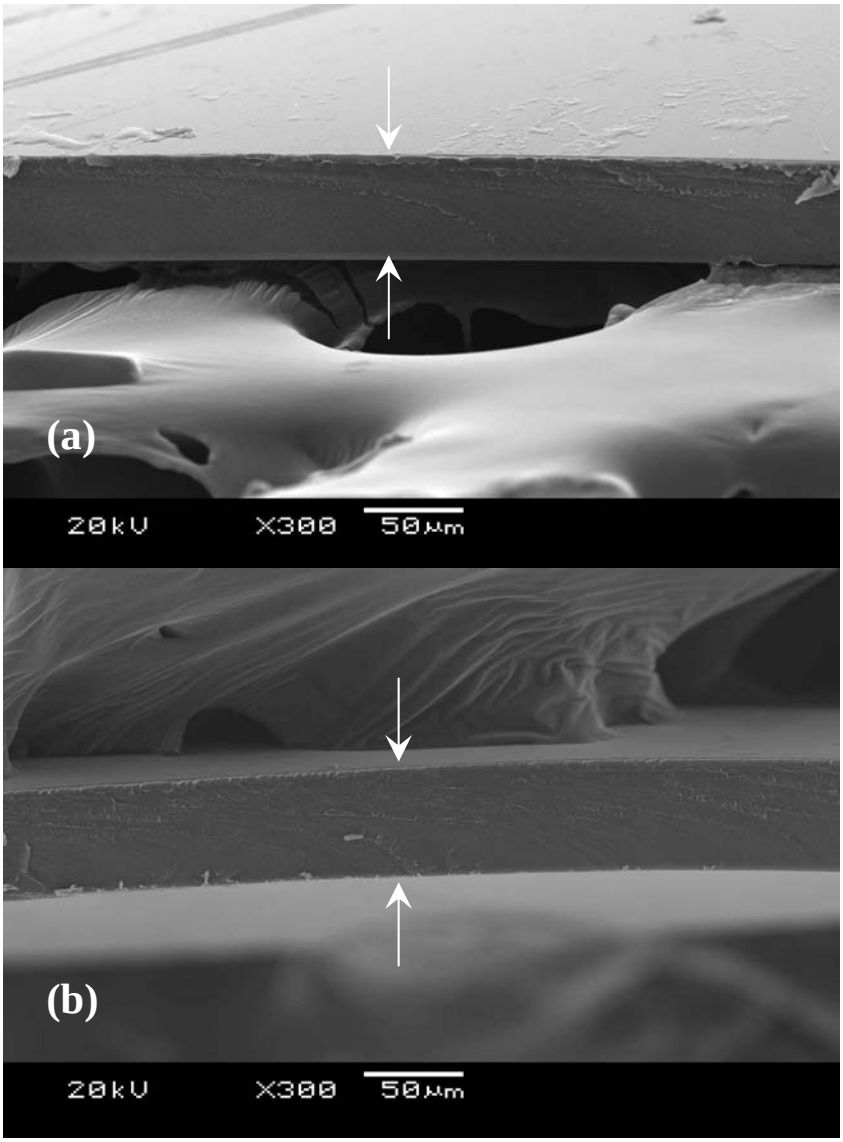

Figure 5.13: Cross-sectional SEM images of the multilayer SPEEK/SPS-DP-60/SPEEK membranes: (a) before and (b) after DMFC evaluation.

To investigate the durability of the multilayer membranes, the cross-section of the membrane (with a center-layer thickness of 15 μm) was characterized by SEM before and after the DMFC evaluation. The DMFC testing of the membrane was carried out for two

weeks (including the overnight shutting down time) by holding the potential at 0.4 V. Fig. 5.13(a) shows the cross-section of the SEEK/SPS-DP-60/SPEEK multilayer membrane before the DMFC evaluation. No clear boundaries between the layers could be observed in the cross section of the multilayer membrane due to the similar main-chain chemical structures of the SPEEK and SPS-DP polymers. Also, the solution-casting procedure used for fabricating the multilayer membrane might have helped to generate stronger interlayer bonding between the different layers. More importantly, as seen in Fig. 5.13(b), no structural delamination is observed in the cross-section of the same membrane after the DMFC evaluation. Unlike the Nafion/SPEEK/Nafion multilayer membrane reported by other researchers [158], the SEEK/SPS-DP-60/SPEEK multilayer membrane shows good structural stability under the fuel cell operating conditions.

5.4 CONCLUSIONS

A series of sulfonated poly (arylene ether sulfone)s with various contents of sulfonic acid groups have been synthesized via a nucleophilic displacement polycondensation reaction and characterized. The sulfonated SPS-DP polymers are thermally stable up to 250 ^{o}C in air, and the T_g, liquid uptake, and proton conductivity of the sulfonated copolymers increase with increasing degree of sulfonation. Although these membranes exhibit lower proton conductivity (0.028 - 0.031 S/cm at 25 ^{o}C) than SPEEK (0.045 S/cm at 25 ^{o}C) and Nafion 115 (0.09 S/cm at 25 ^{o}C), they exhibit a significantly reduced methanol crossover and liquid uptake compared to Nafion and SPEEK membranes.

Taking advantage of the low methanol crossover of these copolymers, a series of multilayer membranes with the SPS-DP-60 copolymer as the methanol-barrier center layer and the high proton-conducting SPEEK as the outer layers have been fabricated and characterized. The multilayer membranes show significantly decreased methanol

crossover without significantly increasing the membrane resistance compared to SPEEK and Nafion 115 membranes. The multilayer membranes with an optimized center-layer thickness of 15 μm show much improved fuel cell performance and power density at 65 and 80 ^{o}C with 1 M methanol solution compared to plain SPEEK membrane due to the much suppressed methanol crossover. The performance of the multilayer membranes could be improved further by (i) optimizing the degree of sulfonation and the thicknesses of the center and outer layers and (ii) employing SPEEK as an ionomer instead of Nafion to reduce the interfacial resistance between the membrane and the catalyst layers.

CHAPTER 6

Sulfonated Poly(ether ether ketone) as an Ionomer for Direct Methanol Fuel Cell Electrodes

6.1 INTRODUCTION

As discussed in the previous chapters, we have investigated various aromatic polymer membranes that can lower the cost and suppress methanol crossover in DMFC. However, with these new membranes, Nafion is often used as an ionomer in the catalyst layer to fabricate the membrane-electrodes assemblies (MEAs). The incompatibility between the polymeric membrane and the ionomer in the catalyst layer can lead to high interfacial resistance and performance loss [168,169].

To overcome this problem, one needs to use the same or similar polymers as both the membrane and electrode ionomer. There have been a few reports on the use of alternative polymers as electrode ionomer in proton exchange membrane fuel cells (PEMFC). Mukerjee and coworkers [170] have attempted to prepare electrodes containing sulfonated poly(arylene ether sulfone)s (SPES) as electrode ionomer for PEMFC. It was shown that the fuel cell performance of the MEAs fabricated with SPES ionomer and SPES membrane is lower than that fabricated with Nafion ionomer and Nafion membrane due to poor kinetics of oxygen reduction reaction with the electrodes containing SPES ionomer. Recently, sulfonated poly (ether ether ketone) (SPEEK) has been explored as electrode ionomer for PEMFC and DMFC with SPEEK membrane [171,172]. However, the performance of the MEA fabricated with SPEEK membrane and SPEEK ionomer was lower than that fabricated with Nafion membrane and Nafion ionomer. This could be related to the lack of effective methods for the dispersion of

SPEEK ionomer in the catalyst ink as well as a lack of optimization of the parameters like ion-exchange capacity (IEC) and content (wt. %) of the SPEEK ionomer in the electrode.

Considering that SPEEK is known to be thermally stable and it exhibits lower methanol crossover than Nafion in DMFC [160,173,174], the optimization of SPEEK as an ionomer in the catalyst layer with employing SPEEK as the membrane is presented in this chapter. The impregnation of SPEEK ionomer into the catalyst electrode was carried out by completely dispersing SPEEK in a water/alcohol based catalyst ink. The performance of the MEAs is evaluated by cyclic voltammetry, AC impedance analysis, and polarization studies in single cell DMFC as a function of the IEC and weight % of the SPEEK ionomer in the electrodes.

6.2 EXPERIMENTAL

6.2.1 Materials

N,N-dimethylformamide (DMF, 99.9%) and isopropyl-alcohol (IPA) were purchased from Fisher Scientific.

6.2.2 Sulfonation of SPEEK

The SPEEK samples were prepared by the procedure as discussed in Chapter 2. To make the SPEEK with different IECs, different reaction times form 25 to 40 h were used.

6.2.3 MEA Fabrication using SPEEK and Nafion as Binders

To fabricate the MEA with SPEEK as a binder, SPEEK was first dissolved in *N,N*-dimethylformamide (DMF) and a desired amount of the SPEEK/DMF solution (14.5 wt. %) was transferred into a water/isopropyl-alcohol (IPA) mixture and sonicated for 30-50 min until the SPEEK polymer was solubilized completely in the water/IPA mixture.

The resultant homogeneous solution was mixed with the catalyst powder, followed by sonication for 1-2 h. The catalyst layer was prepared by brushing the anode or cathode catalyst inks onto a gas diffusion layer (A-6 ELAT/SS/NC/V2 carbon cloth E-TEK Inc.). This alcohol/water based catalyst-SPEEK ink preparation provided an easy coating of the catalyst ink onto the gas diffusion layer due to the use of a lower amount of organic solvents like DMF (9 wt. % DMF in the catalyst ink).

In the case of electrodes containing Nafion ionomer, the catalyst powder was dispersed in a water/IPA mixture, followed by mixing with Nafion solution by sonication for 1 h and painting the resultant ink onto the gas diffusion layer.

The anode catalyst layer consisted of 40 wt. % 1:1 Pt-Ru alloy on Vulcan XC-72 carbon black with either SPEEK or Nafion ionomer. The cathode catalyst layer consisted of 20 wt. % platinum on carbon black with either SPEEK or Nafion ionomer. The Pt-Ru and Pt loadings in the anode and cathode were 1.0 mg/cm^2. For MEA fabrication, the anode and cathode electrodes were hot pressed onto either Nafion or SPEEK membrane. Hot pressing conditions were 140 ^{o}C, 80 psi for 2.5 min and 100 ^{o}C, 40 psi for 3 min, respectively, with Nafion and SPEEK membranes. The resultant MEAs were soaked in 1 M H_2SO_4 solution and rinsed with de-ionized water to remove any remaining organic solvent and convert the SPEEK ionomer in the electrodes into acid form completely. Fuel cell tests were performed using single cell hardware (active area of 5 cm^2) at 65 ^{o}C with 1 M methanol at a flow rate of 2.5 mL/min and humidified oxygen at a flow rate of 200 mL/min without backpressure.

6.2.4 Electrochemical Evaluation of MEAs

Impedance analysis was performed with a Volta Lab 80 potentiostat (PGZ 402 Universal potentiostat) at room temperature. The anode and cathode were supplied, respectively, with 1 M methanol (at a flow rate of 2.5 ml/min) and hydrogen (at a flow

rate of 10 ml/min). The cathode was used as a dynamic hydrogen electrode (DHE) for the measurement of anode impedance. The frequency range was from 100 mHz to 5 kHz and the amplitude of the sinusoidal current signal was 5 mV.

Cyclic voltammetry was also performed using the Volta Lab 80 potentiostat at room temperature. The anode (working electrode) and cathode were supplied, respectively, with humidified nitrogen and hydrogen at a flow rate of 10 mL/min. The potential was scanned between -0.15 and 1.2 V at a sweep rate of 50 mV/s. The impedance and cyclic voltammetry data obtained at room temperature were analyzed to explain the DMFC performance at 65 ^{o}C with an assumption that the trends in the impedance and cyclic voltammetry data are the same regardless of temperature [175].

6.3 RESULTS AND DISCUSSION

6.3.1 Effect of the Ion-exchange Capacity of SPEEK Ionomer

A series of SPEEK polymers was prepared by a sulfonation of PEEK using sulfuric acid for different reaction times. Their IEC, proton conductivity, and water swelling values are giving in Table 6.1. It is seen that the IEC of SPEEK increases from 1.27 to 1.51 meq./g as the sulfonation time increases from 26 to 37 h. The proton conductivity of the SPEEK membranes at room temperature also increases from 0.05 to 0.09 S/cm with sulfonation time. In the case of water swelling at room temperature, while the SPEEK membranes with IEC values of 1.27 to1.33 meq./g exhibit water swelling comparable to that of Nafion, the SPEEK membranes with IEC values of 1.37 to 1.51 meq./g show greater swelling than Nafion.

For the use of the sulfonated polymer as an ionomer in the electrode, the water swelling of sulfonated polymer needs to be taken into account carefully to prevent the electrodes containing sulfonated polymer from being flooded under the fuel cell

operating environment. Although impregnation of a sulfonated polymer with a high IEC into the catalyzed electrode may be preferred with respect to ensuring good proton transfer capability in the electrode, the electrode could suffer from flooding during fuel cell operation due to the excessive swelling of the SPEEK ionomer with high IEC, resulting in a hindrance to the access to reactants (methanol or oxygen) and removal of products (carbon dioxide or water) from the catalyst layer.

Table 6.1: Characterization data of the SPEEK membranes

Sample[a]	Sulfonation time (h)	IEC (meq./g)	Proton Conductivity (S/cm)	Water Swelling (%)
SPEEK 1.27	25	1.27	0.046	35.0
SPEEK 1.33	31	1.33	0.050	36.1
SPEEK 1.37	33	1.37	0.062	45.1
SPEEK 1.51	37	1.51	0.091	56.3
Nafion 115	-	0.92	0.090	34.0

a The numbers refer to the IEC value for each SPEEK sample

To investigate the effect of the IEC of the SPEEK ionomer in the electrodes on the fuel cell performance, a series of electrodes (anode and cathode) containing SPEEK ionomer with different IECs (1.27-1.51 meq./g) was prepared and evaluated in DMFC. The MEAs were fabricated with Nafion 115 to rule out the variations in fuel cell performance that could be caused by the differences in the thickness or IEC values of the SPEEK membrane. Fig. 6.1 shows the dependence of the DMFC performances on the IEC values of the SPEEK ionomer impregnated into both the anode and cathode electrodes. The content of SPEEK ionomer was kept at 20 wt. % in these experiments. As seen in Fig. 6.1, the fuel cell performance improves slightly as the IEC value of the SPEEK ionomer increases from 1.27 to 1.33 meq./g, which could be attributed to better

proton conductivity in the catalyst layers. However, a decrease in DMFC performance is seen on using SPEEK ionomers with IEC > 1.33 meq./g, which is due to a higher water swelling (45-56 %) observed with SPEEK having IEC values of 1.37 - 1.51 meq./g compared to that found with Nafion (34 %) as seen in Table 6.1. This indicates that the impregnation of SPEEK ionomers with high IEC values (> 1.33 meq./g) into the electrodes may result in a decrease in the hydrophobic properties of the electrodes and consequent limitations in the transfer of reactants and products through the catalyst layer.

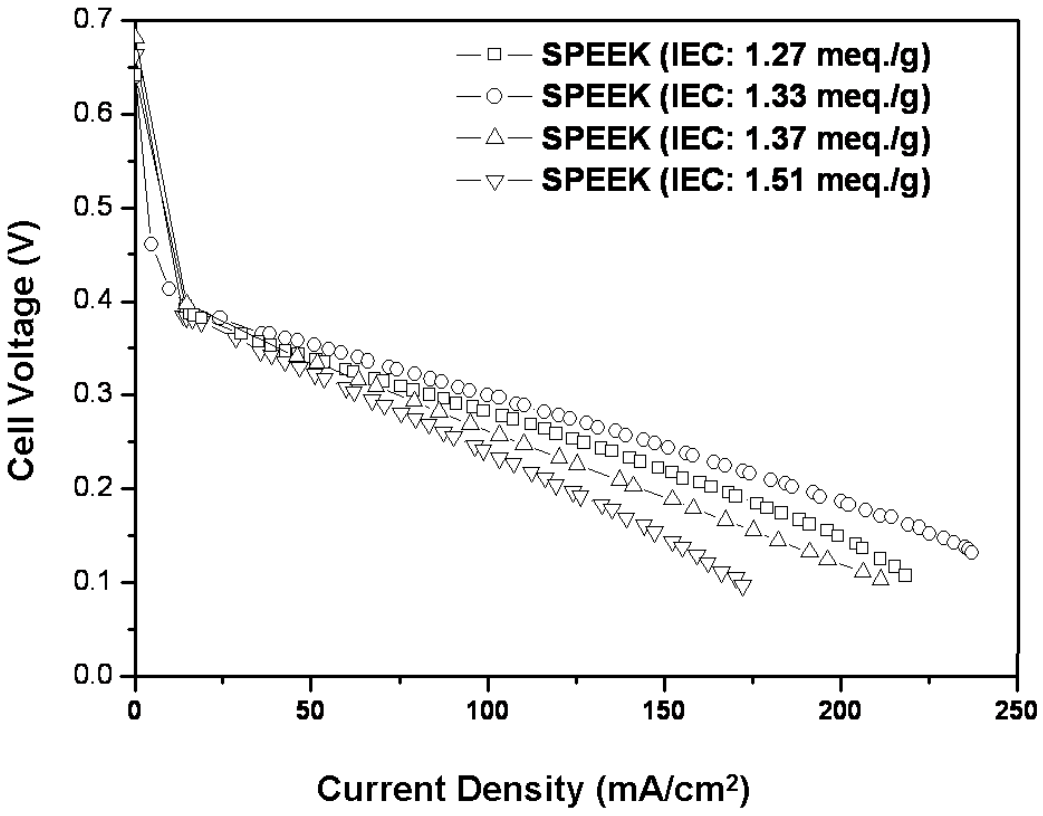

Figure 6.1: Variations of the performances in DMFC of the MEAs fabricated with Nafion 115 membrane and SPEEK ionomer as a function of the IEC value of the SPEEK ionomer with a constant 20 wt. % ionomer. Methanol concentration: 1 M, cell temperature: 65 ^{o}C, and humidified oxygen flow rate: 200 sccm.

6.3.2 Effect of SPEEK Ionomer Content

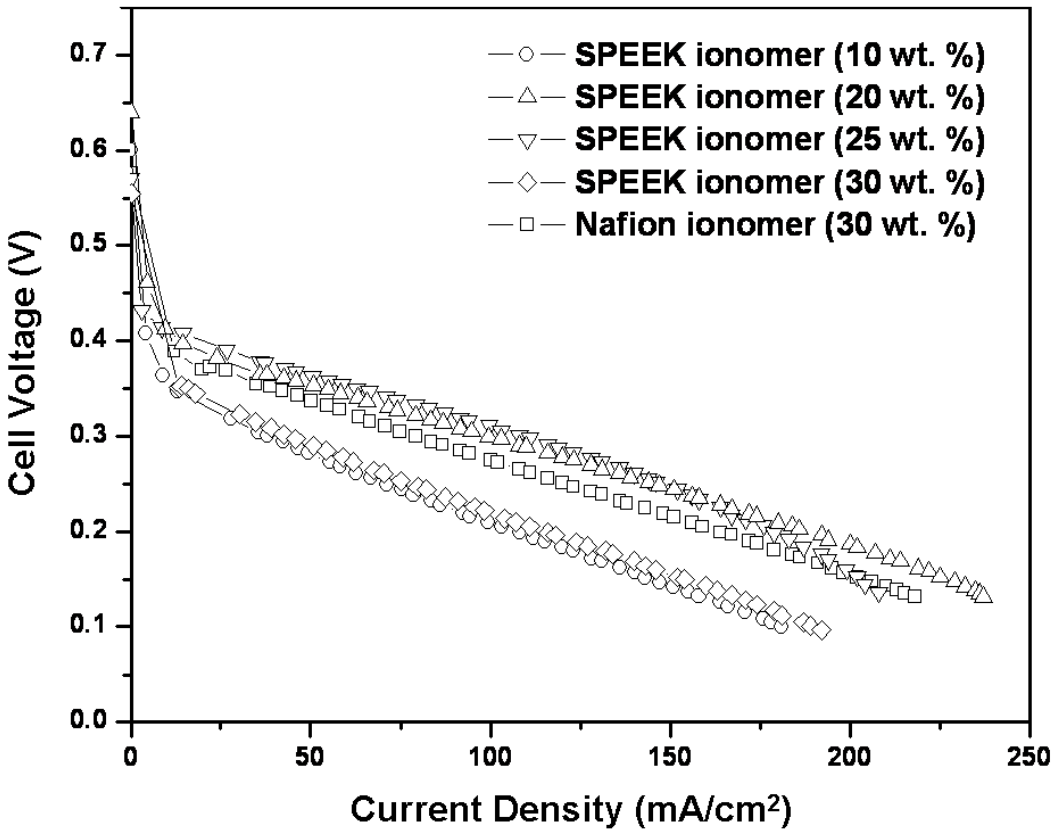

Figure 6.2: Variations of the performance in DMFC of the MEA fabricated with Nafion 115 membrane and SPEEK ionomer as a function SPEEK ionomer content with a constant IEC of 1.33 meq./g. The wt. % values refer to the amount of SPEEK ionomer in the electrodes. Methanol concentration: 1 M, cell temperature: 65 ^{o}C, and humidified oxygen flow rate: 200 sccm.

Fig. 6.2 compares the performances in DMFC as a function of SPEEK ionomer (IEC = 1.33 meq./g) content in both the anode and cathode electrodes. For a reference, the fuel cell performance of a MEA fabricated with the Nafion ionomer in the catalyst layers is also shown. The Nafion content in the anode and cathode catalyst layers was 30 wt. %, which is known as an optimum content for carbon supported catalyst electrodes [176,177]. As seen in Fig. 6.2, the MEAs with 20 or 25 wt. % of SPEEK ionomer in the

catalyst layers show better performance than that with 30 wt. % Nafion ionomer although a mass transfer limitation at high current densities is observed with 25 wt. % SPEEK ionomer. On the other hand, relatively poor performance is seen when the SPEEK ionomer content is too low (10 wt. %) or too high (30 wt. %).

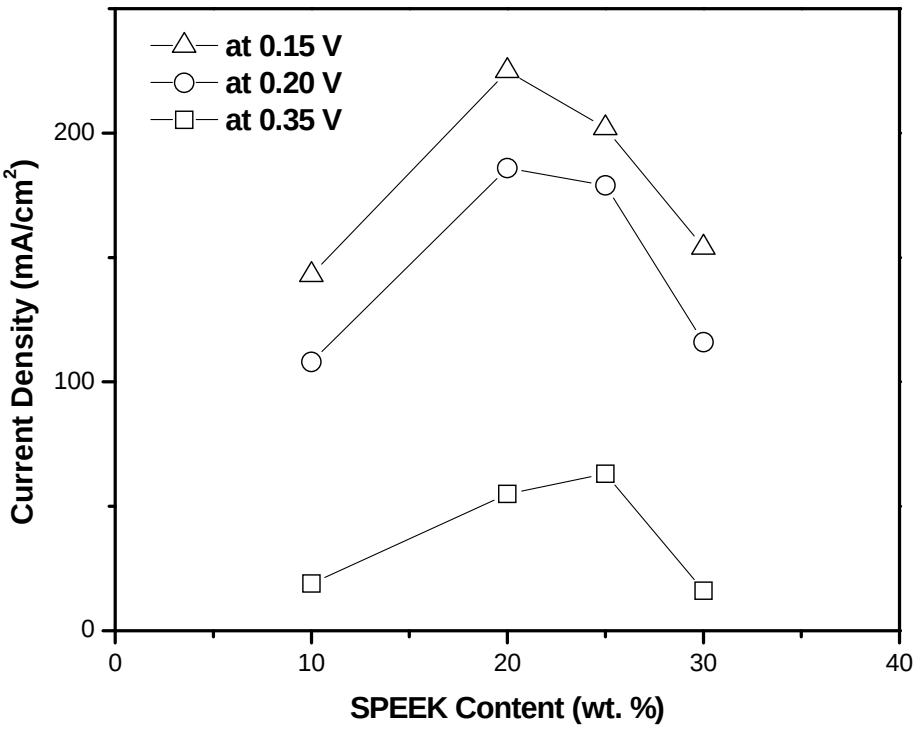

Figure 6.3: Variations of the current density with SPEEK content (IEC = 1.33 meq./g) at different cell voltages.

To have a better comparison, the current densities at different cell voltages are displayed in Fig. 6.3 as a function of SPEEK ionomer (IEC = 1.33 meq./g) content in the catalyst layers. As seen, the current density at a given voltage increases as the loading of the SPEEK ionomer increases from 10 to 20 or 25 wt. % and then decreases with further increase in SPEEK ionomer content. This suggests that the proton conductivity in the

catalyst layer is a critical factor in determining the fuel cell performance particularly at low ionomer content. At higher cell voltages (0.35 V), the current density increases up to 25 wt. % SPEEK ionomer and then decreases at 30 wt. % SPEEK ionomer, while at lower cell voltages (0.15 and 0.2 V), the highest current density increases up to 20 wt. % SPEEK ionomer and then decreases. The latter is because of the water flooding in the catalyst layer on drawing higher current densities (*i.e.* at lower cell voltages).

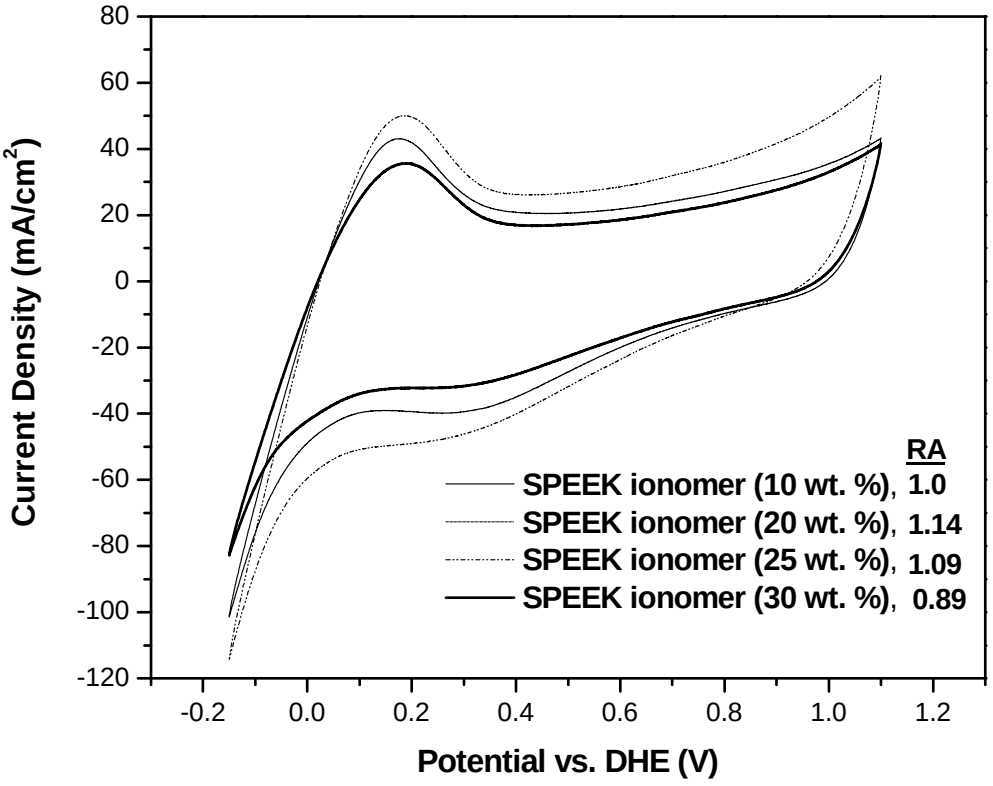

Figure 6.4: Cyclic voltammograms of the anode electrodes having various SPEEK ionomer (IEC = 1.33 meq./g) content. The wt. % values refer to the amount of SPEEK ionomer in the electrodes. The relative hydrogen desorption peak areas (RA) are also indicated for each ionomer content.

Fig. 6.4 displays the cyclic voltammograms of the anode electrodes as a function of SPEEK ionomer (IEC = 1.33 meq./g) content in the electrodes. The relative hydrogen desorption peak areas (RA) determined from the cyclic voltammograms are also indicated in Fig. 6.4. The hydrogen desorption peak area obtained with the anode can be interpreted as the electrochemical active area of the catalyst layer in the electrode where methanol oxidation takes place [175,178]. As seen in Fig. 6.4, the hydrogen desorption peak area increases initially up to 20 wt. % SPEEK ionomer and then decreases. This demonstrates that the electrochemical active area of the catalyst layer is enlarged by adding SPEEK ionomer up to 20 wt. %, while further loading of the SPEEK ionomer, which is an electrical insulator, results in a lowering of the electrochemical active area due to a decrease in the electrical conductivity of the catalyst layer as well as due to the difficulties in the access of the reactants to the electrodes [171,175].

Fig. 6.5 (a) displays the Nyquist plots obtained from the impedance measurements of the MEAs containing different amounts (10-30 wt. %) of SPEEK ionomer (IEC = 1.33 meq./g) in the electrodes. The ohmic resistance determined from the intercept of the real Z axis at high frequency includes membrane resistance, interfacial resistance, and cell hardware resistance [171]. The ionic resistance of the catalyst layer can be excluded because it does not contribute to the ohmic resistance of the MEA at high frequency [177]. Since Nafion 115 was employed as the membrane in all cases, the membrane resistance is constant for all the MEAs and so the interfacial resistance between the membrane and electrode is the factor that influences the high frequency ohmic resistance based on the assumption that the cell hardware resistance is negligibly small. From the Nyquist plots, the ohmic resistance determined from the intercept of the real Z axis at high frequency increases with SPEEK ionomer content. This suggests that the interfacial resistance between the Nafion membrane and the electrodes containing SPEEK ionomer

increases with SPEEK ionomer content due to the incompatibility between the Nafion membrane and the SPEEK ionomer in the electrode. It can be concluded, as already shown in Fig. 6.2, that the improvement in the fuel cell performance as the SPEEK ionomer content increases from 10 to 25 wt. % is primarily due to an expansion of the electrochemical active area in the catalyst layer, whereas the decline in fuel cell performance at 30 wt. % SPEEK ionomer content is a consequence of the combined effects of the decreased electrochemical active area of the electrodes and the relatively high interfacial resistance of the MEA (see Figs. 6.4 and 6.5 (a)).

Fig. 6.5(b) shows the capacitance plots of the anode electrodes as a function of the SPEEK ionomer (IEC = 1.33 meq./g) content. The limiting capacitance determined from the low frequency plateau in the capacitance plot is proportional to the electrochemically effective interfacial area between the catalyst particles and the ionomer, where an electric double layer is formed [179,180] As seen in Fig. 6.5(b), the limiting capacitance increases gradually as the SPEEK content increases from 10 to 25 wt. % and then drops drastically at 30 wt. % SPEEK ionomer. This implies that the interfacial area between the catalyst particles and the SPEEK ionomer increases with SPEEK ionomer content up to 25 wt. %, and decreases upon further increase in SPEEK ionomer content (30 wt. %) as the latter does not lead to any further increase in interfacial area but only results in a decrease in the electrical conductivity of the catalyst layer due to the excessive loading of the SPEEK ionomer (electrical insulator).

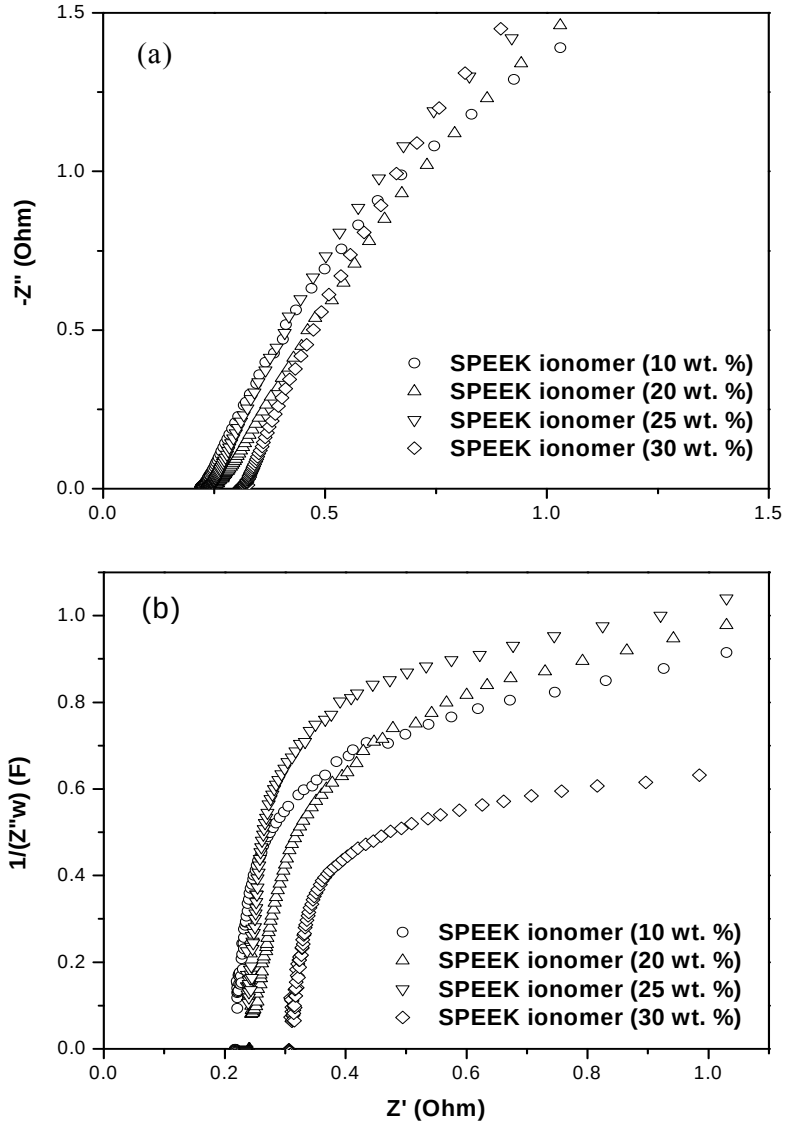

Figure 6.5: (a) Nyquist and (b) capacitance plots obtained with the anode electrodes having various SPEEK ionomer (IEC = 1.33 meq./g) contents. The wt. % values refer to the amount of SPEEK ionomer in electrodes.

6.3.3 Characterization of MEAs with SPEEK Membrane

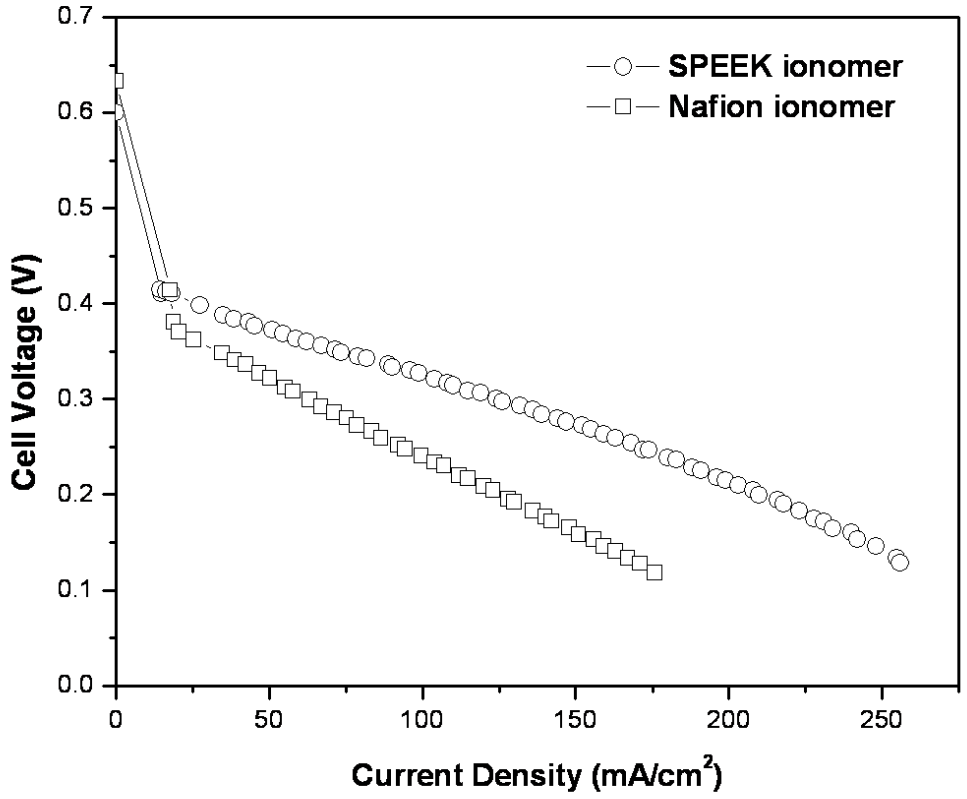

Figure 6.6: Comparison of the performances in DMFC of the MEAs fabricated with the SPEEK membrane (IEC = 1.51 meq./g and thickness = 90 μm) and 20 wt. % SPEEK ionomer (IEC = 1.33 meq./g) or 30 wt. % Nafion ionomer in the electrodes.

To investigate the dependence of the fuel cell performance of SPEEK membranes on the types of ionomer (SPEEK vs Nafion) used in the electrodes, the MEAs consisting of SPEEK membrane and either SPEEK or Nafion ionomer in the electrodes were prepared and characterized in DMFC. The polarization curves of such MEAs are displayed in Fig. 6.6. The SPEEK membrane used was kept identical in all the MEAs with a constant thickness of 90 μm and a constant IEC of 1.51 meq./g. As seen in Fig.

6.6, the MEA with SPEEK ionomer (20 wt. % and IEC = 1.33 meq./g) in the electrodes exhibits distinctly better performance than that with the Nafion ionomer (30 wt. %).

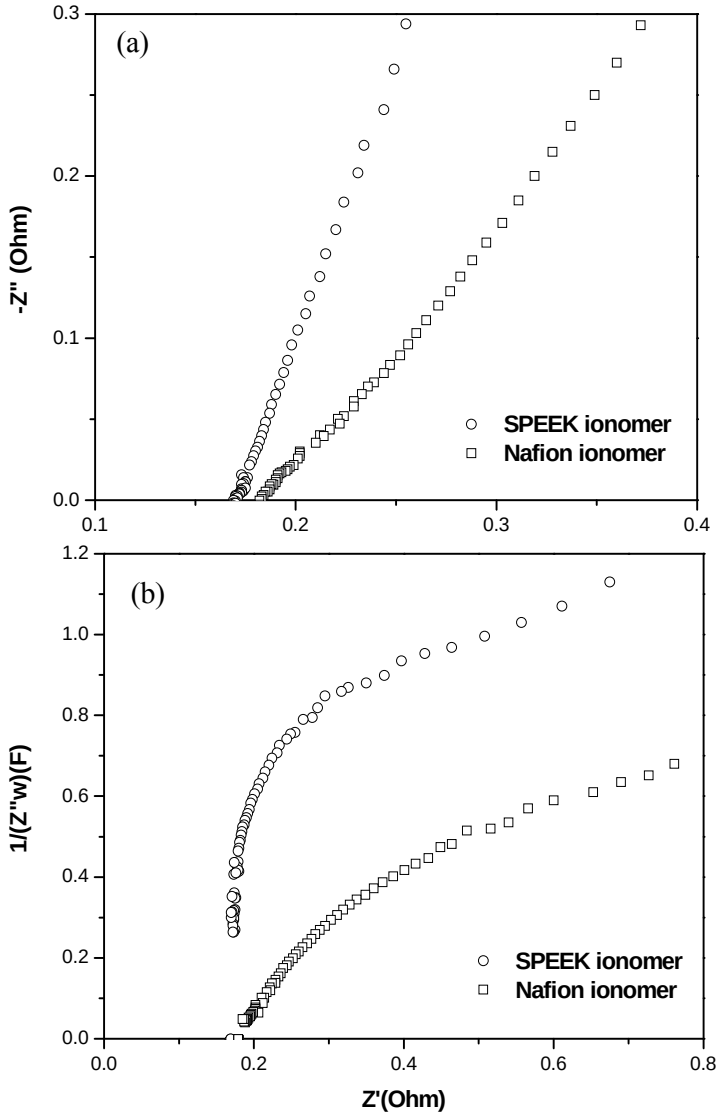

Figure 6.7: (a) Nyquist and (b) capacitance plots obtained with the anode electrodes of the MEAs fabricated with SPEEK membrane (IEC = 1.51 meq./g and thickness = 90 μm) and 20 wt. % SPEEK ionomer (IEC = 1.33 meq./g) or 30 wt. % Nafion ionomer in the electrodes.

To understand the origin of the differences in the fuel cell performances of the different MEAs, AC impedance spectroscopy was performed with the MEAs to evaluate their ohmic resistances and limiting capacitances. Fig. 6.7(a) shows the Nyquist plots obtained with the MEAs containing SPEEK membrane (IEC = 1.51 meq./g and thickness = 90 μm) and either SPEEK (20 wt. % and IEC = 1.33 meq./g) or Nafion (30 wt. %) ionomer in the electrodes. Using the ohmic resistance determined from the intercept of the real Z axis in the high frequency range, the interfacial resistance can be calculated by subtracting the membrane resistance (determined by the impedance measurement with the membrane) from the ohmic resistance. The resultant interfacial resistances of the MEAs are found to be 0.069 and 0.092 Ωcm^2, respectively, for the SPEEK and Nafion ionomers. This indicates the realization of a lower interfacial resistance between the SPEEK membrane and electrodes on replacing the Nafion ionomer by the SPEEK ionomer in the electrodes.

In parallel, to evaluate the interfacial active area of the electrodes depending on the ionomer, the capacitances of the anode electrodes containing either SPEEK or Nafion ionomer were determined and are displayed in Fig. 6.7(b). As seen in Fig. 6.7(b), the limiting capacitance of the electrodes containing SPEEK ionomer is almost two times higher than that of the electrodes containing Nafion ionomer. This can be taken to imply that the SPEEK ionomer is evenly distributed and interconnected through the catalyst layer of the electrode, which results in a large interfacial area where the catalyst particles are in contact with the ionomer network in the catalyst layer.

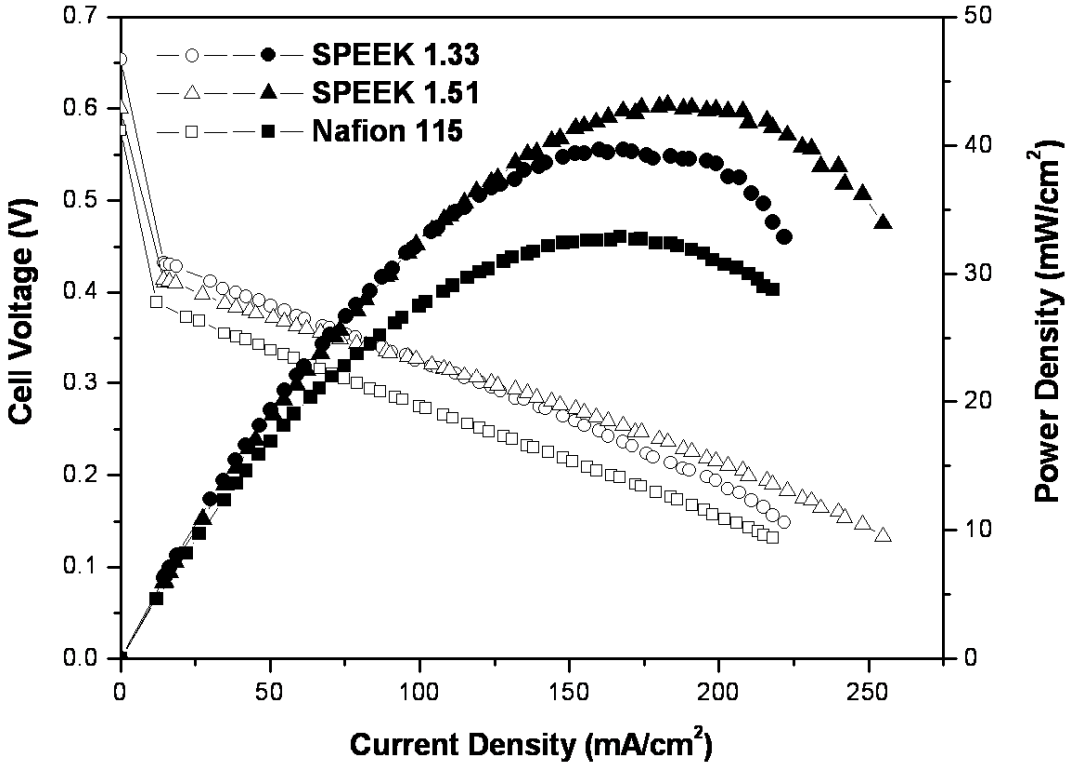

Figure 6.8: Comparison of the performances in DMFC of various MEAs: MEAs fabricated with SPEEK membrane (IEC = 1.33 meq./g and thickness = 70 μm) and 20 wt. % SPEEK ionomer (IEC = 1.33 meq./g), SPEEK membrane (IEC = 1.51 meq./g and thickness = 90 μm) and 20 wt. % SPEEK ionomer (IEC = 1.33 meq./g), and Nafion 115 membrane and 30 wt. % Nafion ionomer.

Fig. 6.8 compares the performances in DMFC of the MEAs prepared with SPEEK membranes having two different IECs (1.33 and 1.51 meq./g) as well as Nafion 115 membrane. 20 wt. % of a SPEEK ionomer with an IEC of 1.33 meq./g was used for preparing the electrodes of the MEAs fabricated with the two SPEEK membranes. The MEA with the Nafion 115 membrane was prepared with Nafion ionomer (30 wt. %) in the electrodes. As seen in Fig. 6.8, the SPEEK membranes with SPEEK ionomer in the electrodes exhibit superior performance in DMFC regardless of the membrane IEC

compared to the MEA fabricated with the Nafion 115 membrane and Nafion ionomer. The polarization loss in the kinetic region at low current densities (10-50 mA/cm^2) is smaller for the MEAs fabricated with SPEEK membrane and SPEEK ionomer in Fig. 6.8 compared to that found with the Nafion membrane and Nafion ionomer, suggesting better electrode kinetics in the former. This is also consistent with that found in Fig. 6.1 where the polarization loss at low current densities is smaller for the MEA fabricated with Nafion membrane and SPEEK ionomer (20 wt. % and IEC = 1.33 meq./g) than that for the Nafion membrane and Nafion ionomer (30 wt. %). Fig. 6.9 compares the methanol crossover current densities for the MEAs as described in the experimental section. The crossover current densities for the MEAs fabricated with the SPEEK membrane (IEC = 1.33 and 1.51 meq./g) and SPEEK ionomer (20 wt. % and IEC = 1.33 meq./g) are lower than that found with the MEA fabricated with Nafion 115 membrane and Nafion ionomer (30 wt. %). This demonstrates that the better performance found in DMFC with the SPEEK membranes and SPEEK ionomer compared to that with Nafion membrane and Nafion ionomer is a result of the combined effects of lower methanol crossover and better electrode kinetics with SPEEK membrane and SPEEK ionomer.

Looking at the power density values in Fig. 6.8, the SPEEK membrane with an IEC of 1.33 meq./g exhibits slightly lower (by 9 %) power density than the SPEEK membrane with an IEC of 1.51 meq./g. This can be attributed to the higher ohmic resistance (0.14 Ωcm^2) of the SPEEK membrane with an IEC of 1.33 meq./g compared to that of the SPEEK membrane with an IEC of 1.51 meq./g (0.1 Ωcm^2). In addition, AC impedance analysis gave interfacial resistance values of 0.042 and 0.069 Ωcm^2, respectively, for the two SPEEK membranes with the IEC values of 1.33 and 1.51 meq./g. This indicates a decrease in the interfacial resistance when the SPEEK membrane and the

SPEEK ionomer have the same IEC values (1.33 meq./g) due to a better compatibility between the membrane and the electrode ionomer.

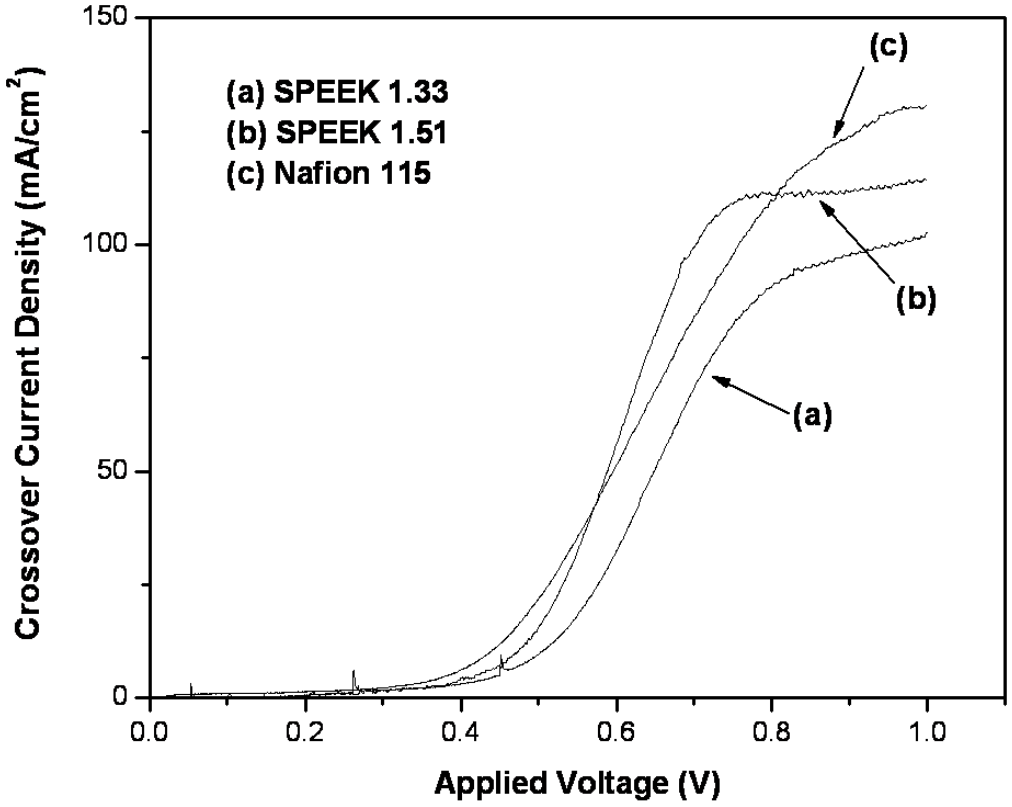

Figure 6.9: Comparison of the methanol crossover current densities of various MEAs: MEAs fabricated with SPEEK membrane (IEC = 1.33 meq./g and thickness = 70 μm) and 20 wt. % SPEEK ionomer (IEC = 1.33 meq./g), SPEEK membrane (IEC = 1.51 meq./g and thickness = 90 μm) and 20 wt. % SPEEK ionomer (IEC = 1.33 meq./g), and Nafion 115 membrane and 30 wt. % Nafion ionomer.

6.4. CONCLUSIONS

A series of SPEEK with different IECs values have been prepared and explored as an ionomer in the electrodes of MEAs. The electrodes containing SPEEK ionomer have

been characterized as a function of the IEC value and content of the SPEEK ionomer by single cell DMFC tests, cyclic voltammetry, and AC impedance spectroscopy. The optimum IEC value and SPEEK ionomer content in the electrodes are found to be, respectively, 1.33 meq./g and 20 wt. %. The MEAs fabricated with SPEEK membrane and SPEEK ionomer exhibit better performance in DMFC than that fabricated with Nafion ionomer, which is attributed to lower interfacial resistance in the MEA and increased electrochemical active area of the catalyst layer. The MEAs fabricated with SPEEK membrane and SPEEK ionomer also show superior performance in DMFC compared to that with Nafion 115 membrane and Nafion ionomer due to lower methanol crossover and better electrode kinetics. Replacement of Nafion ionomer by SPEEK ionomer in the catalyst layer can also provide significant cost savings as SPEEK is less expensive than Nafion.

CHAPTER 7

Summary

With an aim to develop low-cost, high performance membrane materials with low methanol crossover for direct methanol fuel cells (DMFC), the following systems have been investigated:

- *Blend membranes based on acid-base interactions:* Polymer systems consisting of an acidic polymer sulfonated poly(ether ether ketone) (SPEEK) and various basic polymers such as (polysulfone-4-nitro-benzimidazole (PSf-NBIm), polysulfone-1*H*-Perimidine (PSf-PImd), and polysulfone-5-amino-benzotriazole (PSf-BTraz)).

- *Polymers with an additive base:* Sulfonated polysulfone (SPSf) and SPEEK with *N*,*N'*-Bis-(1H-benzimidazol-2-yl)-isophthalamide (BBImIP) as an additive.

- *Multilayer membranes:* Trilayer membranes consisting of novel sulfonated poly(arylene ether sulfone) as a methanol-barrier center layer and SPEEK as outer layers.

In addition, with an aim to overcome the high interfacial resistance between the aromatic polymer membrane and Nafion ionomer in the electrode, membrane-electrode assemblies (MEAs) with SPEEK as an ionomer have also been fabricated and investigated.

Various basic polymers such as PSf-NBIm, PSf-PImd, and PSf-BTraz have been synthesized by a condensation reaction starting from carboxylated polysulfone. These

basic polymers have then been blended with the acidic polymer SPEEK and characterized by ion-exchange capacity, proton conductivity, liquid uptake, ionic cluster size, fuel cell performance, and methanol crossover measurements. Although all the blend membranes show a larger ionic cluster size compared to that in plain SPEEK due to the insertion of the N-heterocylce side groups of the basic polymers into the ionic cluster formed by the sulfonic acid groups of SPEEK as evidenced by SAXS and TEM data, they exhibit lower liquid uptake in water and methanol/water solutions and reduced methanol crossover due to the hydrophobicity and methanol blocking effect of the N-heterocycle groups. The blend membranes with an optimized basic polymer content exhibit better performance in DMFC than plain SPEEK and Nafion 115 membranes due to an enhancement in proton conduction and a reduction in methanol crossover through acid-base interactions.

The microstructure, electrochemical performance, and methanol crossover of these blend membranes have been compared with those of SPEEK/PSf-BIm (polysulfone bearing benzimidazole) and SPEEK/PSf-ABIm (polysulfone bearing 2-amino-benzimidazole). The SPEEK/PSf-PImd blend membrane shows the lowest methanol crossover among all the blend systems investigated due to the largest size of the 1*H*-Perimidine group. The SPEEK/PSf-BTraz blend membrane shows the highest proton conductivity and power density due to the easiest hopping proton conduction through the 5-amino-benzotriazole groups. The study demonstrates that blend membranes consisting of aromatic polymers with sulfonic acid groups and aromatic polymers with N-heterocycle groups is an effective strategy to enhance proton conductivity and lower methanol crossover in DMFC.

N,*N*'-Bis-(1H-benzimidazol-2-yl)-isophthalamide (BBImIP) has been synthesized and explored as an additive in sulfonated aromatic polymer membranes like SPSf and SPEEK for use in DMFC. Both the SPSf/BBImIP and SPEEK/BBImIP blend membranes

offer an important advantage of suppressed methanol crossover in DMFC compared to their plain counterparts SPSf or SPEEK membranes. While the SPSf/BBImIP blend membranes (0.5 – 4.0 wt.% BBImIP) show lower performance than plain SPSf in DMFC due to the lower proton conductivity, the SPEEK/BBImIP blend membranes (1.0 – 3.0 wt.% BBImIP) exhibit performance in DMFC similar to or better than that of plain SPEEK membrane. The study demonstrates that blending N-heterocycles like amino-benzimidazole with sulfonated polymers offers an effective way to suppress methanol crossover through the membrane. The low methanol permeability could result in better long-term performance and lower cathode catalyst loading in DMFC.

A series of sulfonated poly (arylene ether sulfone)s (SPS-DP) with various sulfonic acid contents have been synthesized via a nucleophilic displacement polycondensation reaction and characterized. The SPS-DP polymers are thermally stable up to 250 ^{o}C at air. The liquid uptake and the proton conductivity of the sulfonated copolymers increase with increasing degree of sulfonation. These membranes exhibit a significantly reduced methanol crossover and liquid uptake compared to Nafion and SPEEK membranes with lower proton conductivities (0.028 - 0.031 S/cm at room temperature). To take advantage of the low methanol permeability property of the SPS-DP polymer, a series of multilayer membranes in which SPS-DP-60 copolymer forms a methanol-barrier center layer and SPEEK with a higher proton conductivity forms the outer layers have been fabricated and characterized. The investigation shows that multilayer membranes could significantly suppress methanol crossover without increasing the membrane resistance drastically. The multilayer membranes with an optimized center-layer thickness of 15 μm show much improved fuel cell performance and power density at 65 and 80 ^{o}C with 1 M methanol solution compared to plain SPEEK membrane due to the much suppressed methanol crossover.

A series of MEAs have been prepared with SPEEK membrane and SPEEK with different IEC values and contents as an ionomer in the electrodes. The electrochemical properties of the resultant MEAs have been investigated in DMFC by single cell DMFC tests, cyclic voltammetry, and AC impedance spectroscopy. The optimum IEC value and SPEEK ionomer content in the electrodes are found to be, respectively, 1.33 meq./g and 20 wt. %. Due to the lower interfacial resistance in the MEA and increased electrochemical active area of the catalyst layer, the MEAs fabricated with SPEEK membrane and SPEEK ionomer exhibit better performance in DMFC than that fabricated with Nafion ionomer. The MEAs fabricated with SPEEK membrane and SPEEK ionomer also show superior performance in DMFC compared to that with Nafion 115 membrane and Nafion ionomer due to lower methanol crossover and better electrode kinetics. Replacement of Nafion ionomer by SPEEK ionomer in the catalyst layer can also provide significant cost savings as SPEEK is less expensive than Nafion.

Bibliography

[1] International Energy Outlook.United States Energy Information Administration.

[2] R. O'Hayre, S-W Cha, W. Colella, F. B. Prinz, John Wiley and Sons Inc., Fuel cell fundamentals, 2nd edition, 2009.

[3] S. Srinivasan, R. Mosdale, P. Stevens, C. Yang, Annu. Rev. Energ. Env. 24 (1999) 281.

[4] B. D. McNicol, D. A. J. Rand, K. R. Williams, J. Power Sources 100 (2001) 47.

[5] B. Yang, Ph.D. dissertation, The University of Texas at Austin, August, 2004.

[6] S. McIntosh and R. J. Gorte, Chem. Rev. 104 (2004) 4845.

[7] Russell H. Jones (Editor) and George J. Thomas (Editor). Materials for the Hydrogen Economy (Hardcover), CRC press.

[8] X. M. Ren, P. Zelenay, S. Thomas, J. Davey, S. Gottesfeld, J. Power Sources 86 (2000) 111.

[9] J. Lin, J. K. Lee, M. Kellner, R. Wycisk, and P. N. Pintauro, J. Electrochem. Soc., 153, A1325 (2006).

[10] US Patent No. 3061658

[11] M. S. Wilson, S. Gottesfeld, J. Appl. Electrochem. 22 (1992) 1.

[12] E.A. Ticianelli, C. R. Derouin, A. Redondo and S. Srinivason, J. Electrochem. Soc. 135 (1988) 2209.

[13] M. S. Wilson and S. Gottesfeld, J. Electrochem. Soc. 139 (1992) L28.

[14] M. S. Wilson, J. A. Valerio and S. Gottesfeld, Electrochim. Acta 40 (1995) 355.

[15] S. Mukerjee and S. Srinivasan, J. Electroanal. Chem. 357 (1993) 201.

[16] J. Shim, D.- Y. Yoo, and J-S. Lee, Electrochim. Acta 45 (2000) 1943.

[17] E. Antolini, R. R. Passos, and E. A. Ticianelli, Electrochim. Acta 48 (2002)263.

[18] M. Neergat, A. K. Shukla, and K. S. Gandhi, J. Appl. Electrochem. 31 (2001) 373.

[19] A. K. Shukla, R. K. Raman, N. A. Choudhury, K. R. Priolkar, P. R. Sarode, S. Emura, and R. Kumashiro, J. Electroanal. Chem. 563 (2004) 181.

[20] J. Yang and J. J. Xu, Electrochem. Commun. 5 (2003) 306.

[21] A. Restovic, E. Rý´os, S. Barbato, J. Ortiz and J. L. Gautier, J. Electroanalytical Chem. 522 (2002) 141.

[22] S. Mulljzr, K. Stiuebel and O. HAAS, Electrochim. Acta 39 (1994) 1661.

[23] T. Kishi, F. Shimizu, and T. Nagai, Surf. Technol. 21 (1984)109.

[24] R. W. Reeve, P. A. Christensen, A. Hamnett, S. A. Haydock, and S. C. Roy, J. Electrochem. Soc. 145 (1998) 3463.

[25] D. R. McIntyre, A. Vossen, J. R. Wilde, and G. T. Burstein, J. Power Source 108 (2002) 1.

[26] J.L. Fernandez, V. Raghuveer, A. Manthiram, and A.J. Bard, J. Am. Chem. Soc. 127 (2005) 13100.

[27] V. Raghuveer, A. Manthiram, and A.J. Bard, J. Phys. Chem. 109 (2005) 22909.

[28] V. Raghuveer, P.J. Ferreira, and A. Manthiram, Electrochem. Commun. 8 (2006) 807.

[29] H. Liu and A. Manthiram, Electrochem. Commun. 10 (2008) 740.

[30] C. Roth, N. Martz, F. Hahn, J.-M. Leger, C. Lamy, and H. Fuess, J. Electrochem. Soc. 149 (2002) E443.

[31] A. J. Dickinson, L. P. L. Carrette, J. A. Collins, K. A. Friedrich, and U. Stimming, Electrochim. Acta 47 (2002) 3733.

[32] J. H. White and A. F. Sammells, J. Electrochem. Soc. 140 (1993) 2169.

[33] A. K. Shukla, M. K. Bavikumar, A. S. Arico, G. Candino, V. Antonucci, N. Giordano, and A. Hamnett, J. Appl. Electrochem. 25 (1995) 528.

[34] H. Zhang, Y. Wang, E. R. Fachini, and C. R. Cabrera, Electrochem. Solid-State Lett. 2 (1999) 437.

[35] K. Lasch, L. Jorissen, and J. Garche, J. Power Sources 84 (1999) 225.

[36] V. Neburchilov, J. Martin, H. J. Wang, and J. J. Zhang, J Power Sources 169 (2007) 221.

[37] M. A. Hickner, H. Ghassemi, Y. S. Kim, B. R. Einsla, and J. E. McGrath , Chem. Rev 104 (2004) 4587.

[38] W.Y. Hsu and T. D. Gierke, J. Membr. Sci. 13 (1983) 307.

[39] C. Gavach, G. Pamboutzouglou, M. Nedyalkov, and G. Pourcelly, J. Membr. Sci. 45 (1989) 37.

[40] T. D. Gierke, G. E. Munn, F. C. Wilson, J. Polym. Sci. Polym. Phys. Ed. 19 (1981) 1687.

[41] K. T. Adjemian, S. J. Lee, S. Srinivasan, J. Benziger, A. B. Bocarsly, J. Electrochem. Soc. 149 (2002) A256.

[42] M.W. Verbrugge, J. Electrochem. Soc. 136 (1989) 417.

[43] R. Savinell, E. Yeager, D. Tryk, U. Landau, J. Wainright, D. Weng, K. Lux, M. Litt, and C. Rogers, J. Electrochem. Soc. 141 (1994) L46.

[44] J. T. Wang, S. Wasmus, and R. F. Savinell, J. Electrochem. Soc. 143 (1996) 1233.

[45] P. Colomban (Ed.), Proton Conductors: Solids, Membranes and Gels-Materials and Devices (Chemistry of Solid State Materials, No 2), Cambridge University Press, 1992.

[46] S. Agro, T. DeCarmine, S. DeFelice, L. Thoma, Annual Progress Report for the DOE Hydrogen Program, 2005, p. 790, US Department of Energy (DOE).

[47] Howell, Keynote Paper the Fifth International Membrane Science & Technology Conference (IMSTEC ’03), Sydney, Australia, November 10–14, 2003.

[48] P. Colomban (Ed.), Proton Conductors: Solids, Membranes and Gels-Materials and Devices (Chemistry of Solid State Materials, No 2), Cambridge University Press, 1992.

[49] K. D. Kreuer, Solid State Ionics 136 (2000) 149.

[50] T. Ueki and M. Watanabe, Macromolecules 41 (2008) 3739.

[51] Y.Z. Fu, Ph.D. dissertation, The University of Texas at Austin, May, 2007.

[52] S.-Z. Ren, G.-Q. Sun, C.-N. Li, Z.-X. Liang, Z.-M. Wu, W. Jin, Q. Xin, and X.-F. Yang, J. Membr. Sci. 282 (2006) 450.

[53] P .L. Antonucci, A.S. Aric´o, P. Cret´ı, E. Ramunni, V. Antonucci, Solid State Ionics 125 (1999) 431.

[54] C-Y Yen, C-H Lee, Y-F Lin, H-L Lin, Y-H Hsiao, S-H Liao, C-Y Chuang, and C. Ma, J. Power Sources 173 (2007) 36.

[55] V. Tricoli, J. Elelectrochem. Soc. 145 (1998) 3798.

[56] R.-C. Jiang, Y. Zhang, S. Swler, X. Wei, C. Erkey, H. R. Kunz, and J. M. Fenton, Electrochem. Solid-State Lett. 8 (2005) A611.

[57] E. H. Jung, U. H. Jun, T. H. Yang, D. H. Peak, D. H. Jun, and S. H. Kim, International Journal of Hydrogen Energy 32 (2007) 903.

[58] J. Liu, H. T. Wang, S. A. Cheng, and K.-Y. Chan, J. Membr. Sci. 246 (2005) 95.

[59] N. W. Deluca and Y. A. Elabd, J. Membr. Sci. 282 (2006) 217.

[60] L. Li, J.-F. Drillet, Z. Mácová, R. Dittmeyer, and K. Jüttner, Russian Journal of Electrochemistry 42 (2006) 1193.

[61] E. B. Easton, B. L. Langsdorf, J. A. Hughes, J. Sultan, Z. G. Qi, A. Kaufman, and P. G. Pickup, J. Electrochem. Soc. 150 (2003) C735.

[62] A. Sungpet, J. Membr. Sci. 226 (2003) 131.

[63] M. A. Smit, A. L. Ocampo, M. A. Espinosa-Medina, and P. J. Sebastian, J. Power Sources 124 (2003) 59.

[64] T. Shimizu, T. Naruhashi, T. Momma, and T. Osaka, Electrochemistry 70 (2002) 991.

[65] V. Saarinen, O. Himanen, T. Kallio, G. Sundholm, and K. Kontturi, J. Power Sources 163 (2007) 768.

[66] L. J. Hobson, H. Ozu, M. Yamaguchi, and S. Hayasea, J. Electrochem. Soc. 148 (2001) A1185.

[67] P. X. Xing, G. P. Robertson, M. D. Guiver, S. D. Mikhailenko, K. P. Wang, and S. Kaliaguine, J. Membr. Sci. 229 (2004) 95.

[68] B. Yang and A. Manthiram, Electrochem. Solid-State Lett. 6 (2003) A229.

[69] Y. -Z. Fu and A. Manthiram, J. Power Sources 157 (2006) 222.

[70] C. Genies, R. Mercier, B. Sillion, N. Cornet, G. Gebel, and M. Pineri, Polymer, 42 (2001) 359.

[71] J. H. Fang, X. X. Guo, S. Harada, T. Watari, K. Tanaka, H. Kita, and K. Okamoto, Macromolecules 35 (2002) 9022.

[72] J. A. Kerres, J. Membr. Sci. 185 (2001) 3.

[73] R. Nolte, K. Ledjeff, M. Bauer, and R. Mulhaupt, J. Membr. Sci. 83 (1993) 211.

[74] K. Miyatake, Y. Chikashige, and M. Watanabe, Macromolecules 36 (2003) 9691.

[75] R. Guan, H. Zou , D. P. Lu, C. L. Gong, and Y. F. Liu, European Polymer Journal 41 (2005) 1554.

[76] N. Asano, M. Aoki, S. Suzuki, K. Miyatake, H. Uchida, and M. Watanabe, J. Am. Chem. Soc. 128 (2006) 1762.

[77] P. X. Xing, G. P. Robertson, M. D. Guiver, S. D. Mikhailenko, and S. Kaliaguine, J. Polym. Sci.: Part A 42 (2004) 2866.

[78] Y. Gao, G. P. Robertson, M. D. Guiver, and X. G. Jian, J. Polym. Sci.: Part A 41 (2003) 497.

[79] Y. Gao, G. P. Robertson, D. -S Kim, M. D. Guiver, S. D. Mikhailenko, X. Li, and S. Kaliaguine, Macromolecules 40 (2007) 1512.

[80] A. S. Badami, A. Roy, H.-S. Lee, Y. X. Li, and J. E. McGrath, J. Membr. Sci. 328 (2009) 156.

[81] W. L. Harrison, F. Wang, J. B. Mecham, V. A. Bhanu, M. Hill, Y. S. Kim, and J. E. McGrath, J. Polym. Sci.: Part A 41 (2003) 2264.

[82] F. Wang, M. Hickner, Y. S. Kim, T. A. Zawodzinski, and J. E. McGrath, J. Membr. Sci. 197 (2002) 231.

[83] J. H. Fang, X. X. Guo, S. Harada, T. Watari, K. Tanaka, H. Kita, and K. Okamoto, Macromolecules 35 (2002) 9022.

[84] C. Genies, R. Mercier, B. Sillion, R. Petiaud, N. Cornet, G. Gebel, and M. Pineri, Polymer 42 (2001) 5097.

[85] Y.Woo, S.Y. Oh, Y. S. Kang, and B.S.Jung, J. Membr. Sci. 220 (2003) 31.

[86] K. Ramya and K. S. Dhathathreyan, J. Appl. Polym. Sci. 88 (2003) 307.

[87] K. Ramya, B. Vishnupriya, and K. S. Dhathathreyan, J. New Mat. Electrochem. Syst. 4 (2001) 115.

[88] B. Vishnupriya, K. Ramya, and K. S. Dhathathreyan, J. Appl. Polym. Sci. 83 (2002) 1792.

[89] W. L. Harrison, F. Wang, J. B. Mecham, V. A. Bhanu, M. Hill, Y. S. Kim, and J. E. McGrath, J. Polymer Sci.: A 41 (2003) 2264.

[90] H. Ghassemi, J. E. McGrath, and T. A. Zawodzinski, Polymer 47 (2006) 4132.

[91] B. J. Liu, Y. S. Kim,W. Hu, G. P. Robertson, B. S. Pivovar, and M. D. Guiver, J. Power Sources 185 (2008) 899.

[92] B. J. Liu, G. P. Robertson, D.-S. Kim, M. D. Guiver, W. Hu, and Z. H. Jiang, Macromolecules 4 (2007) 1934.

[93] K. D. Kreuer, J. Membr. Sci. 185 (2001) 29.

[94] D. D'Alelio, Ion-exchanger, US Patent 2366007 (1944).

[95] R. Nolte, K. Ledjeff, M. Bauer, and R. Mülhaupt, J. Membr. Sci. 83 (1993) 211.

[96] J. Kerres, W. Cui, and W. Schnurnberger, US Patent 08/868943 (1997).

[97] J. Kerres, W. Zhang, and W. Cui, J. Polym. Sci.: Part A: Polym. Chem. 36 (1998) 1441.

[98] J. Kerres, W. Cui, and M. Junginger, J. Membr. Sci. 139 (1998) 227.

[99] M. L. Vona, E. Sgreccia, S. Licoccia,G. Alberti, L. Tortet, and P. Knauth, J. Phys. Chem. B 113 (2009) 7505.

[100] M. H. Jeong, K.-S. Lee, and J.-S. Lee, Macromolecules 42 (2009) 1652.

[101] Y. S. Oh, H.-J. Lee, M. Yoo, H.-J. Kim, J. Han, and T.-H. Kim, J. Membr. Sci. 323 (2008) 309.

[102] P. Donoso, W. Gorecki, C. Berthier, F. Defendini, C. Poinsignon, and M. B. Armand, Solid State Ionics 28 (1988) 969.

[103] J. Przyluski, A. Zalewska, J. Maron, and W. Wieczorek, Polish J. Chem. 71 (1997) 968.

[104] M. F. Daniel, B. Desbat, F. Cruege, O. Trinquet, and J. C. Lassegues, Solid State Ionics 28 (1988) 637.

[105] Y. L. Ma, J. S. Wainright, M. H. Litt, and R .F. Savinell, J. Electrochem. Soc. 151 (2004) A8.

[106] J. S. Wainright, J.T. Wang, D. Weng, R.F. Savinell, and M. Litt, J. Electrochem. Soc. 142 (1995) L121.

[107] J. S. Wainright, J.T. Wang, R. Savinell, M. Litt, H. Moaddel , C. Rogers, In: S. Srinivasan, D.D. Macdonald, A.C. Khandkar (Eds.), Electrode Materials and Processes for Energy Coversion and Storage, Pennington, NJ, 1995, p. 255.

[108] D. Weng, J. S. Wainright, U. Landau, and R. F. Savinell, J. Electrochem. Soc. 143 (1996) 1260.

[109] Q. F. Li, H.A. Hjuler, and N.J. Bjerrum, J. Appl. Electrochem. 31 (2001) 773.

[110] J. A. Kerres, J. Membr. Sci. 185 (2001) 3.

[111] B. Kosmala and J. Schauer, J. Appl. Polym. Sci. 85 (2002) 1118.

[112] K. Bouzek, S. Moravcová, Z. Samec, and J. Schauer, J. Electrochem. Soc. 150 (2003) E329.

[113] M. Walker, K.-M. Baumgärtner, M. Kaiser, J. Kerres, A. Ullrich, and E. Räuchle, J. Appl. Polym. Sci. 74 (1999) 67.

[114] L. Jörissen, V. Gogel, J. Kerres, and J. Garche, J. Power Sources 105 (2002) 267.

[115] J. Kerres, A. Ullrich, F. Meier, Th. Häring, Solid State Ionics 125 (1999) 243.

[116] J. Kerres, A. Ullrich, Th. Häring, , in: Extended Abstracts of the 3rd International Symposium on New Materials for Electrochemical Systems, Montreal, Canada, 4–8 July 1999, pp. 231–232.

[117] J. Kerres, A. Ullrich, Th. Häring, W. Preidel, M. Baldauf, and U. Gebhardt, J. New Mater. Electrochem. Syst. 3 (2000) 229.

[118] J. Kerres, A. Ullrich, T. Häring, Modifikation von Engineeringpolymerenmit N-basischen Gruppen und mit Ionenaustauschergruppenin der Seitenkette, D. Patent 198 36 514.4

[119] Y.-Z. Fu, A. Manthiram and M. D. Guiver, Electrochem. Solid-State Lett. 10 (2007) B70.

[120] S. M. Haile, D.A. Boysen, C.R.I. Chisholm, and R.B. Merle, Nature 410 (2001) 910.

[121] D. A. Boysen, T. Uda, C.R.I. Chisholm, and S.M. Haile, Science 303 (2004) 68.

[122] D.A. Boysen, C.R.I. Chisholm, S.M. Haile, S.R. and Narayanan, J. Electrochem. Soc. 147 (2000) 3610.

[123] K. D. Kreuer, Annu. Rev. Mater. Res. 33 (2003) 333.

[124] N. Kuwata, N. Sata, T. Tsurui, and H. Yugami, Jpn. J. Appl. Phys., Part 1 44 (2005) 8613.

[125] T. Hibino, A. Hashimoto, M. Suzuki, M. Sano, J. Electrochem. Soc. 149 (2002) A1503.

[126] J. H. Shim, J. S. Park, J. An, T. M.Gur, S. K. Kang and F. B. Prinz, Chemistry of Materials, (2009).

[127] B. Yang and A. Manthiram, Electrochem. Solid-State Lett. (2003) A229

[128] Y. -Z. Fu and A. Manthiram, J. Power Sources 157 (2006) 222

[129] X. Ren, T. E. Springer, T. A. Zawodzinski, and S. Gottesfeld, J. Electrochem. Soc. 147 (2000) 466.

[130] K. D. Kreuer, J. Membr. Sci. 185 (2001) 29.

[131] Q. Guoa, P. N. Pintaurob, H. Tang, and S. O'Connora, J. Membr. Sci. 154 (1999) 175 (1999)

[132] F. Lufrano, I. Gatto, P. Staiti, V. Antonucci, and E. Passalacqua, Solid State Ionics 145 (2001) 47.

[133] N. Asano, K. Miyatake, M. Watanabe, and C. Mater., Chem. Mater. 16 (2004) 2841.

[134] O. Yamada, Y. Yin, K. Tanaka, H. Kita, and K. Okamoto, Electrochim. Acta 50 (2005) 2655.

[135] J. M. Song, K. Miyatake, H. Uchida, and M. Watanabe, Electrochim. Acta 51 (2006) 4497.

[136] J. T. Wang, S. Wasmus, and R. F. Savinell, J. Electrochem. Soc., 143 (1996) 1233.

[138] A. Schechter and R. F. Savinell, Solid State Ionics 147 (2002) 181.

[139] A. Ainla and D. Brandell, Solid State Ionics 178 (2007) 581.

[140] L. Jörissen, V. Gogel, J. Kerres, and J. Garche, J. Power Sources 105 (2002) 267.

[141] B. Kosmala and J. Schauer, J. Appl. Polym. Sci. 85 (2002) 1118.

[142] K. Bouzek, S. Moravcová, Z. Samec, and J. Schauer, J. Electrochem. Soc. 150 (2003) E329.

[143] J. A. Kerres, Fuel Cells 5 (2005) 230.

[144] Y.-Z. Fu, A. Manthiram, and M. D. Guiver, Electrochem. Commun. 8 (2006) 1386.

[145] Y. -Z. Fu, A. Manthiram, and M. D. Guiver, Electrochem. Commun. 9 (2007) 905.

[146] M. D. Guiver, S. Croteau, J. D. Hazlett, and O. Kutowy, British Polymer Journal 23 (1990) 29.

[147] K. A. Mauritz, J. Macromol Sci. Rev. Macromol. Chem. Phys. C 28 (1988) 65.

[148] R. A. W. A. Lefelar, Macromolecules 17 (1984) 1145.

[149] B. Yang and A. Manthiram, J. of Power Sources 153 (2006) 7.

[150] Z. Zhou, S. Li, Y. Zhang, M. Liu, and W. Li, J. Am. Chem. Soc. 127 (2005) 10824.

[151] N. Grier, J. of Coat. Technol. 48 (1976) 50.

[152] K. Miyatake, Y. Chikashige, and M. Watanabe, Macromolecules 36 (2003) 9691.

[153] T. B. Norsten, M. D. Guiver, J. Murphy, T. Astill, T. Navessin, S. Holdcroft, B. L. Frankamp, V. M. Rotello, and J. Ding, Adv. Funct. Mater. 16 (2006) 1814.

[154] Y. Gao, G. P. Robertson, M. D. Guiver, S. D. Mikhailenko, X. Li, S. Kaliaguine, Polymer, 47 (2006) 808.

[155] D. S. Kim, Y. S. Kim, M. D. Guiver, B. S. Pivovar, J. Membr. Sci. 321 (2008) 199.

[156] J. K. Lee, W. Li, and A. Manthiram, J. Membr. Sci. 330 (2009) 73.

[157] T. R. Farhat and P. T. Hammond, Adv. Funct. Mater. 16 (2006) 433.

[158] D. M. DeLongchamp and P. T. Hammond, Langmuir 20 (2004) 5403.

[159] F. D. Martino, N. Vatistas, and V. Tricoli, J. Electrochem. Soc. 156 (2009) B59.

[160] B. Yang and A. Manthiram , Electrochem. Comm. 6 (2004) 231.

[161] Y. C. Si, J. -C Lin, H. R. Kunz, and J. M. Fenton, J. Electrochem. Soc. 151 (2004) A463.

[162] R. C. Jiang, H. R. Kunz and J. M. Fentona, J. Electrochem. Soc. 153 (2006) A1554.

[163] W. Li, A. Bellay, Y.-Z. Fu, and A. Manthiram, J. Power Sources 180 (2008) 719.

[164] Y. Gao, G. P. Robertson, M. D. Guiver, S. D. Mikhailenko, X. Li, and S. Kaliaguine, Macromolecules 37 (2004) 6748.

[165] D. Xing and J. Kerres, J. New Mat. Electrochem. Systems 9 (2006) 51.

[166] J. K. Lee and J. Kerres, J. Memb. Sci. 294 (2007) 75.

[167] J. K. Lee, W. Li, and A. Manthiram, J. Power Sources 180 (2008) 56.

[168] B. S. Pivovar and Y. S. Kim, J. Electrochem. Soc. 154 (2007) B739.

[169] Y. S. Kim, M. J. Summer, W. L. Harrison, J. S. Riffle, J. E. McGrath, and B.S. Pivovar, J. Electrochem. Soc. 151 (2004) A2150.

[170] C. Ma, L. Zhang, S. Mukerjee, D. Ofer, and B. Nair, J. Membr. Sci. 219 (2003) 123.

[171] E. B. Easton, T. D. Astill, and S. Holdcroft, J. Electrochem. Soc. 152 (2005) A752.

[172] H. Y. Jung, K. Y. Cho, K. A. Sung, W. K. Kim, and J. K. Park, J. Power Sources 163 (2006) 56.

[173] P. Xing, G. P. Robertson, M. D. Guiver, S. D. Mikhailenko, K. Wang, and S. Kaliauine, J. Membr. Sci. 229 (2004) 95-106.

[174] F. Trotta, E. Drioli, G. Moraglio, E.B. Poma, J. Appl. Polym. Sci. 70 (1998) 477-482.

[175] J. H. Kim, H. Y. Ha, I. H. Oh, S. A. Hong, H. N. Kim and H. I. Lee, Electrochim. Acta 50 (2004) 801.

[176] Z. Qi and A. Kaufman, J. Power Sources 113 (2003) 37.

[177] G. Li and P.G. Pickup, J. Electrochem. Soc. 150 (2003) C745.

[178] A. Pozio, M. De Francesco, A. Cemmi, F. Cardellini, and L. Giorgi, J. Power Sources 105 (2002) 13.

[179] M. C. Lefebvre, R. B. Martin, and P.G. Pickup, Electrochem. Solid-State Lett. 2 (1999) 259.

[180] Z. Siroma, T. Sasakura, K. Yasuda, M. Azuma, and Y. Mizazaki, J. Electroanal. Chem. 546 (2003) 73.

List of Publication Related to This Work

1. W. Li, A. Bellay, Y.-Z. Fu, and A. Manthiram, "*N*,*N'*-Bis-(1H-benzimidazol-2-yl)-isophthalamide as an Additive in Sulfonated Polymer Membranes for Direct Methanol Fuel Cells", *Journal of Power Sources* **180**, 719 (2008).

2. W. Li, Y.-Z. Fu, A. Manthiram, and M. D. Guiver, "Blend Membranes Consisting of Sulfonated Poly(ether ether ketone) and Polysulfone Bearing 4-nitro-benzimidazole for Direct Methanol Fuel Cells", *Journal of the Electrochemical Society* **156,** B258 (2009).

3. W. Li, B. Norris, P. Snodgrass, K. Prasad, A. Stockett, V. Pryamitsyn, C. Bielawski, V. Ganesan, A. Manthiram, "Evaluating the Role of Additive pKa on the Proton Conductivities of Blended Sulfonated Poly(Ether Ether Ketone) Membranes", *The Journal of Physical Chemistry B*. (Accepted)

4. J. K. Lee, W. Li and A. Manthiram, "Sulfonated Poly(ether ether ketone)s Ionomers for Direct Methanol Fuel Cell Electrodes", *Journal of Power Sources* **180**, 56 (2008)

5. J. K. Lee, W. Li, A. Manthiram, and M. D. Guiver, "Blend Membranes Based on Acid-base Interactions for Operation at High Methanol Concentrations", *Journal of the Electrochemical Society* **156**, B46 (2009).

6. J. K. Lee, W. Li, and A. Manthiram, "Poly(arylene ether sulfone)s containing pendant sulfonic acid groups as membrane materials for direct methanol fuel cells" *Journal of membrane Science* **330**, 73 (2009).

7. W. Li, A. Manthiram, and M. D. Guiver, "Blend Membranes Consisting of Sulfonated Poly(ether ether ketone) and 1*H*-Perimidine Tethered Polysulfone for Direct Methanol Fuel Cells", *Electrochemcial and Solid-State Letters*, submitted in June 2009.

8. W. Li and A. Manthiram, "Sulfonated Poly(arylene ether sulfone) as a Methanol-barrier Layer in Multilayer Membranes for Direct Methanol Fuel Cells", *Journal of Power Sources*, submitted in July 2009.

Vita

Wen Li was born in Beijing, China on Januanry 29, 1980, the son of Jingshun Li and Peihua Zhao. After completing his study at Beijing No.4 High School, China, in 1998, he entered Tsinghua University, Beijing, China. He received the B.S. degree in Chemical Engineering in July 2002 and M.S. degree in Chemical Engineering in July 2005 from Tsinghua University. In August 2005, he entered the Graduate School of the University of Texas at Austin.

Permanent address: Room 2-302, Kang Ju Nan Qu, Mi Yun County, Beijing, China, 101500.

This dissertation was typed by Wen Li.